SOUTHWEST RESEARCH INSTITUTE®

COMPARISON OF FIRE PROPERTIES OF AUTOMOTIVE MATERIALS AND EVALUATION OF PERFORMANCE LEVELS

FINAL REPORT
SwRI® Project No. 01.05804
October 2003
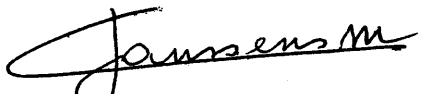Consisting of 369 Pages

Prepared by:

Karen C. Battipaglia
A. Leigh Griffith, M.S.
Jason P. Huczek, M.S.
Marc L. Janssens, Ph.D.
Michael A. Miller, M.S.
Keith R. Willson, Ph.D.
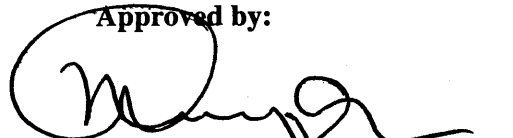
Prepared for:

Department of Transportation
National Highway Traffic Safety Administration (DOT/NHTSA)
Crashworthiness Research, NRD-11
400 Seventh Street, SW, Room 5301
Washington, DC 20590

Submitted by:

Marc L. Janssens, Ph.D.
Director
Department of Fire Technology

Approved by:

Michael G. MacNaughton, Ph.D.
Vice President
Chemistry and Chemical
Engineering Division

EXECUTIVE SUMMARY

This report describes the results of a research program that was conducted at Southwest Research Institute (SwRI®) between July 2002 and October 2003 on behalf of the National Highway Traffic Safety Administration (NHTSA). Results of a parallel research program performed for the Motor Vehicle Fire Research Institute (MVFRI) are reported as well. The two programs are referred to as the "NHTSA project" and the "MVFRI project," respectively.

The primary objectives of the NHTSA project were

1. To identify or develop a small-scale test methodology to rate automotive materials consistent with actual fire performance in vehicle burns; and

2. To establish levels of performance for this test methodology that would significantly alter the fire outcome in terms of injury or survivability.

According to the National Fire Protection Association (NFPA) statistics, a front-end collision followed by an engine compartment fire is one of two scenarios that account for the majority of fatalities in motor vehicle fires. The other scenario involves a rear-end collision resulting in a ruptured fuel tank and an underbody pool fire. Because the fire performance of materials and components is not expected to have a significant effect on the second scenario, the focus of the NHTSA project is on the engine fire scenario.

The "test methodology" defines the test apparatus, the procedure that needs to be followed, and the results to be reported. An extensive literature survey was conducted to identify candidate test apparatuses and determine appropriate test conditions. The Cone Calorimeter (ASTM E 1354) was identified as the most suitable test apparatus. Heat fluxes in the range of 10 to 60 kW/m^2 were found to be representative of thermal exposure conditions in motor vehicle fires that originate in the engine compartment. The literature survey also included a detailed review of recent full-scale vehicle burns in support of the analysis to meet the second objective of the NHTSA project. It was determined from this review that engine fires become a threat to occupants trapped in the passenger compartment when a critical size of approximately 400 kW is reached.

For the experimental part of the NHTSA project, 18 exterior automotive parts (outside the passenger compartment) were selected from a passenger van and a sports coupe. The vehicles were previously tested in full-scale by Factory Mutual (FM) as part of a previous research program funded by General Motors Corporation (GM). Three types of measurements were made in the NHTSA project:

1. Micro-scale tests were performed using modulated differential scanning calorimetry (MDSC) to determine thermal physical properties of the materials.

2. Small-scale fire tests were conducted in the Cone Calorimeter (ASTM E 1354) at 20, 35, and 50 kW/m² to obtain ignition, heat release, and smoke production data over a range of exposure conditions. The materials were also tested in general accordance with the Federal Motor Vehicle Safety Standard (FMVSS) 302. Exterior materials do not have to meet the FMVSS 302 requirements, but the test data were obtained to serve as a baseline. Additional Cone Calorimeter tests were also obtained on a subset of the components that were coated with a metallic film.

3. Intermediate-scale calorimeter or ICAL (ASTM E 1623) tests were performed at the same heat fluxes as in the Cone Calorimeter to obtain heat release rate and smoke production rate data for six of the 18 components.

The peak heat release rates measured in the Cone Calorimeter and ICAL expressed on the basis of the initially exposed area are reasonably consistent below 350 kW/m². At higher heat release rates, the ICAL values are significantly higher due to the contribution of a pool fire of molten material that forms below the specimen holder. However, the aforementioned review of full-scale vehicle burn test data revealed that plastic pool fires underneath the engine do not have a significant effect on fire growth before the critical size of 400 kW is reached. Consequently, heat release rates measured in the Cone Calorimeter at the appropriate heat flux level can be used to predict full-scale fire growth.

A simple model was developed to estimate fire growth in the engine compartment of a motor vehicle based on Cone Calorimeter data for the materials and components involved. This model assumes a slab geometry and resulted in the following equation that can be used for design purposes

$$\dot{Q} = A_0 \dot{Q}''(1.5)^{\frac{2(t-t_{ig})}{t_{ig}}}$$

where $\dot{Q}$ is the heat release rate of the fire in kW, A_0 is the area initially ignited (assumed to be 0.0079 m²), $\dot{Q}''$ is the peak heat release rate measured in the Cone Calorimeter at 35 kW/m², t is the time in seconds, and t_{ig} is the time to ignition measured in the Cone Calorimeter at 35 kW/m² in seconds. The time to reach 400 kW can therefore be calculated from

$$t = t_{ig}\left[1 + 1.233\ln\left(\frac{400}{0.0079\dot{Q}''}\right)\right]$$

This equation can be used to establish Cone Calorimeter criteria based on an acceptable fire growth rate. A fire performance graph of $\dot{Q}''$ versus t_{ig} was developed consisting of a set of curves for different fire growth rates (6 minutes to 400 kW, 8 minutes to 400 kW, *etc.*). Data points that fall below a specific curve will require more than the corresponding time to reach 400 kW. The fire performance graph also contains a curve for the FMVSS 302 test. Materials with a peak heat release rate of 240 kW/m^2 or less when tested in the Cone Calorimeter at 35 kW/m^2 will not support flame propagation in the FMVSS 302 test. Materials with a peak heat release rate exceeding 240 kW/m^2 are expected to meet the FMVSS 302 burn rate requirements if the ratio of peak heat release rate to ignition time is 12 kW/s-m^2 or less.

Additional Cone Calorimeter tests were performed on two materials protected with a metallic coating. Four different coating systems were applied. One of the coatings was applied in two thicknesses on two of the four substrates. In general, the coatings resulted in delayed ignition times, but did not significantly affect the peak heat release rate. Consequently, it was demonstrated that the use of metallic coatings is a viable option to improve fire performance and delay fire growth in the engine compartment of a motor vehicle.

The MVFRI project involved additional measurements of toxic gases in the duct for most of the Cone Calorimeter tests. Concentrations of CO, CO_2, HCl, HCN, and NO_x were measured continuously during each test with a Fourier Transform InfraRed (FTIR) spectrometer. The concentration measurements were used to calculate yields, *i.e.*, the total mass of each toxic gas generated during flaming combustion divided by the mass loss of the fuel over the same period. CO yields obtained in this study are comparable in magnitude, but consistently lower than values reported in the literature for the same generic classes of materials. This can be explained by the fact that the literature values were obtained in the Fire Propagation Apparatus (ASTM E 2058) under reduced ventilation conditions compared to the Cone Calorimeter. The use of the measured yields to calculate a fractional effective dose in real engine fires is also discussed.

Three materials were selected from the set of 18 for an evaluation in two commonly used toxicity test procedures. The Airbus Directive (ABD) 0031 procedure is based on the NBS smoke chamber (ASTM E 662) and involves supplemental gas analysis. The International Maritime Organization (IMO) smoke and toxicity test procedure is detailed in Part 2 of Annex 1 to the *International Code for Application of Fire Test* Procedures (FTP Code) and is based on a modified

version of the NBS smoke chamber as described in International Organization for Standardization (ISO) Standard 5659 Part 2. Both procedures specify acceptance criteria that include limiting concentrations of CO, HCl, HCN, NO_x, and a few additional gases. The three materials that were selected had the lowest, median, and highest peak CO concentrations in the Cone Calorimeter tests of all the materials that were tested. The material with low peak CO concentration was a PVC and exceeded the limits for HCl in the IMO and Airbus tests. The material with median CO in the Cone Calorimeter failed the IMO test, and the material with high CO in the Cone Calorimeter marginally met the IMO and Airbus requirements. It can be concluded from these tests that the CO concentrations in the Cone Calorimeter are not consistent with those in box-type toxicity tests. This can be explained by the fact that plenty of excess air is continuously supplied in the Cone Calorimeter, while the oxygen concentration in the IMO and Airbus smoke chambers typically drops below ambient during a test. It is not clear which of the two types of conditions is more representation of real engine fire conditions.

TABLE OF CONTENTS

TABLE OF CONTENTS

LIST OF FIGURES

LIST OF TABLES

LIST OF TABLES

LIST OF TEST STANDARDS

Airbus Industries ABD 0031 Airbus Directives (ABD) and Procedures for Fire – Smoke – Toxicity (FST), 2002.

American Society for Testing and Materials

ASTM C 1166 *Standard Test Method for Flame Propagation of Dense and Cellular Elastomeric Gaskets and Accessories*.

ASTM D 568 *Standard Test Method for Rate of Burning and/or Extent and Times of Burning of Flexible Plastic in a Vertical Position*.

ASTM D 635 *Standard Test Method for Rate of Burning and/or Extent and Time of Burning of Plastics in a Horizontal Position*.

ASTM D 2859 *Standard Test Method for Ignition Characteristics of Finished Textile Floor Covering Materials*.

ASTM D 3675 *Standard Test Method for Surface Flammability of Flexible Cellular Materials Using a Radiant Heat Energy Source*.

ASTM E 162 *Standard Test Method for Surface Flammability of Materials Using a Radiant Heat Energy Source*.

ASTM E 648 *Standard Test Method for Critical Radiant Flux of Floor-Covering Systems Using a Radiant Heat Energy Source*.

ASTM E 662 *Standard Test Method for Augoignition Temperature of Liquid Chemicals*.

ASTM E 800 *Standard Test Method for Measurement of Gases Present or Generated During Fires,*.

ASTM E 906 *Standard Test Method for Heat and Visible Smoke Release Rates for Materials and Products*.

ASTM E 1354 *Standard Test Method for Heat and Visible Smoke Release Rates for Materials and Products Using an Oxygen Consumption Calorimeter*.

ASTM E 1623 *Standard Test Method for Determination of Fire and Thermal Parameters of Materials, Products, and Systems Using an Intermediate Scale Calorimeter (ICAL)*.

ASTM E 2058 *Standard Test Method for Measurement of Synthetic Polymer Material Flammability Using a Fire Propagation Apparatus (FPA)*.

Federal Aviation Regulations (FAR) 25.853 *Flammability Requirements of Aircraft Seat Cushions*, Part 25 *Compartment Interiors*.

FMVSS 302 *Motor Vehicle Interior Materials Fire Test*

GM 269 M *Flammability Test for Fire Retardant Polymers*.

IMO A.653 *Recommendation on improved fire test procedures for flammability of bulkhead, ceiling and deck finish materials*.

ISO 5659 Part 2 *Determination of optical density by a single-chamber test*.

ISO 5660 Part 1 *Reaction-to-fire tests -- Heat release, smoke production and mass loss rate -- Part 1: Heat release rate (cone calorimeter method)*.

ISO 5660 Part 2 *Reaction-to-fire tests -- Heat release, smoke production and mass loss rate -- Part 2: Smoke production rate (dynamic measurement)*.

Nordtest NT Fire 047 *Combustible products: Smoke gas concentrations, continuous, FTIR analysis*.

UL 94 *Standard for Tests for Flammability of Plastic Materials for Parts in Devices and Appliances*.

LIST OF SYMBOLS

$\dot{Q}$	Heat release rate of the fire (kW)
$\dot{Q}''$	Peak heat release rate measured in the Cone Calorimeter (kW/m^2)
A_0	Area initially ignited (m^2)
CHF	Critical heat flux (kW/m^2)
c_v	Specific heat (kJ/kg-K)
D_s	Optical Density
FHP	Fire hazard parameter
FPI	Fire propagation index (m$^{5/3}$/kW$^{2/3}$-s$^{1/2}$)
HRP	Heat response parameter (–)
HRR	Heat release rate (kW/m^2)
HRR$_0$	Intrinsic heat release rate (kW/m^2)
I_s	Flame spread index
k_v	Thermal conductivity (kW/m-K)
L	Distance to the center
PHRR	Peak heat release rate (kW/m^2)
$\dot{Q}$	Heat release rate of the fire (kW)
$\dot{Q}''$	Peak heat release rate measured in the Cone Calorimeter (kW/m^2)
R	Radius
t	Time (sec)
t_{400}	Time to 400 kW (s)
T_d	Decomposition temperature (°C)
T_g	Glass Transition temperature (°C)
t_{ig}	Time to ignition (sec)
T_m	Melt transition tempereature (°C)
TRP	Thermal response parameter (kW-s$^{1/2}$/m^2)
Y	Yield (g/g/)
α_v	Thermal diffusivity (mm^2/s)
δ	Thickness (mm)
ρ	Density (kg/m^3)

1.0   INTRODUCTION

This report describes the results of a research program that was conducted between July 2002 and October 2003 on behalf of the National Highway Traffic Safety Administration (NHTSA). Results of a parallel research program performed for the Motor Vehicle Fire Research Institute (MVFRI) are reported as well. The two programs are referred to as the "NHTSA project" and the "MVFRI project," respectively. Except for the intermediate-scale calorimeter (ICAL) tests, which were conducted at the Pacific Fire Laboratory (PFL) in Kelso, WA, the work for these two projects was performed at SwRI in San Antonio, TX.

The primary objectives of the NHTSA project were

1. To identify or develop a small-scale test methodology to rate automotive materials consistent with actual fire performance in vehicle burns; and

2. To establish levels of performance for this test methodology that would significantly alter the fire outcome in terms of injury or survivability.

The NHTSA project was a follow-up to an earlier program conducted at SwRI as part of a settlement between General Motors Corporation (GM) and the U.S. Department of Transportation [1]. The report of this earlier study, referred to as the "GM project," has not been published yet and is currently under review. The GM project focused on materials and components inside the passenger compartment. The NHTSA project uses a similar approach for exterior materials and extends the analysis by establishing levels of performance.

The additional work performed for MVFRI was motivated by the fact that recent full-scale vehicle burn tests indicated that smoke toxicity might be an issue [2]. Additional funding was provided by MVFRI to supplement a large number of the small-scale tests for NHTSA with toxic gas measurements. In addition, a subset of the materials was evaluated according to commonly used smoke toxicity test protocols required for materials used in other modes of transportation. The intent was to generate additional data, so that the smoke toxicity issue can be addressed in the development of a small-scale test method and performance levels for NHTSA.

2.0   APPROACH

The NHTSA project consists of three tasks as described below.

2.1   Task 1: Survey of Test Methodologies

This task consists of four parts.

1. The literature survey for the GM project will be updated to find recent publications that have appeared since the survey was conducted.

2. The reports from the FM full-scale vehicle burns were not available when the survey was conducted for GM and need to be studied in great detail. The full-scale test data obtained by FM will be extremely valuable to determine heat flux histories experienced by automotive components in real fires. The exposure conditions in the chosen test methodology will need to be consistent with these full-scale measurements.

3. SwRI will evaluate the data obtained by FM using the Fire Propagation Apparatus. These data will help SwRI determine the scope of materials already tested and give SwRI an indication of where data on more materials may be necessary.

4. A table will be compiled of all potential test methods with their advantages/disadvantages.

2.2   Task 2: Automotive Component Fire Tests

2.2.1   Task 2a: Selection and Procurement of Materials

Exterior components will be selected from vehicles tested in full-scale by FM. This selection set will be guided by material flammability studies conducted at The National Institute for Standards and Technology (NIST) on parts of a minivan and a sports coupe [3, 4].

2.2.2   Task 2b: Material Characterization

Thermodynamic characteristics of the materials from the selected components will be evaluated by modulated differential scanning calorimetry (MDSC). The analytical objectives of this task will focus on correlating the thermodynamic characteristics with the measured flammability behavior of the selected materials as determined by small-scale fire test methods. These correlations in relation to pre-ignition thermal and molecular behavior will enable the flammability properties of polymeric automotive materials presently in use to be categorized on a fundamental basis; for example, relative to polymer resin and filler composition. This level of understanding will become

particularly useful in selecting or engineering alternative materials or material modifications that might exhibit substantially improved fire performance in specific component applications, and which such alternatives would serve as suitable substitutes for the standard automotive polymers.

2.2.3   Task 2c: Small-Scale Flammability Tests

Based on the approach that was followed for the GM project, it is expected that the Cone Calorimeter will be used for this task. Samples of all materials will be tested in duplicate at 20, 35, and 50 kW/m^2. In addition to the full Cone Calorimeter tests, a number of tests will be conducted to determine the time to ignition at lower heat fluxes. The Cone Calorimeter data will be used to generate material properties that are useful to predict full-scale fire behavior. FMVSS 302 data will be obtained for all materials to serve as a baseline for Task 3b.

2.2.4   Task 2d: Intermediate- Scale Calorimeter (ICAL) Tests

Six components will be selected for testing in the ICAL apparatus. Single ICAL tests will be performed at 20, 35, and 50 kW/m^2 incident heat flux to one face of the component. The tests will be conducted in general accordance with ASTM E 1623, except that the sample will be ignited with a small pilot flame at a predetermined time. The flame will be inserted in the stream of pyrolysis gases at a time that will be calculated from the Cone Calorimeter ignition data to minimize heat release rate variations due to random ignition time fluctuations. The ICAL was developed for testing of planar specimens, and special sample holders will have to be constructed to accommodate odd-shaped automotive components.

2.2.5   Task 2e: Alternative Materials and/or Material Modifications

The purpose of this task is to identify new materials or viable modifications to the standard ones that endow superior fire performance, and which can serve as suitable substitutes for standard automotive polymeric components. In particular, coating technologies that are amenable to under the hood polymeric components will be specifically sought out in this task by employing surface engineering capabilities already established at SwRI. The potential benefit that surface metallization of standard polymeric materials might bring to the fire performance of such materials or components will be determined experimentally under this task.

2.3   Task 3: Full-Scale Fire Test Comparison with Component Results

After completion of Task 2 four types of data will be available for the three sets of materials:

1.   Material composition and fundamental thermal physical data obtained in Task 2b;
2.   Cone Calorimeter ignition and heat release rate data for the materials from Task 2c;

3. Intermediate-scale ignition and heat release rate component data from Task 2d; and

4. Large-scale fire performance data for the system of components from FM vehicle burns.

These data sets are interconnected as shown in Figure 1. If reasonably accurate component and system models were available, the Cone Calorimeter data could be used to predict fire performance of complete components. Moreover, calculated component performance could be combined to estimate the performance of the system. Thus, Cone Calorimeter acceptance criteria could be defined to obtain a specific performance level for the system. This three-tier approach has been applied with great success for other complex systems such as upholstered furniture and electric cables [5, 6]. The same approach will be used here to accomplish the objectives of the NHTSA project.

```
┌─────────────────────────────────────────────────┐
│   Composition and Thermal Physical Properties     │
└─────────────────────────────────────────────────┘
                        ↕
┌─────────────────────────────────────────────────┐
│              Cone Calorimeter Data                │
└─────────────────────────────────────────────────┘
                  Component Model
                        ↕
┌─────────────────────────────────────────────────┐
│        Intermediate-Scale Calorimeter Data        │
└─────────────────────────────────────────────────┘
                   System Model
                        ↕
┌─────────────────────────────────────────────────┐
│            Full-Scale Vehicle Burn Data           │
└─────────────────────────────────────────────────┘
```
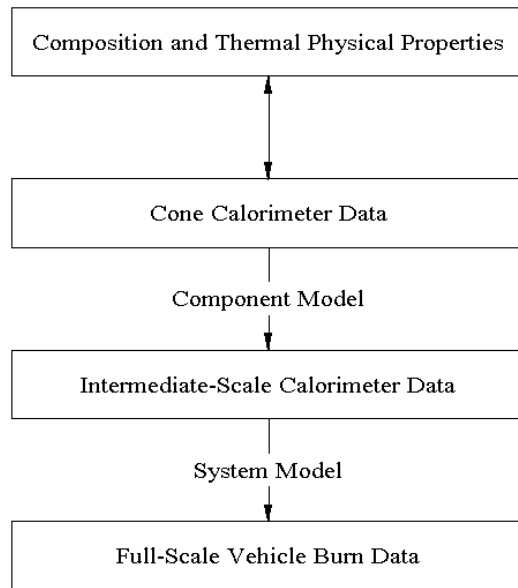
Figure 1. Relationship Between the Different Data Types.

2.3.1   Task 3a: Identify or Develop a Test Methodology for Automotive Materials

The preferred test apparatus (Cone Calorimeter) will be confirmed. Details of the test protocol (heat flux level(s), number of replicate tests, data to be reported, *etc.*) will be determined.

2.3.2   Task 3b: Establish Levels of Performance

The second objective of the NHTSA project is to define specific levels of performance and acceptance criteria that are consistent with full-scale fire performance. The latter will most likely be based on the time for the fire to spread to the passenger compartment and conditions to become untenable (faster is worse). The system and component models will be used to translate different levels of full-scale performance into corresponding levels of performance in the Cone Calorimeter.

Acceptance criteria can then be defined on the basis of a Cone Calorimeter performance level that corresponds to an acceptable full-scale fire performance level, *i.e.*, an acceptable time to onset of untenable conditions in the passenger compartment. This will fulfill the second of the two objectives of the project.

3.0   SELECTION OF TEST METHODOLOGY

3.1   Literature Survey Update

An extensive literature survey of publications on motor vehicle fire safety and related subjects was conducted as part of the GM project. The objectives of the survey were to identify the predominant motor vehicle fire scenarios that result in fatalities and to gain a better understanding of motor vehicle fire growth mechanisms and associated thermal exposure conditions. The survey for GM included conference proceedings, journal articles, reports, *etc.* published prior to December 31, 2001. In the NHTSA project, the survey was updated through June 30, 2003. Many of these publications describe work that was done as part of the GM-DOT settlement. These publications can be downloaded from NHTSA Docket #3588 [2-4, 7-51]. Five types of publications on motor vehicle fire safety were included in the NHTSA survey:

1. *Automobile Fire Statistics [52, 53].* Statistics provide information on likely ignition scenarios and potential paths of fire propagation, and their importance in terms of life safety. The most complete statistics on motor vehicle fires are published by the National Fire Protection Association (NFPA). The most recent report dates back to 2000 and was covered in the survey for the GM project.

2. *Full-Scale Vehicle Burn and Component Test Reports [54-57].* Many full-scale vehicle burn tests have been conducted. The purpose of most of these tests was to obtain data for fire engineering design of parking structures, road tunnels, *etc.* Older tests were instrumented with thermocouples, but more recent experiments include heat flux and energy release rate data. The most useful and complete data of this kind were obtained at FM as part of the GM-DOT settlement. A detailed summary of some of these tests is provided in the next section [2, 19, 27].

3. *Reports on Small-Scale Flammability Tests on Materials Used in Automobiles [58-60].* Numerous reports have been published on the flammability of materials used in automobiles. Most of these studies focus on performance of materials

tested according to FMVSS 302. However, a few recent publications present ignition, heat release, and smoke production data for automotive materials.

4. *Other Publications on Fires in Automobiles [61, 62].* Accident reports, publications on computer modeling and investigation of motor vehicle fires, and legislative documents concerning automobile fire safety contain useful information.

5. *Reports of Similar Studies for Other Modes of Transportation [58, 63-67].* Several studies have been performed to relate small-scale flammability data with performance in real fires for materials used in passenger cabins of commercial aircraft, rail transportation vehicles, and ships. There are analogies between these investigations and the NHTSA project. A survey of these investigations revealed some valuable information.

The recent publications that were reviewed in this study confirm the conclusions that were reached in the survey conducted earlier for GM. According to NFPA statistics, a front-end collision followed by an engine compartment fire is one of two scenarios that account for the majority of fatalities in motor vehicle fires. The other scenario involves a rear-end collision resulting in a ruptured fuel tank and an underbody pool fire. Because the fire performance of materials and components is not expected to have a significant effect on the second scenario, the focus of the NHTSA project should be on the engine fire scenario. Full-scale vehicle burn test data indicate that incident heat fluxes to components in the engine compartment in this scenario range from 10 to 60 kW/m^2. Incident heat fluxes to materials inside the passenger compartment are between 20 and 40 kW/m^2 prior to flashover.

3.2 Review of Recent Full-Scale Vehicle Burn Tests

3.2.1 Summary of Full-Scale Fire Test of Caravan

The test vehicle was a crash-tested 1996 Dodge Caravan Sport. In the crash test, a moving barrier traveling at a velocity of 65 mph, struck the vehicle on the front left corner. Approximately five minutes after impact, a fire started in the area of the battery and power distribution center (PDC). The fire was allowed to burn for approximately five minutes, at which point, it was manually extinguished. The fire test was conducted on November 13, 1996. An electrical igniter was used to artificially start a fire in the engine compartment. The results of that fire test are discussed below.

3.2.1.1　Ignition

The fire was started artificially using an electrical igniter placed between the battery and power distribution center (PDC). The igniter was made by winding Nichrome wire (24 AWG, length = 350 cm, resistance = 12 Ω) around four pieces of polypropylene sheet (0.1 × 10 × 15 cm, mass = 110 g) cut from the environmental housing of a Dodge Caravan battery. The polypropylene sheet was included in the igniter to replace material consumed by the fire during the crash test.

Electrical power was supplied to the igniter from a variable-tap transformer. At the start of this test, the power output of the transformer was adjusted to approximately 80% of full power (approximately 95 VAC). The power-output of the transformer was increased to 100% of full power (approximately 120 VAC) 5½ minutes after the start of the test. When flames were observed in the engine compartment, approximately 10 minutes after the start of the test, the transformer was turned off, cutting electrical power to the igniter.

Neither the temperature of the igniter, nor the current through the heating wire was measured during this test. Heat generated by the igniter was estimated from the resistance of the heating wire and the applied voltage: 0.8 kW at 95 VAC and 1.2 kW at 120 VAC.

3.2.1.2　Flame Spread in Engine Compartment

Heat from the igniter caused plastic in the igniter and in the components contacting the igniter to thermally degrade, producing a plume of gray smoke that rose from the left side of the engine compartment for approximately 10 minutes before the gaseous thermal degradation products ignited spontaneously. Flames were first detected in the area above the battery and PDC. The hood liner ignited shortly after the battery and PDC. Flames spread to the right side of the engine compartment along the hood liner and the heating, ventilation, and air conditioning (HVAC) air intake cowl. Burning thermoplastic melt flowed into the left headlamp assembly eventually igniting the bumper fascia and other combustible components in the front of the engine compartment.

3.2.1.3　Flame Spread into Passenger Compartment Through the Windshield

A small fire plume emerged from the rear edge of the hood approximately 15 seconds after ignition (610 seconds after energizing the igniter). As more combustible material in the engine compartment ignited, the fire plume grew in height. Increasing pressure in the engine compartment created by the growing fire also increased the velocity of gas flow from the engine compartment, pushing the fire plume rearward against the windshield. The polymer film in the windshield started to burn about 4 minutes after ignition. Pieces of flaming windshield fell into the passenger compartment, igniting the top of the instrument panel, the carpet in front of the passenger seat, the

deployed passenger airbag, and the inboard armrest of the front passenger seat. Hot gases produced by the burning objects in the passenger compartment accumulated below the roof, causing the front of the headliner and upper sections of the A-pillar trim to ignite between 10 and 11 minutes after flames were first observed in the engine compartment. Flames spread along the headliner toward the rear of the vehicle, with the interior of the vehicle approaching the flashover stage when the fire was extinguished starting at 11 minutes after ignition.

3.2.1.4 Flame Spread into Passenger Compartment Through the Dash Panel

Physical inspection of the test vehicle after the test and analysis of the test data indicated that flames also spread into the instrument panel through two of the openings in the dash panel. These included the pass-through for the refrigerant lines and the air intake for HVAC system. The pass-through closures in both of these openings were dislodged during the crash test. Flame-spread through the openings in the dash was slower than flame-spread through the windshield, and appeared to have been driven by a pressure gradient across the dash panel that developed as the fire in the engine compartment grew.

3.2.1.5 Conditions for Test Termination

Five criteria were established before the test to guide the decision to stop the tests and extinguish the fire. The intent of these criteria was to allow flames to spread into the passenger compartment sufficiently, so that the principle fire paths could be determined, while preserving physical evidence of fire paths that were not readily visible during the test or in any of the videos of the test. This physical evidence would be lost be lost if the test vehicle was allowed to burn completely.

- When the air temperature in the passenger compartment measured between the front seats at the height of an adult occupant exceeded 200°C and was increasing rapidly, or

- When the concentration of carbon monoxide in the passenger compartment exceeded 1% and was rising rapidly, or

- When flames visibly impinged on one or both front seats, or

- When the head-lining covering the forward section of the roof was in flames, or

- When flashover in the passenger compartment was evident.

After flames were first observed in the engine compartment, an attempt was made to evaluate these criteria continuously. As flames spread into the passenger compartment, conditions changed rapidly allowing insufficient time for objective evaluation of each of these criteria.

The test was stopped shortly after observing flames along the entire lower surface of the headliner, and the air horn was sounded a second time to signal the end of the test. The fire was extinguished with a fine water mist. At first, the water mist was directed through the driver's side window to extinguish burning objects in the passenger compartment. The fire in the engine compartment, the burning front grill and bumper fascia, and several small burning pools of melted plastic under the vehicle were extinguished after suppressing flames inside the vehicle.

A general observation from the video records was the lack of any significant ground fires under the engine compartment that might have spread into the passenger compartment, which explains the lack of fire damage around openings through the lower portion of the dash panel. These areas were not exposed to flame. See Table 1 for a summary of the test events for the Caravan.

3.2.2   Summary of Full-Scale Fire Test of Camaro

The test vehicle was a crash-tested 1997 Chevrolet Camaro. In the crash test, the vehicle was towed into a fixed steel pole. No fire was observed during this crash test, nor was there evidence of fire present in the test vehicle upon post-crash inspection. An artificial means of starting a fire in the engine compartment was employed, and the results of the fire test are discussed below. The fire test was conducted on October 1, 1997.

3.2.2.1   Ignition

A circular propane torch was installed at the rear of the right side of the engine compartment so that the flames impinged on the upper and lower cases of the HVAC module. The torch was constructed from stainless steel tubing (o.d. = 6.4 mm) and had a ring-shaped section (i.d. = 5.1 cm) with 12 holes (diameter = 1.3 mm) evenly spaced around the ring. The holes were pointed toward the ring axis at a 45° angle.

Propane was supplied to the torch from an external propane tank. The flow rate of the propane to the torch was 3.0 NTP l/min; this equates to 4.2 kW. A coiled nichrome heating wire was installed just above the torch and was used to ignite the propane gas. Electrical power was supplied to the heating wire using a variable tap transformer connected to 120 VAC. The nichrome wire was preheated for 30 seconds before propane flow was initiated.

Table 1. Summary of Test Events for the Caravan.

Time (min:sec)	Event
0:00	Start of Test – Igniter is supplied with power.
0:05 – 10:00	Smoke observed rising above the area around the battery and PDC .
10:02	Ignition of pyrolysate from battery case and PDC housing.
10:17	Ignition of hood liner, flames spread to left and rear edges of hood.
11:02	At this point, flame spread had expanded only slightly around the battery case and PDC housing. However, it had spread far enough ignite the HVAC air intake cowl.
12:02	Hood liner began to pull away from hood and cotton shoddy underneath ignited. The burning cotton felt increased the heat release rate and flames spread along the HVAC air intake cowl and ignited the paint on the exterior surface of the hood.
12:32	Flames begin to contact the windshield directly along its lower edge. Flame height against windshield is approximately 13 cm.
13:02	Most of battery, PDC housing, and the forward edge of the HVAC air intake cowl, in the left side of the engine compartment were burning. Also, flowing thermoplastic melt was observed, but there was no burning on the floor. This portion of the engine compartment was deformed during the crash test and prevented the flowing of melted burning plastic to flow to the floor. This increased the burning intensity in the engine compartment.
13:37	Ignition of windshield laminate.
14:02	Ignition of headlight assembly; flame height against windshield is approximately 26 cm.
14:37	A triangular section of the windshield fell onto the instrument panel, leaving a hole 15 cm wide in front of the steering wheel.
15:32	Differential pressure at dash panel is positive for the first time, meaning the pressure was greater in the engine compartment than the passenger compartment. This trend continued for the remainder of the test. Flame height against windshield is approximately 33 cm.
16:02	Flames spread downward on the bumper fascia and bumper energy absorber. This led to the formation of a pool fire on the ground under the left front corner of the engine compartment.
16:32	Flame height against windshield is approximately 40 cm.
16:37	The size of the hole in the windshield increases horizontally and vertically by a factor of 3 and 2, respectively.
16:47	Flames were in contact with the exterior surface of the silencer pad. Flame height against windshield is approximately 27 cm.
17:02	Ignition of instrument panel.
17:32	Several large sections of the windshield fell into the right side of the passenger compartment, igniting the deployed passenger airbag, the passenger seat, and the carpet in front of the passenger seat. The concentrations of the measured combustion gases (measured 6 inches below the headliner) also started to accumulate in the passenger compartment.
19:32	A layer of heated combustible gases (produced by thermal decomposition of materials in the instrument panel, the deployed air bags, the interior trim panels, the front seats, and the carpet) accumulated below the headliner of the test vehicle and ignited.
20:02	Flames begin to emerge from the driver's door window.
20:32	Radiation ignited the deployed driver's air bag and upper surfaces of the seat backs on the driver and front passenger seats.
20:47	Signal to end the test was given. A fine water mist was sprayed into the passenger compartment through the window in the driver's door. The water mist extinguished the burning upper layer within a few seconds, causing a rapid drop in air temperature in the passenger compartment. The water mist was then directed into the hole in top of the instrument panel, which extinguished the fire in the instrument panel and cooled melted plastic components rapidly without appreciably disrupting their shapes. Finally, the water mist was sprayed through the gaps between the crushed hood and left fender to suppress flames in the engine compartment.

3.2.2.2 Flame Spread in the Engine Compartment to HVAC Upper Case

To start the test, the propane torch was ignited and allowed to burn for two minutes. It could be seen from the video that after the propane torch was shut off, there was sustained flaming above the igniter. It was also seen from the video that neither the upper nor lower cases of the HVAC module were burning after 3 minutes post-ignition. However, the specific area of burning was out of the field of view of either camera. Components in this area included sections of the engine and transmission wiring harness and hoses to the HVAC heater core.

At 3 minutes after ignition, flames were visible under the dash upper extension panel to the left of the engine, approximately 2 inches to the left of the igniter.

Burning polymer melt was observed dripping onto the inboard section of the HVAC upper case, right exhaust manifold heat shield, and right valve cover starting between 1½ – 2 minutes after ignition. Just after 3 minutes from ignition, a section of the HVAC upper case near one of the heater hoses was burning. Burning pools of melted plastic were seen on the exhaust manifold heat shield. This burning pool self-extinguished approximately two minutes later, at 5 minutes post-ignition. Flames spread on the HVAC module downward on the upper case between 3 and 6 minutes post-ignition.

3.2.2.3 Flame Spread Laterally and Forward in the Engine Compartment

It was not possible to visually observe the entire lateral and forward flame spread with video cameras. Instead, temperature data were analyzed to track the propagation of flames in places out of the field of view of video cameras. It was assumed that where a temperature of 600°C was observed, that flames were present. Thermocouples were located on components in the upper section of the engine compartment and just under the HVAC air inlet screen. The temperature contours that were developed for this analysis could not be used to approximate the downward flame spread in the engine compartment or flame spread from the engine compartment to the passenger compartment.

The temperature analysis suggests that flames emerged from under the upper dash extension panel, above the area where the propane torch was located, between 3 and 4 minutes post-ignition. It can be seen from the video that flames reached the air inlet screen at the base of the windshield, in the area above the propane torch, at about 3½ minutes post-ignition. The timing of the flame spread to the right air inlet screen estimated from temperature data are consistent with the timing of flame spread to this area observed by video.

The temperature data further suggest that flames spread laterally at the rear of the engine compartment along the air inlet screen and forward from the area where the propane torch was located between 4 and 8 minutes post-ignition. Video showed that flames emerged from the forward edge of the left upper dash extension panel under the dislodged battery top between 8 and 8½ minutes post-ignition. Temperature data show temperatures greater than 600°C in this area at 10 minutes post-ignition, suggesting that flames spread to the left air inlet screen above the dislodged battery top between 9 and 10 minutes.

Flames spread laterally and forward on both sides of the engine compartment between 10 and 16 minutes post-ignition. When the test was ended at about 16 minutes post-ignition, flames had spread laterally to the right upper side panel and forward on the right side of the engine compartment to the upper radiator support cross-member. Flames had spread laterally to the left upper side panel in the rear of the engine compartment and forward to the engine air cleaner housing in the right side of the engine compartment.

The inner edge of the right front fender, which was broken during the crash test, ignited between 6 and 8 minutes post-ignition. The right front wheel well liner ignited between 10 and 11 minutes post-ignition. Burning pieces of the right front fender fell off the vehicle and onto the floor beginning at 13½ minutes post-ignition. Overall, the pattern of flame spread derived by temperature data analysis was consistent with what was actually observed on video.

3.2.2.4 Flame Spread to Fluids Under the Test Vehicle

Pieces of burning material started to fall into the mixture of oil, brake fluid, and engine coolant that was pooled under the engine compartment of the test vehicle at about 8½ minutes post-ignition. The state of this material (melted or solid plastic) could not be determined from the test data or by observation. Some of this burning material self-extinguished shortly after falling into the fluid pool and other pieces continued to burn until the test was ended and the fire extinguished. It could not be determined whether the fluid mixture ignited in the area around the pieces of plastic that continued to burn. At the time the test was ended, flames had not spread across the surface of the pooled fluids away from the burning material that fell from the vehicle.

3.2.2.5 Flame Spread into the Passenger Compartment Through the Windshield

Flame spread through the windshield was characterized by analyzing the video records from some of the exterior and interior cameras, the recorded temperatures, and the infrared imaging data.

Flames began to contact the windshield between 3 and 4 minutes post-ignition, when flames emerged from the engine compartment along the rear edge of the deformed hood. The height and width of the fire plume along the rear edge of the deformed hood increased between 4 and 10 minutes post-ignition. The windshield inner layer started to soften and stretch along the cracks in the glass outer layer between 8 and 9 minutes. The lower portion of the windshield fell onto the instrument panel at approximately 11:10 post-ignition. The windshield that fell onto the instrument panel was not burning at this time.

Pieces of the broken windshield continued to fall into the passenger compartment until the test was concluded at approximately 16 minutes post-ignition. The instrument panel, the deployed passenger's airbag, and the front passenger's seat cushion were charred where pieces of the windshield had fallen. Fragments of the windshield were embedded in the residue from the dash sound barrier and instrument panel upper trim panel on the right side of the windshield support panel. It was not possible to determine the times of ignition of the instrument panel upper trim or the windshield inner layer.

However, estimated temperature profiles on the instrument panel upper trim indicate that flames spread rearward on the top of the right side of the instrument panel between 12 and 13 minutes post-ignition.

3.2.2.6 Flame Spread into the Passenger Compartment Through the Dash Panel

The recorded temperatures as well as the pattern of fire damage in the instrument panel and on the dash panel, as observed during post-test inspection, were used to characterize flame spread through the dash panel.

There was no evidence of heat or fire damage around the brake linkage pass-through, the steering column pass-through, the two tears in the dash panel, or the seam opening at the lower right corner of the dash panel.

Estimated temperature profiles in the HVAC module and the defroster nozzle and air distributor assembly indicate that flames spread rearward into the instrument panel through the HVAC module. These temperature profiles indicate that flames spread into the auxiliary A/C evaporator and blower upper case and heater front case between 10 and 11 minutes post-ignition. Flames started to spread laterally to the right into the air inlet housing between 12 and 13 minutes post-ignition and to the left into the air distributor case between 14 and 15 minutes post-ignition. Flames spread rearward into the right side of the defroster nozzle and air distributor assembly case

between 14 and 15 minutes post-ignition. The video documentation is consistent with the observations made from the temperature data.

The video shows flames below the right side of the instrument panel at 13 minutes post-ignition. Melted and charred plastic was observed below the right side of the instrument panel after this test. The carpet in this area started to burn before the test was ended. These observations suggest that downward flame spread in this area involved burning material falling from the HVAC module, the defroster nozzle and air distributor assembly, and the instrument panel compartment box onto the carpet below the right side of the instrument panel.

The development of a pressure gradient across the dash panel did not appear to play a significant role in the flame spread from the engine compartment to the passenger compartment. Data recorded from pressure taps in the test vehicle indicate that the pressure on both sides of the dash panel started to decrease relative to atmospheric pressure between 8 and 9 minutes post-ignition. The measured pressures at the exterior and interior surfaces of the dash panel were approximately equal until 11½ minutes post-ignition. The pressure at the interior surface was greater than the pressure at the exterior surface of the dash between 11½ and 12½ minutes post-ignition.

3.2.2.7 Heat and Fire Damage to the Headlining Panel and Front Seats

The pattern of heat and fire damage to the headlining panel, estimated temperature profiles along the lower surface of the headlining panel, and data recorded from thermocouples positioned below the headlining panel and downward toward the front seat cushions indicated that a burning upper layer did not develop in the passenger compartment during this test.

Estimated temperature profiles along the lower surface of the headlining panel indicate that exposure to heat and flames occurred between 15 and 16 minutes post-ignition. Temperatures along the headlining panel were less than 50°C until the first section of windshield fell inward onto the instrument panel at approximately 11 minutes post-ignition.

As flames spread rearward on the right side of the top of the instrument panel, the fire plume from the top of the instrument panel rose upward through opening in the windshield. Temperatures along the forward edge of the headlining panel increased to between 150 and 200ºC by 15 minutes post-ignition. Development of higher temperatures along the headlining panel between 15 and 16 minutes post-ignition correlate with the timing of flame-spread through the top of the instrument panel above the center console.

3.2.2.8 End of Test – Extinguishment

A fine water mist was used to extinguish the fire in the test vehicle at approximately 16 minutes post-ignition. This type of extinguishment was preferred since the water mist would cool the molten plastic rapidly, preserving the geometric shape of the plastic at that instant, while avoiding the damage that can be caused by a high-pressure water stream. After the signal was given to end the test, the water mist was first directed into the passenger compartment through the right side window to extinguish the flames in the interior of the vehicle. The water mist was then directed toward the engine compartment to extinguish flames outside of the passenger compartment. Table 2 lists the test events for the Camaro.

Table 2. Summary of Test Events for the Camaro.

Time (min:sec)	Event
0:00	Ignition of propane torch.
2:00	Propane torch turned off .
2:15	Flames visible on the right air inlet screen.
4:00 – 6:00	Flames spread laterally in the engine compartment.
8:00 – 9:00	A measurable pressure difference develops across dash panel.
11:10	Sections of the windshield fall onto the instrument panel, upper trim panel.
14:00	Deployed passenger airbag ignites and burns.
14:55	Flames emerge through the defroster outlet in instrument panel upper trim panel.
15:50	Test ended.

3.2.3   Summary of Full-Scale Fire Tests of Camaro with Flame Retardant (FR) Treated HVAC Module

Two 1999 Chevrolet Camaro vehicles were tested in this study. One vehicle (control vehicle) was tested as received after the crash test and the other vehicle (FR vehicle) was tested with a flame retardant treated HVAC module.

The control vehicle was crash-tested on October 27, 1999, and the FR vehicle was crash-tested on October 13, 1999. In each crash test, the vehicle was towed into a fixed steel pole. There was no discussion of fire being observed during these crash tests in this report.

An artificial means of starting a fire in the engine compartment was employed, and the results of the fire tests are discussed below. The control vehicle fire test was conducted on February 17, 2000. The FR vehicle fire test was conducted on February 21, 2000.

3.2.3.1 HVAC Modules

The HVAC module in the control vehicle was assembled from service part components purchased from a Chevrolet dealership. None of the materials in the control HVAC module contained active flame retardants. Polypropylene and polyester parts of the HVAC module in the FR vehicle were treated with flame retardants. Table 3 provides the base polymers of components in the FR HVAC module that contained flame retardants. Table 4 lists the chemical additives in the polypropylene and polyester components for the control and FR vehicle HVAC modules.

Table 3. Base Polymer in HVAC Components.

Component	Base Polymer
Air Inlet and Outlet Housing	Polypropylene
Auxiliary A/C Evaporator and Blower Upper Case	Polypropylene
Auxiliary A/C Evaporator and Blower Lower Case	Polyester
Heater Front Case	Polypropylene
Heater Rear Case	Polypropylene
Heater Case	Polypropylene
Air Distribution Case	Polypropylene

Table 4. Additives in the Base Polymer Components in Control and FR HVAC Modules.

	Polypropylene *	Polyester
Control HVAC Module	$Ca(CO_3)$	Glass fiber Clay Cissel
FR HVAC Module	Decabromodiphenyleneoxide SbO_3 Zn-compounds	Glass fiber SbO_3 $Al_2O_3 \bullet (SiO_2)$

* The resin used to make the polypropylene parts in the FR vehicle HVAC module had a V-0 rating according to UL 94.

3.2.3.2 Ignition

The fire was started artificially using electrical igniters placed in the air cleaner housings in the engine compartment of the test vehicles. The igniters were made by winding Nichrome wire (24 AWG, length = 350 cm, resistance = 12 Ω) around four pieces of polypropylene sheet ($0.1 \times 10 \times 15$ m, mass = 110 g). Electrical power was supplied to the heating wire using a variable tap transformer connected to 120 VAC, which produced approximately 1.2 kW of heat. Table 5 shows the ignition timing for both tests.

Table 5. Ignition Timing.

	Time Post-Ignition (min:sec)	
	Control Vehicle	**FR Vehicle**
Electrical Power On	-1:39	-5:18 *
Ignition	0:00	0:00
Electrical Power Off	1:10	1:00

* The transformer malfunctioned and did not supply power to the heating wire for the first three minutes of the test.

3.2.3.3 Flame Spread in the Engine Compartment

The initial fuel for the fire was the polypropylene sheets from the igniter and the filter element in the air cleaner. Flames spread from the air cleaner housing rearward to the air inlet screen along the lower edge of the windshield, then laterally along the air inlet screen toward the right side of the engine compartment.

The crash-induced gap between the air cleaner housing cover and the air cleaner housing was larger in the FR vehicle than in the control vehicle, which allowed flames to emerge from the air cleaner 150 seconds sooner in the FR fire test as opposed to the control fire test. Table 6 provides a summary of flame spread in the control vehicle fire test, and Table 7 provides a summary of flame spread for the FR vehicle fire test.

Table 6. Summary of Flame Spread in Control Vehicle.

Time (min:sec)	Event
0:00	Ignition of igniter.
3:30	Flames from the igniter and air cleaner element begin to emerge from the rear of the air cleaner housing.
4:40	The air inlet screen had ignited, and flames had started to spread laterally along the hood lace seal on the air inlet screen.
5:40	Ignition of right edge of the HVAC air inlet screen, a section of wiring harness on top of the right front wheel house, and the inner edge of the right fender.
7:00 – 9:00	Combustible materials in the front of the left side of the engine compartment ignited.
7:50	Video camera moved away from test vehicle.
8:00	Pieces of the windshield had separated and fallen into the passenger compartment.
10:00 – 13:00	Both sides of the A/C evaporator core were heated by flames.
11:30	The auxiliary A/C evaporator and blower lower case were exposed to flames in the area above the right exhaust manifold.
12:30	Flames had spread rearward along the top of the instrument panel to the passenger airbag cover and deployed passenger air bag.
12:47	Flame spread into the passenger compartment through the windshield opening had progressed to the rear of the instrument panel upper trim panel and pieces of burning windshield started to fall inward.
13:00	End of Test – fire extinguished.

The patterns of burn damage observed in and around the engine compartments of the test vehicles were similar. In both cases, sections of glass fiber mat from the hood silencer pad had detached from the hood and were on top of the left side of the engine, the generator, the HVAC module, and the left wheelhouse panel. During both tests, the left and right outer fender panels ignited, burned, and fell to the ground.

Table 7. Summary of Flame Spread in FR Vehicle.

Time (min:sec)	Event
0:00	Ignition of igniter.
1:00	Flames from the igniter and air cleaner element begin to emerge from the rear of the air cleaner housing.
3:00	The air inlet screen had ignited and flames had started to spread laterally along the hood lace seal on the air inlet screen.
4:00	Ignition of right edge of the HVAC air inlet screen, a section of wiring harness on top of the right front wheel house, and the inner edge of the right fender.
4:30	Video camera moved away from test vehicle.
8:00	Pieces of the windshield had separated and fallen into the passenger compartment.
9:00 – 11:00	Combustible materials in the front of the left side of the engine compartment ignited.
11:30	The auxiliary A/C evaporator and blower lower case were exposed to flames in the area above the right exhaust manifold.
12:30	Flames had spread rearward along the top of the instrument panel to the passenger airbag cover and deployed passenger air bag.
12:50	Flame spread into the passenger compartment through the windshield opening had progressed to the rear of the instrument panel upper trim panel and pieces of burning windshield started to fall inward.
13:00	End of Test – fire extinguished.

3.2.3.4 Flame Spread into the Passenger Compartment Through the Windshield

Flame spread through the windshield was characterized by analyzing the video records from some of the exterior and interior cameras, the recorded temperatures, and the post-fire inspection.

As flames spread laterally to the right along the rear of the engine compartment, the exterior surfaces of the windshields in both test vehicles were exposed to heated gases and flames from the burning air inlet screens. Radiation from the flames heated the windshields and caused the windshield inner layers to soften and stretch and the lower portions of the windshield to sag onto the instrument panel top covers. The patterns of fire damage observed in the passenger compartments of the test vehicles after these tests are consistent with flame spread through the windshield.

3.2.3.5 Ignition of the Auxiliary A/C Evaporator and Blower Upper Case

Sections of the auxiliary A/C evaporator and blower upper case that were in the engine compartments of the test vehicles had ignited at some point before these tests were concluded. This was discovered upon post-test inspection of the vehicles. This was also evident by the photographic documentation. In both tests, the plastic had melted and sagged onto the A/C evaporator cores. Some material in both HVAC modules was consumed by fire, and the residue on top of the A/C evaporator core was burned and charred.

From the temperature data, both faces of the A/C evaporator core in the control vehicle HVAC module were exposed to flames. However, the A/C evaporator core in the FR vehicle was never exposed to temperatures that would suggest flames had been present.

The HVAC module in the control vehicle was more extensively fractured than the HVAC module in the FR vehicle. This difference was deemed to be a result of the variability of the crash test. Temperature distributions of the control HVAC module suggested that heated gases and flames from the engine compartment penetrated the section of the HVAC module exterior to the dash panel through the openings, which were created during the crash test. Post-test inspection of the HVAC modules from the test vehicles indicated that only the sections of the auxiliary A/C evaporator and blower upper cases that were above the A/C evaporator core had burned.

There was no evidence of fire damage to the auxiliary A/C evaporator and blower lower cases in either of the test vehicles, which indicated that the polyester resin in this component did not ignite and burn during these tests. The video record, the temperature data, and the post-test inspections indicate that flames did not spread through the HVAC modules into the instrument panels of either test vehicle.

3.2.3.6 Conditions in the Passenger Compartment

Air temperatures in the passenger compartments of the test vehicles were measured with aspirated thermocouples. One aspirated thermocouple assembly was installed between the front seats in each of the test vehicles and was oriented vertically. Air temperatures peaked at 160°C at 12:56 post-ignition for the control vehicle and at 114°C at 12:58 post-ignition for the FR vehicle. For both tests, the temperatures decreased as distance below the headlining increased. This indicates that a uniform upper smoke layer did not develop before extinguishment for either vehicle.

Heat flux transducer/radiometer assemblies were located above both front seats in the test vehicles. These instruments measured the convective and radiative heat fluxes to vertical, forward-

facing planes approximately 30 inches above the centers of the seat cushions. In both tests, an increase in radiative heat flux was evident at approximately 7 minutes post-ignition. This corresponds with the timing of sections of the windshield falling inward onto the dash panel. The peak radiative heat flux recorded during the control vehicle test was 15.9 kW/m^2 at 12:49 post-ignition. The peak radiative heat flux recorded during the FR vehicle test was 15.8 kW/m^2 at 12:51 post-ignition. The convective heat fluxes did not change significantly from background levels during these tests.

During these tests, combustion products such as smoke and carbon monoxide entered the passenger compartments of the test vehicles before flames spread to the instrument panel upper trim panel. The amount of smoke and the concentration of carbon monoxide in the passenger compartment of the FR vehicle were significantly greater than the amount of smoke and the concentration of carbon monoxide in the passenger compartment of the control vehicle.

In point of fact, at 7 minutes post-ignition in the control vehicle, a few diffuse streams of smoke were visible within the passenger compartment. At 7 minutes post-ignition in the FR vehicle passenger compartment, smoke almost completely obscured the headlining trim panel. The peak carbon monoxide concentration in the passenger compartment of the control vehicle was measured at 38 ppm, which occurred at 7:03. The peak carbon monoxide concentration in the passenger compartment of the FR vehicle was measured at 1024 ppm, which occurred at 6:35. In both tests, smoke and carbon monoxide cleared from the passenger compartment at approximately 7 minutes post-ignition. This corresponds to when the windshield first started to collapse.

3.2.4   Critical Fire Size

In the Caravan and Camaro tests, flame spread into the passenger compartment occurred before conditions became untenable due to temperature and toxicity. In both tests, the heat release recorded at this time was approximately 400 kW. The results reported for the control and FR vehicle tests were not as detailed, but a critical fire size of 400 kW appears to be reasonably consistent with a significant increase in the threat to occupants trapped in the passenger compartment.

3.3   Fire and Thermal Properties of Automotive Materials

Several fire and thermal properties of automotive components have been documented and published in various sources. Many of these properties and parameters have been measured or calculated as part of this project and will be discussed in subsequent sections. These data are useful as a point of reference and for comparison to determined values as part of the NHTSA project. Also,

some of these values have been correlated with small-scale fire properties, which will reinforce the developed levels of performance discussed in Section 5.3.

Tables 8 and 8a tabulate several of these quantities for the Dodge Caravan. These data are taken from an FM paper, "A Study of the Flammability of Plastics in Vehicle Components and Parts" [50]. Table 9 gives a similar set of data for Chevrolet Camaro automotive components. This information is taken from, "Thermal Properties of Automotive Polymers, IV - Parts of a Camaro" [35].

Table 8. 1996 Dodge Caravan Material Properties.

Part Description	δ(mm)	$\rho_v \times 10^{-3}$(kg/m^3)	c_v (kj/kg-K)	k_v x10^9(kW/m-K)	$k\rho c$	α_v (mm^2/s)	T_{ig} (°C)
Battery Cover	5	0.90	2.216	0.20	1.92	0.10	443
Resonator Structure	5	1.06	2.082	0.20	2.70	0.09	374
Resonator Intake Tube	6	1.15	1.745	0.22	2.70	0.11	374
Air Ducts	5	1.04	1.934	0.20	4.25	0.10	443
Brake Fluid Reservoir	20	0.90	2.247	0.20	ND	0.10	ND
Kick Panel Insulation	5	1.95	1.141	0.21	7.78	0.09	374
Headlight Assembly (Clear)	5	1.19	2.061	0.20	4.10	0.08	497
Headlight Assembly (Black)	5	1.19	2.061	0.20	4.10	0.08	497
Fender Sound Reduction Foam	16	0.13	1.624	0.16	74.42	0.76	497
Hood Liner Face	25	0.66	1.319	0.15	16.33	0.17	374
Windshield Wiper Structure	5	1.64	1.140	0.75	1.52	0.40	497

Table 8a. 1996 Dodge Caravan Material Properties.

Part Description	T_d (°C)	CHF (kW/m^2) Measured	CHF (kW/m^2) Calculated	TRP Measured	TRP Calculated	FPI	Y_s
Battery Cover	423	15	13	454	342	12	0.071
Resonator Structure	430	10	13	277	241	14	0.072
Resonator Intake Tube	430	10	13	277	241	ND*	0.100
Air Ducts	ND	15	15	333	230	11	0.080
Brake Fluid Reservoir	ND	ND	ND	ND	ND	ND	0.082
Kick Panel Insulation	255	10	7	215	142	18	0.070
Headlight Assembly	445	20	23	434	264	9	0.113
Fender Sound Reduction Foam	401	20	20	146	62	27	0.098
Hood Liner Face	325	10	6	174	98	23	0.022
Windshield Wiper Structure	414	20	20	483	434	8	0.100

* ND = Not Defined

Table 9. 1997 Chevrolet Camaro Material Properties.

Part Description	$\rho_v \times 10^{-3}(kg/m^3)$	T_m (°C)	T_g (°C)	T_d (°C)
Front Wheel Well Liner	0.88	123, 164	ND	282
Air Inlet	0.89	119, 156	24	352
Hood Insulator	0.08	Amorphous	36	336
Radiator Inlet/Outlet Tank	1.18	261	102	430
Engine Cooling Fan	1.44	219	40	430
Power Steering Fluid Reservoir	1.4	261	35	425
Blower Motor Housing	1.22	159	ND	295

3.4 Candidate Test Methods

Tables of the most relevant potential test methodologies have been compiled. Table 10 gives a summary of the most common small-open-flame test methods that are currently used for some regulatory purpose. These methods are referred to as "Small Flame Exposure" test methods. Table 11 gives a summary of the most common radiant heat exposure test methods that are currently used for some regulatory purpose. These methods are referred to as "Radiant Exposure" test methods. Table 12 gives a summary of the advantages and disadvantages to the various test methods outlined in Tables 10 and 11.

Based on the outlined advantages and disadvantages in Table 12, the updated literature review, and analysis of both the full-scale and small-scale test reports available, it is concluded that the test method described in ASTM E 1354, *Standard Test Method for Visible Heat and Smoke Release Rates for Materials and Products Using an Oxygen Consumption Calorimeter,* is overall the best candidate test methodology for quantifying the flammability of automotive component materials.

Reports from FM tests of the Caravan and Camaro vehicles show that measured heat fluxes on the wall dividing the engine and passenger compartment were typically between 25 and 50 kW/m². In previous testing of automotive interior materials, Cone Calorimeter testing was performed at heat fluxes of 20, 35, and 50 kW/m². Therefore, tests will be performed at the same level in order to allow for a comparison between the performance of the exterior materials and interior materials.

Table 10. Summary of "Small Flame Exposure" Test Methods.

	Area of Regulation	Summary of Method
FMVSS 302	U.S. DOT uses this method to regulate the flammability of materials used in the interiors of passenger vehicles.	Five specimens, measuring 4 × 14 in. × nominal thickness, in the horizontal position are exposed to a 1½-inch high Bunsen burner flame for 15 seconds. The rate of flame spread over measured length is observed, and the maximum permitted flame spread rate is 4 in./min.
FAR 25.853	This standard is used to test the materials and components in cabins and holds of transport aircraft in the U.S. It is also recommended in the Federal Register Vol. 47 No. 228, for testing of rail transit upholstery seating material.	Depending on what type of material is being tested, the orientation of the specimen can be vertical, horizontal, at 45°, or at 60°. In each case, three specimens are tested with a Bunsen or Tirrill burner at a specified height and exposed for a specified duration. For each procedure, there are classifications based on burn length, flame spread rate, after flame time, glow time, and flame time of drippings. For rail transit upholstery seating materials, testing is conducted to FAR 25.853 and the flame time cannot exceed 10 seconds and the burn length cannot exceed 6 inches.
ASTM C 1166	Appendix B of Part 238 to the Code of Federal Regulations (CFR) uses this standard test to regulate the flammability performance of elastomeric gaskets and accessories in rail transportation vehicles.	Six specimens, measuring 1 × 18 × ½-in. thick, are exposed to a 38-mm high Bunsen burner flame for 15 or 5 minutes for dense or cellular materials, respectively. The samples are tested in the vertical position, and the remaining unburned length of the specimen is measured. The average flame propagation for the six runs is reported.
UL 94	This test standard contains several test procedures in different orientations and with slightly different exposures. The UL listing of a given electrical appliance is generally contingent on the classifications of plastics tested in these procedures.	Depending on the type of classification required, materials are tested to UL 94HB, 94V-0, 94V-1, 94V-2, 94HBF, 94HF-1, 94HF-2, 94-5V, 94VTM-0, 94VTM-1, or 94VTM-2. The main difference between all of these different procedures is the orientation of the test specimen. Most of these procedures test two sets of five specimens each, nominally measuring between 5 and 6 in. long and ½ - 2 in. wide with a ½-in. maximum thickness. All of these procedures expose the specimen to a Bunsen or Tirrill burner flame with a height between ¾ and 5 in. long and a duration between 3 and 60 seconds, depending on the material tested. Each procedure classifies the material by several factors, including average burning rate, self-extinguishment, after flame time, burning droplets, glow or incandescence time, and/or burn-through.

Table 10 (Continued). Summary of "Small Flame Exposure" Test Methods.

	Area of Regulation	Summary of Method
ASTM D 2859	This test standard applies to floor coverings installed in buildings.	Eight specimens, each measuring 9×9 in., are exposed to the burning of a methenamine tablet, lit with a match. The material passes the test if the charred area is less than or equal to 1 in. from the inner edge of the 8-in. diameter steel plate lying on top of the floor covering sample.
ASTM D 635	Building codes use this test to classify the burning behavior of rigid plastics in the horizontal position.	Ten specimens, each $5 \times \frac{1}{2}$-in. $\times$ usual thickness, in the horizontal position, are exposed to a 1-in. long Bunsen burner flame for 30 seconds. The building codes classify a plastic as CC2 if its maximum burning rate is $\frac{1}{4}$ in./min for a thickness greater than 0.05 in.
ASTM D 568	Building codes use this test to classify the burning behavior of rigid plastics in the vertical position.	Ten specimens, each 1×18 in., in the vertical position, are exposed to a 1-in. long Bunsen burner flame until the specimen ignites or a maximum of 15 seconds. Test specimens less than 0.05 inch thick are required to be tested to this procedure, and a passing result is a specimen that is not completely consumed within 2 minutes.
ASTM D 2863	The U.S. Navy uses this test procedure to qualify (in part) composite materials and composite material systems for use in Naval submarines. The National Aeronautics and Space Administration (NASA) also uses this test procedure	15 to 30 specimens are tested for each material qualified in order to systematically bracket the minimum oxygen concentration necessary for combustion. Combustion is defined, for self-supporting polymers, when either the specimen has burned for 3 minutes or when flames have spread 2 in. below the top of the specimen. For the Navy specification, tests are conducted at 25, 75, and 300°C, and the minimum requirement for qualification is 35, 30, and 21%, respectively.
GM 269M	General Motors has proposed using this method to evaluate flammability of engine compartment sound absorbing materials.	A 12×4-in. sample with a thickness between 1/16 and 5/16 inch is placed in a frame and mounted at a 45° angle. The whole system is placed on a load cell in an enclosed test chamber. Two infrared heaters, placed parallel to each 4-in. wide side of the test sample are used to preheat both surfaces. After the desired surface temperature is reached, the sample is exposed to a 4-inch high Meeker burner flame for 15 seconds. If the sample ignites, it is allowed to burn for 5 minutes or until self-extinguishment. If it does not ignite or self-extinguishes within 10 seconds of removal of the burner, the ignition procedure is repeated 8 times. Mass loss of the sample is recorded as well as mass of dripping with a second load cell. Other qualitative data and observations are also derived. To date, there is no consensus for pass/fail criteria.

Table 11. Summary of "Radiant Exposure" Test Methods.

	Area of Regulation	Summary of Method
ASTM E 906	The Federal Aviation Administration (FAA) uses this standard (FAR 25-61) to qualify interior materials in aircraft.	Three specimens, each measuring 4×4 in. nominally, with a maximum thickness of 2 inches are exposed vertically to a radiant ignition source ($35 \ kW/m^2$) for 5 minutes. The heat release rate is measured by a series of temperature measurements, *i.e.*, a thermopile. According to FAA regulations, materials tested must not have a peak heat release rate of $\geq 65 \ kW/m^2$ nor a total heat release of $\geq 65 \ kW \cdot min/m^2$.
ASTM E 662 With or Without Toxicity Measurements	The FAA, the Federal Railroad Administration (FRA) and the U. S. Navy use this test method to regulate interior finish materials.	*FAA*: Three vertically oriented specimens are exposed to $25 \ kW/m^2$ in the presence of a series of 6 multi-flamelet burners. Two burners impinge directly on the sample, and the other four are positioned vertically in the gas stream. Depending on the type of material being tested, there are different requirements for passing the test. In general, the specific optical density of a tested material must be ≤ 100 in the first 90 seconds of the test and ≤ 200 in the first 4 minutes. All materials used in the pressurized area of the fuselage must be tested for toxicity. The products of combustion are sampled for concentrations of CO, HCl, HCN, HF, NO_x and SO_2. The FAA has concentration requirements for each compound at 90 seconds and 4 minutes. *FRA*: Three specimens are exposed to $25 \ kW/m^2$ with and without the presence of a series of 6 multi-flamelet burners. Two burners impinge directly on the sample, and the other four are positioned vertically in the gas stream. In general, the specific optical density of a tested material must be ≤ 100 in the first 90 seconds of the test and ≤ 200 in the first 4 minutes. *Navy*: Three specimens are exposed to $25 \ kW/m^2$ with and without the presence of a series of six multi-flamelet burners. Two burners impinge directly on the sample, and the other four are positioned vertically in the gas stream. The maximum optical density must be observed ≤ 200 seconds into testing.
ASTM E 1995	The International Maritime Organization (IMO) uses this test method to regulate interior finish materials.	*IMO*: Three horizontally oriented specimens are exposed to $25 \ kW/m^2$ with and without the presence of a single pilot flame and three specimens are exposed to $50 \ kW/m^2$ without the presence of a single pilot flame. In general, the specific optical density of a tested material must be ≤ 200. In addition, the products of combustion are sampled for concentrations of CO, HBr, HCl, HCN, HF, NO_x and SO_2. The IMO has maximum concentration requirements for each compound.

Table 11 (Continued). Summary of "Radiant Exposure" Test Methods.

	Area of Regulation	Summary of Method
ASTM E 648	The FRA uses this test method to qualify flooring materials on rail transit vehicles.	Three horizontally mounted specimens, each measuring 10×41 in. nominally, are exposed to a radiant ignition source ranging from 1 to 10 kW/m^2. A propane pilot is applied perpendicular to the long edge of the sample and ignition and/or flame spread is observed. After a series of tests, the critical heat flux for ignition can be determined. The FRA requires a critical radiant flux of ≥ 5 kW/m^2.
ASTM E 162	The FRA uses this test method to qualify most of the component materials installed on rail transit vehicles. The U.S. Navy also uses this standard to approve interior composite material systems for submarine applications.	Four specimens, each measuring 6×18 in. nominally, are mounted vertically at 30° to the radiant panel (operating temperature – 670°C). A gas pilot burner is placed at 15 to 20° to the specimen and is applied from a distance of approximately 1¼ inches to the upper edge. The test is run until flame has spread 15 inches down the specimen or a maximum of 15 minutes has elapsed. A flame spread index (I_s) is calculated from measured flame spread and a heat evolution term, which relates the difference between the time temperature curve of the tested sample to that of a standard reference material. *FRA*: Depending on the type of material, there are different requirements for I_s. For windows and light diffusers, $I_s \leq 100$. For thermal and acoustic insulation, $I_s \leq 25$. For most of the other interior materials in a transit vehicle, the maximum I_s allowed is 35. *Navy*: For interior materials installed in a naval submarine, the maximum allowable value for I_s is 20.
ASTM D 3675	This test method is a variant of the ASTM E 162. However, it targets the cushioning of seating materials specifically. The FRA uses this test to qualify the cushion of the seating material in transit vehicles.	The test procedure is functionally identical to the ASTM E 162, outlined above, with two exceptions: (1) the test specimens are retained in the holder with a sheet of 20-gauge hexagonal steel wire mesh placed against the surface of the test face, (2) the exposure time is equal to the time it takes to spread the full length of the specimen (18 inches) or 15 minutes, whichever comes first. According to FRA regulations, $I_s \leq 25$.

Table 11 (Continued). Summary of "Radiant Exposure" Test Methods.

	Area of Regulation	Summary of Method
ASTM E 1317	The IMO uses this test method to qualify interior finishes for use on bulkheads, ceilings, and decks. The test method and acceptance criteria are described in IMO Resolution A.653. IMO Resolution A.687(17) is nearly identical, but only applies to primary deck coverings, and, as such, requires steel as a substrate for the material tested. This same apparatus is used in ASTM E 1317.	Three specimens, each measuring $6 \times 31\frac{1}{2}$ in., are mounted vertically in a frame and subjected to a radiant ignition source, which is positioned at a 15° angle to the specimen. Specimens of normal thickness < 2 inches are tested at their full thickness adhered to a representative substrate. Specimens of normal thickness > 2 inches are tested with extra material cut away, such that the thickness of the sample tested is 2 inches. An acetylene-air pilot flame is positioned adjacent to the sample, and the length is adjusted to approximately 9 in. The time to ignition is observed, and flame spread is recorded manually by the operator in 2-inch increments. The duration of the test is 10 minutes if the sample ignites, or until all flaming has ceased, or if flame spreads across the entire length of the specimen. Four key parameters are measured or derived from this testing: the critical flux at extinguishment, the heat for sustained burning, the total heat release, and the peak heat release rate. The IMO has different acceptance criteria for each of these parameters depending on if the tested material is a floor covering or if it is a wall, ceiling, or bulkhead covering.
ASTM E 2058	Not currently used in any regulatory manner. However, FM has proposed using this apparatus as a way to quantify the relative material flammability of automotive components. This work is published and available on the NHTSA public docket #3588.	This test method has three separate procedures involving material flammability: an ignition procedure, a combustion test procedure, and a fire propagation procedure. For each procedure, at least 3 specimens, each measuring 4×4 in., are exposed to an external heat flux of 0 to 65 kW/m^2 at an oxygen concentration of 21 to 40% by volume. The ignition procedure determines the time required from the application of an externally applied heat flux to a horizontal specimen until ignition of that specimen. Ignition is considered to have occurred when at least 4 seconds of sustained flaming is observed on or over most of the specimen surface. The combustion procedure is conducted to measure the chemical and convective heat release rates, the mass loss rate, and the effective heat of combustion of a horizontal specimen at a given externally applied heat flux and oxygen concentration (maximum of 40% by volume). The fire propagation test procedure is performed to determine the chemical heat release rate of a vertical specimen during upward fire propagation and burning.

Table 11 (Continued). Summary of "Radiant Exposure" Test Methods.

	Area of Regulation	Summary of Method
ASTM E 1354	The IMO and the U.S. Navy use this test method or its International Organization for Standardization (ISO) equivalent (ISO 5660) to qualify material flammability of component and/or composite materials. Appendix B to Part 238 of CFR Title 49 requires testing of materials with small surface areas at 50 kW/m^2 and to have $t_{ig}/q_{max} \geq 1.5$. In addition, NIST used the Cone Calorimeter apparatus to test various automotive vehicle components from the interior, engine compartment, and fuel tank areas. This testing was performed as part of the GM-DOT settlement agreement. Similar testing was performed at SwRI for a number of interior automotive parts from a Chevrolet Cavalier. This work was also performed as part of the GM-DOT settlement agreement. An independent study of material flammability of automotive components was published by Dr. Marcelo Hirschler of GBH International, Inc. The main conclusion of this paper was that the flammability (ignitability and heat release rates) of plastics in automobiles is higher than that of generic plastics used in buildings.	This test method exposes a 4 × 4 in. specimen (horizontal or vertical) to a radiant heat flux ranging from 0 to 100 kW/m^2. Typically, three specimens are tested for repeatability, and the average is reported. This method yields several properties and/or parameters that are relevant to the tested material's flammability. These include time to ignition, heat release rate (oxygen consumption calorimetry), total heat released, smoke production rate, total smoke released, mass loss rate (burning rate), effective heat of combustion, critical heat flux for ignition, thermal response parameter, and heat of gasification. *IMO*: In the standard for qualifying marine materials for high-speed craft as fire-restricting materials, the IMO requires testing of materials used for furniture or other components, according to ISO 5660, which utilizes the Cone Calorimeter apparatus. *Navy*: Uses this test method to qualify materials installed on naval submarines. Several criteria exist for a material's flammability to be accepted. A series of ignitability tests are performed and, at each specified heat flux (25, 50, 75, and 100 kW/m^2), the time to ignition (300, 150, 90, and 60 seconds) is given as a minimum requirement. In addition, maximum peak and average heat release rates are specified for a given heat flux. At 100 kW/m^2 irradiance, the peak heat release rate must not exceed 150 kW/m^2 and the average over 300 seconds must not exceed 120 kW/m^2. At 75 kW/m^2 irradiance, the peak heat release rate must not exceed 100 kW/m^2 and the average over 300 seconds must not exceed 100 kW/m^2. At 50 kW/m^2 irradiance, the peak heat release rate must not exceed 65 kW/m^2, and the average over 300 seconds must not exceed 50 kW/m^2. At 25 kW/m^2 irradiance, the peak heat release rate must not exceed 50 kW/m^2, and the average over 300 seconds must not exceed 50 kW/m^2. The Navy also uses the Cone Calorimeter apparatus to measure the concentrations of several products of combustion continuously during a test at 25 kW/m^2 irradiance. The maximum concentrations allowed of CO, CO_2, HCN, and HCl are 200 ppm, 4% by volume, 30 ppm, and 100 ppm, respectively.

Table 12. Summary of Advantages and Disadvantages of Test Methods.

	Advantages	Disadvantages
All "Small Flame Exposure" Tests*	Inexpensive screening tool that could be used as a method to separate the average material from the subpar material in terms of flammability.	Does not reflect a "real" fire scenario. The heat exposure is too limited and can yield false positives for various materials.
ASTM E 906	Yields a material's heat release rate from a radiant heat exposure. This method is more representative of a real fire scenario.	This method measures heat release rate by way of a thermopile. This method of measurement is obsolete. It would be more relevant if oxygen consumption calorimetry were used.
ASTM E 662	Provides a standard way to measure the optical density of the smoke produced by a burning material. Can be used effectively as a ranking tool.	Data collected in this test are only relevant to this particular test method; they cannot be extrapolated to the material outside the geometry of the test method. In addition, the static state of the test method may influence the burning rate of the material, *i.e.*, the buildup of smoke in the test chamber may affect the rate at which a material burns.
ASTM E 648	Provides a standard way to measure the flame spread of a burning floor covering. Can be used effectively as a ranking tool.	The data collected in this test are only relevant to this particular test method and its geometry. It does not address how a floor covering might burn and spread flame in full scale when it occurs in the same direction as surrounding air flow.
ASTM E 162	Provides a standard way to measure the flame spread of a burning wall or ceiling covering. Can be used effectively as a ranking tool.	The data collected in this test are only relevant to this particular test method and its geometry. It does not address how a wall or ceiling covering might burn and spread flame in full-scale.

* Although GM269M includes radiant heat exposure, the advantages and disadvantages of "small flame exposure" tests largely apply to this test also.

Table 12 (Continued). Summary of Advantages and Disadvantages of Test Methods.

	Advantages	Disadvantages
ASTM D 3675	Provides a standard way to measure the flame spread of a burning seat cushion (flexible cellular material). Can be used effectively as a ranking tool.	The data collected in this test are only relevant to this particular test method and its geometry. It does not address how a seat cushion might burn and spread flame in full-scale.
ASTM E 1317	Provides a standard way to measure the flame spread of a burning wall or ceiling covering. Can be used effectively as a ranking tool.	The data collected in this test are only relevant to this particular test method and its geometry. This method measures heat release rate by way of a thermopile. This method of measurement is obsolete.
ASTM E 2058	Can be operated at a wide range of heat fluxes and oxygen concentrations, which can be varied to simulate various relevant fire scenarios. This test method yields relevant engineering data such as heat release rate, mass loss rate, effective heat of combustion, *etc*., which can be used as input to fire models as part of a fire risk and hazard assessment.	Due to the use of high-temperature heating lamps, the specimens are required to be blackened, which can influence test results. The gas pilot flame used is not always the best method for igniting pyrolyzates. This test apparatus can require significant maintenance in the way of calibration of instrumentation and various troubleshooting that is inherent with sophisticated apparatuses.
ASTM E 1354	Can be operated at a wide range of heat fluxes, which can be varied to simulate various relevant fire scenarios. This test method yields relevant engineering data such as heat release rate, mass loss rate, effective heat of combustion, *etc*., which can be used as input to fire models as part of a fire risk and hazard assessment.	The flow field over the sample surface complicates the analysis of ignition data. This test apparatus can require significant maintenance in the way of calibration of instrumentation and various troubleshooting that is inherent with sophisticated apparatuses.

4.0 AUTOMOTIVE COMPONENT FIRE TESTS

4.1 Selection and Procurement of Materials

Originally, the test matrix was to be set up so that parts from 3–4 different vehicles could be tested. The vehicle models would be chosen based on full-scale fire tests conducted at FM, and the test reports would be referenced for comparison purposes. However, full-scale tests on only two of the four vehicles have been reported, so instead, materials were chosen from these two vehicle models. Ten parts were selected from the 1996 Dodge Caravan and eight components were selected from the 1997 Chevrolet Camaro.

Some parts had different components that were tested separately. For example, the composition of the headlight assembly consisted of a clear plastic piece and a black plastic piece. Whenever the automotive component was non-homogeneous, both components and/or sides were tested in the Cone Calorimeter. Table 13 provides an overview of the different parts that were obtained for testing and includes part numbers for each. A description and photographs of the parts can be found in Appendix A.

Table 13. List of Test Components and Part Numbers.

Vehicle	Part ID	Part Number
1996 Dodge Caravan	Battery Cover	5235267AB
	Resonator Structure	4861057
	Resonator Intake Tube	53030508
	Air Ducts	4678345
	Break Fluid Reservoir	4683264
	Kick Panel Insulation	4860446
	Headlight Assembly	4857041A
	Fender Sound Reduction Foam	4716345B
	Hood Liner Face	4716832B
	Windshield Wiper Structure	4716051
1997 Chevrolet Camaro	Front Wheel Well Liner	10296526
	Air Inlet	10297291
	Hood Insulator	10278015
	Radiator Inlet/Outlet Tank	52465337
	Engine Cooling Fan	22098787
	Power Steering Fluid Reservoir	26019594
	Windshield with Laminate	10310333
	Blower Motor Housing	52458965

4.2   Material Characterization

The analytical objective of this element of the study was to correlate the microscopic properties of the selected component materials, as determined by thermal analysis, with the measured flammability behavior of the selected materials as determined by laboratory- and component-scale comparative methods, *i.e.*, Cone Calorimeter and ICAL tests as described in subsequent sections. Of particular interest was the correlative relationship between the microscopic thermal behavior of the selected polymeric materials and the time to ignition that transpired under radiant heat flux for macroscopic quantities of the same material. In this context, the latent heats of endothermic phase transitions and exothermic heats of reaction of the material measured microscopically provided a bridge to the pre-ignition behavior of material flammability tests.

Differential scanning calorimetry (DSC) is a technique in which the difference in energy input into a material and a reference material is measured as a function of temperature. In this study, a modulated differential scanning calorimetry (MDSC) procedure was used for the analysis. In the MDSC technique, the specimen is exposed to a steady rising temperature modulated by small-amplitude, sinusoidal temperature oscillations. In addition to providing a determination of the total heat flow into or from the specimen, such as in conventional DSC, the MDSC technique allows for the mathematical separation of the total heat flow into reversing and non-reversing components (as determined from the complex Fourier components of the sinusoidal thermal perturbations). Reversible heat flow is associated with reversible thermal phenomena that occur within a specimen regardless of its thermal history, such as the first- or second-order transitions and heat capacity of the material. Non-reversible heat flow is associated with thermal phenomena in which the state of matter is kinetically controlled and present in a quasi-stable state, as opposed to the thermodynamically most favorable state.

In the present study, the separation between reversible and non-reversible heat flow was used predominantly to resolve the actual temperatures at which complex phase transitions (first- and second-order) occurred within the polymeric components. However, the total heat-flow thermograms were used to determine the endothermic enthalpies for first-order phase transitions, *i.e.*, melt transition for the crystalline fraction of the polymeric component, as well as any exothermic enthalpies of reaction. This was done to account for the total endothermic heat-flow history, such as latent heats of fusion, or exothermic heat-flow history, such as reactive exotherms, that occur in polymeric components of this kind under conditions of radiant heat flux prior to the time of ignition of the material. In this way, the microscopic scalability of Cone Calorimeter measurements could be

assessed. This microscopic scalability will be discussed in the context of what will be termed the "downward scalability" of Cone Calorimeter measurements in the analysis section of this report.

Specimens for MDSC analysis (5 to 15 mg in mass) were heated from room temperature to 300°C at a constant rate of 3°C/min with a superimposed thermal modulation of approximately 1 °C/min. For each component material, duplicate specimens were excised from the component and analyzed under a nitrogen gas environment at a flow rate of 30 mL/min. Between each analysis, the sample compartment of the MDSC instrument was allowed to cool to room temperature while purging with copious amounts of nitrogen for not less than five minutes. Thermograms of the total, reversible, and non-reversible heat flows were recorded as a function of the ramp temperature, the originals of which are attached in Appendix B.

The results of MDSC measurements are summarized in Tables 14 and 15, which show for each vehicle group and component material tested the temperature at which endothermic and, if applicable, exothermic phenomena occur, along with the corresponding enthalpy for each thermal event. As indicated in these tables, no attempt was made to elucidate second-order phase transitions - either the amorphous fraction of the polymeric material or a substantially amorphous polymer component - that occurred below room temperature. Only in one case was there a substantially amorphous polymer with a glass transition above room temperature represented in the vehicle component selection. This component was the headlight structure from the Dodge Caravan, whose base polymer consisted of polycarbonate. With that exception all remaining materials subjected to MDSC analysis exhibited crystalline polymer morphologies with well-defined first-order melt transitions.

Table 14. MDSC Thermal Measurements of Component Materials from the Dodge Caravan.

Dodge Caravan Part No.	Description	Base Polymer Composition	Endothermic Melt Transition 1 (°C)	Endothermic Heat of Fusion 1 (J/g)	Endothermic Melt Transition 2 (°C)	Endothermic Heat of Fusion 2	Exotherm (°C)	Exothermic Heat of Reaction (J/g)
45235267AB	Battery Cover	Polyethylene	128.25	235.3	NA	NA	NA	NA
4683264	Brake Fluid Reservoir	Polypropylene	167.89	137.5	NA	NA	NA	NA
4716051	Wiper Structure	SMC/Polyester	77.25	60.98	NA	NA	50.19	11.95
5303058	Resonator Intake Tube	Polypropylene/EPDM	161.21	60.61	NA	NA	68.29	2.738
4861057	Resonator Structure	Polypropylene	166.64	88.27	NA	NA	NA	NA
4857041A	Headlight Structure, Black	Polycarbonate	143.37	NA	NA	NA	NA	NA
4857041A	Headlight Structure, Clear	Polycarbonate	143.26	NA	NA	NA	NA	NA
Second-order (amorphous) glass transition, T_g								

Table 15. MDSC Thermal Measurements of Component Materials from the Chevrolet Camaro.

Chevrolet Camaro Part No.	Description	Base Polymer Composition	Endothermic Melt Transition 1 (°C)	Endothermic Heat of Fusion 1 (J/g)	Endothermic Melt Transition 2 (°C)	Endothermic Heat of Fusion 2	Exotherm (°C)	Exothermic Heat of Reaction (J/g)
22098787	Radiator Cooling Fan	Nylon 6	59.79	1.283	221.37	54.08	NA	NA
260194594	Power Steering Reservoir	Nylon 6/6	265.3	55.94	NA	NA	NA	NA
52465337	Radiator Inlet/Outlet Tank	Nylon 6/6	264.82	59.19	NA	NA	NA	NA
10297291	Air Inlet	Polyethylene/Polypropylene	113.16	10.58	168.39	64.84	234.34	6.559
10296526	Front Wheel Well Liner	Polypropylene	168.46	88.39	NA	NA	240.29	7
52458965	Blower Motor Housing	Polypropylene	166.74	101	NA	NA	249.09	NA

4.3   Small-Scale Fire Tests

4.3.1   Introduction

An extensive series of small-scale tests was conducted on samples prepared from the parts that were obtained as described in Section 4.1. Two test procedures were used for the NHTSA project: FMVSS 302 and ASTM E 1354 (Cone Calorimeter). Additional smoke and toxicity tests were performed for the MVFRI project according to Airbus and IMO test procedures. The FMVSS testing was performed for two major reasons. First, to see if the components in the engine compartment would pass the test even though it is not required (only required for passenger compartment materials). Second, to link the regulatory test results to Cone Calorimeter results, if possible, in the data analysis.   Cone Calorimeter tests were performed to obtain engineering data for hazard assessment of these materials. Smoke and toxicity tests were performed on the materials to gather data on the toxic effects of these materials.

4.3.2   FMVSS 302 Tests

4.3.2.1   Test Procedure

All tests were conducted in general accordance with FMVSS 302. The test is performed by inserting a horizontal 4 × 14-in. sample into a metal test cabinet and exposing the open edge of the specimen to a Bunsen burner flame. The specimen is exposed to the flame for 15 seconds and then the time for the flame to travel a distance of 10 inches is recorded. A passing material must have a flame spread less than 4 in./min or 102 mm/min.

4.3.2.2   Test Matrix

A detailed test matrix for the FMVSS 302 testing is provided in Table 16. The materials tested are not required to pass the standard because they are all exterior materials. The tests were performed for these materials in order to provide a baseline performance measure for all materials, and a reference point for exterior materials to the current requirements for automotive component flammability. Typically, two tests were performed on each material, and if ample material was available, a third test was run.

Table 16. FMVSS 302 Test Matrix.

	1996 Dodge Caravan	1997 Chevrolet Camaro
Battery Cover	X	
Resonator Structure	X	
Resonator Intake Tube	X	
Air Ducts	X	
Break Fluid Reservoir	X	
Kick Panel Insulation	X	
Headlight Assembly (Black)	X	
Fender Sound Reduction Foam	X	
Hood Liner Face	X	
Windshield Wiper Structure	X	
Front Wheel Well Liner		X
Air Inlet		X
Hood Insulator		X
Radiator Inlet/Outlet Tank		X
Engine Cooling Fan		X
Power Steering Fluid Reservoir		X
Windshield with Laminate		X
Blower Motor Housing		X

4.3.2.3   Specimen Preparation

The test specimens were prepared as specified in FMVSS 302. For many of the materials, it was not possible to obtain a continuous 4 × 14-in. long specimen. For these materials, the test specimen was constructed by placing together flat pieces of material such that ridges and joinings were minimized on the sample surface. Test specimens were held in place by the retainer frame.

4.3.2.4   FMVSS 302 Test Results

FMVSS 302 test results for the two vehicles tested under this program are presented in Table 17. These tables include test observations along with whether or not the material passed the test. A material meets the test requirements if its burn rate does not exceed 102 mm/min. Although engine components are not required to pass the FMVSS 302 test, it is not surprising that each component tested did, in fact, pass the test.   It is logical to expect engine compartment materials to be more resistant to heat than passenger compartment materials due to the environmental differences of the two occupancies. The next step is to try and correlate the average burning rates to engineering flammability data obtained in the Cone Calorimeter.

Table 17. FMVSS 302 Test Results for the Dodge Caravan and Chevrolet Camaro.

Model	Material	Observations/Comments			Average Burn Rate (mm/min)	Pass/Fail
		Run 1	Run 2	Run 3		
1996 Dodge Caravan	Battery Cover	Flaming droplets at 36 sec	Flaming droplets at 23 sec	Flaming droplets at 24 sec	68.48	Pass
	Resonator Structure	Melting at 114 sec, Dripping at 120 sec, Burning Floor at 152 sec	Dripping at 108 sec, Burning on Floor at 120 sec	---	50.72	Pass
	Resonator Intake Tube	Flaming droplets at 26 sec	---	---	55.84	Pass
	Air Ducts	Flaming droplets at 46 sec	Flaming droplets at 36 sec	---	36.46	Pass
	Brake Fluid Reservoir	Dripping at 64 sec, Burning on Floor at 244 sec	---	---	19.61	Pass
	Kick Panel Insulation	Could not sustain burning	Ignited and self-extinguished before the first mark	Ignited and self-extinguished before the first mark	0.00	Pass
	Headlight Assembly (Black)	Ignited and self-extinguished before the first mark	Ignited and self-extinguished before the first mark	Ignited and self-extinguished before the first mark	0.00	Pass
	Fender Sound Reduction Foam	Flaming droplets at 6 min, 53 sec	Flaming droplets at 6 min, 8 sec	---	36.23	Pass
	Hood Liner Face	Ignited and went out after removal of pilot flame	Ignited and went out after removal of pilot flame	Ignited and went out after removal of pilot flame	0.00	Pass
	Windshield Wiper Structure	Ignited and went out after removal of pilot flame	Ignited and went out after removal of pilot flame	Ignited and went out after removal of pilot flame	0.00	Pass
1997 Chevrolet Camaro	Front Wheel Well Liner	Dripping at 45 sec, Flaming droplets at 52 sec, Burning on floor at 186 sec	Dripping at 39 sec, Flaming droplets at 50 sec, Burning on floor at 162 sec	---	37.09	Pass
	Air Inlet	Ignited and went out after removal of pilot flame	Flaming droplets at 105 sec, Burning on floor from 105 sec until end of test	Flaming droplets at 105 sec, Burning on floor from 105 sec until end of test	14.80	Pass
	Hood Insulator	Ignited and went out after removal of pilot flame	Ignited and went out after removal of pilot flame	Ignited and went out after removal of pilot flame	0.00	Pass
	Radiator Inlet/Outlet Tank	Ignition, but no dripping, no flaming on floor	Ignited and self-extinguished before the first mark	---	2.25	Pass
	Engine Cooling Fan	Ignited and self-extinguished before the first mark	Ignited and self-extinguished before the first mark	---	0.00	Pass
	Power Steering Fluid Reservoir	Ignited and went out after removal of pilot flame	Ignited and went out after removal of pilot flame	Ignited and went out after removal of pilot flame	0.00	Pass
	Windshield with Laminate	Ignited and self-extinguished before the first mark	Ignited and self-extinguished before the first mark	Ignited and self-extinguished before the first mark	0.00	Pass
	Blower Motor Housing	Flaming droplets at 37 sec	Flaming droplets at 41 sec	---	31.83	Pass

4.3.3 ASTM E 1354 Cone Calorimeter Tests

4.3.3.1 Test Procedure

All tests were conducted in general accordance with ASTM E 1354-02a, in the horizontal orientation, with the edge frame and spark igniter. Two types of tests were performed: full Cone Calorimeter tests and ignition tests. The full tests were terminated after flameout and data were recorded as specified in ASTM E 1354. The ignition tests were terminated two minutes after sustained flaming was observed.

Full Cone Calorimeter tests were generally conducted in duplicate at three heat flux levels: 20, 35, and 50 kW/m^2. The justification for the choice of heat flux levels is discussed in Sections 3.1 and 3.4. If the two results had a large discrepancy, a third test was performed.

Up to four additional ignition tests were performed at heat flux levels below 20 kW/m^2. The objective was to bracket the critical heat flux, which is the maximum heat flux at which ignition does not occur for very long exposures, to within ± 1 kW/m^2. If sustained flaming did not occur within 10 minutes, "No Ignition" was recorded and the heat flux was increased until flaming did occur. For some materials, the critical heat flux was greater than 20 kW/m^2.

4.3.3.2 Test Matrix

The parts and components of the 1996 Dodge Caravan tested in the Cone Calorimeter are listed in Table 18. The number of replicate tests at each level and the number of ignition tests are also given in this table. The same information for the 1997 Chevrolet Camaro is presented in Table 19.

4.3.3.3 Specimen Preparation

Test Specimens were generally prepared according to the procedure in ASTM E 1354 for products that are at least 6 mm (1/4 in.) in thickness, *i.e.*, without a substrate. In most cases, parts were large enough so that complete 100 × 100-mm specimens could be cut. In some cases specimens had to be pieced together as shown in Figure 2.

Table 18. Cone Calorimeter Test Matrix for Parts of the 1996 Dodge Caravan.

	Full Cone Calorimeter Tests			Ignition Tests	Appendix C Pages
	20 kW/m^2	35 kW/m^2	50 kW/m^2		
Battery Cover	3	2	2	4	1-6
Resonator Structure	2	2	2	4	7-12
Resonator Intake Tube	2	2	2	4	13-18
Air Ducts	2	2	2	4	19-24
Brake Fluid Reservoir	2	3	2	4	25-30
Kick Panel Insulation	2	2	2	4	31-36
Headlight Assembly (Black)	1	2	2	3	37-42
Headlight Assembly (Clear)	2	2	2	3	43-48
Fender Sound Reduction Foam	2	2	2	3	49-54
Hood Liner Face	3	2	2	3	55-60
Windshield Wiper Structure	2	2	2	4	61-66

Table 19. Cone Calorimeter Test Matrix for Parts of the 1997 Chevrolet Camaro.

	Full Cone Calorimeter Tests			Ignition Tests	Appendix C Pages
	20 kW/m^2	35 kW/m^2	50 kW/m^2		
Front Wheel Well Liner	3	2	2	4	67-72
Air Inlet	3	2	2	3	73-78
Hood Insulator	3	3	3	6	79-84
Radiator Inlet/Outlet Tank	2	2	2	4	85-90
Engine Cooling Fan	2	2	2	4	91-96
Power Steering Fluid Reservoir	2	2	3	4	97-102
Windshield with Laminate	2	2	2	3	103-108
Blower Motor Housing	2	2	2	5	109-114
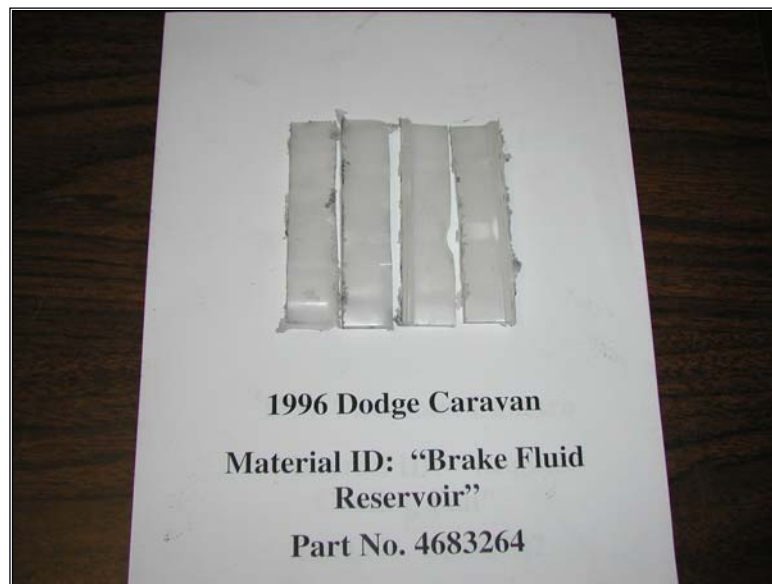
Figure 2. Cone Calorimeter "Pieced" Test Sample.

4.3.3.4   ASTM E 1354 Test Results

Complete results and graphs as required by the ASTM E 1354 and ISO 5660 Cone Calorimeter standards are compiled in Appendix C. The page numbers in Appendix C for the different tests are listed in Tables 18 and 19. Both standards require that tests be conducted in triplicate. In the interest of time and money, materials were conducted in duplicate if enough specimens were available. The heat release rate graphs in Appendix C indicate the repeatability was typically very good. A third test was conducted only if there was a major discrepancy between the two results. Ignition times for all tests are given in Tables 20 and 21.

4.3.3.5   Supplemental Toxic Gas Measurements

A ThermoNicolet Magna 560 Fourier Transform Infrared (FTIR) spectrometer was used to determine the concentration of several toxic compounds present in the smoke produced by each material tested in the Cone Calorimeter (see Section 4.3.3.2). This additional scope of work was performed under separate contract with funding provided by MVFRI (SwRI Project No. 01.06287). The concentration measurements were combined with gas flow rates measured by the Cone Calorimeter to provide a yield in terms of mass of material lost during the burning period.

4.3.3.5.1   Test Procedures

The method used to collect gas samples and determine the concentrations of the various gases is based on ASTM E 800 (2001), *Standard Guide for Measurement of Gases Present or Generated During Fires*, and the SAFIR report entitled "Smoke Gas Analysis by Fourier Transform Infrared Spectroscopy – The SAFIR Project." ASTM E 800 describes various analytical methods and sampling considerations for the measurement of carbon monoxide (CO), carbon dioxide (CO_2), hydrogen chloride (HCl), hydrogen cyanide (HCN), and oxides of nitrogen (NO_x), as well as other compounds not considered here. According to E 800, gaseous samples should be representative of the composition at the point of sample, and data provided by the analytical instrument should be accurate for the composition at the point of sample. The SAFIR report describes specific methods and procedures for gas sampling, spectral calibration, and data analysis. Nordtest Standard NT FIRE 047, *Combustible Products: Smoke Gas Concentrations, Continuous FTIR Analysis* provided additional guidance in the development of this method.

Table 20. Ignition Data for Parts of the 1996 Dodge Caravan (NI = No Ignition in 10 min).

Battery Cover Flux (kW/m²)	t_{ig} (s)	Resonator Structure Flux (kW/m²)	t_{ig} (s)	Resonator Intake Tube Flux (kW/m²)	t_{ig} (s)	Air Ducts Flux (kW/m²)	t_{ig} (s)
15	NI	**10**	NI	**10**	NI	**10**	NI
17	NI	**11**	NI	**11**	NI	**12**	NI
19	NI	12	546	12	299	13	186
20	290	15	312	16	94	15	187
20	224	20	163	20	115	20	94
20	387	20	135	20	111	20	86
20	86	35	44	35	27	35	31
35	24	35	43	35	26	35	38
35	23	50	18	50	13	50	15
50	7	50	20	50	15	50	17
50	9						

Brake Fluid Reservoir Flux (kW/m²)	t_{ig} (s)	Kick Panel Insulation Flux (kW/m²)	t_{ig} (s)	Headlight Assembly Flux (kW/m²)	t_{ig} (s)	Fender Sound Red. Foam Flux (kW/m²)	t_{ig} (s)
8	NI	**12**	NI	**20**	NI[C]	**8**	NI
9	NI	**14**	NI	**20**	NI	**9**	NI
10	484	**15**	NI	**20**	NI	10	158
12	367	16	378	**23**	NI[C]	20	3
20	142	20	47	**24**	513[C]	20	4
20	152	20	56	**25**	367[C]	35	2
35	62	35	32	35	747	35	2
35	58	35	31	35	395	**50**	1
35	52	50	24	35	433[C]	**50**	1
50	32	50	22	35	398[C]		
50	40			35	NI		
				36	NI		
				38	217		
				40	104		
				50	71 [C]		
				50	31		
				50	33		
				50	60 [C]		

[C] Clear Lens

Hood Liner Face Flux (kW/m²)	t_{ig} (s)	Windshield Wiper Struct. Flux (kW/m²)	t_{ig} (s)
13	NI	**11**	NI
14	NI	12	590
15	241	13	565
20	21	15	368
20	NI	20	146
20	16	20	159
35	4	35	79
35	8	35	86
50	4	50	49
50	4	50	41

Note: Heat fluxes that are in **BOLD** were not used in the calculation of FPI or TRP

Table 21. Ignition Data for Parts of the 1997 Chevrolet Camaro (NI=No Ignition in 10 min).

Front Wheel Well Liner		Air Inlet		Hood Insulator		Radiator Inlet/Outlet Tank	
Flux (kW/m^2)	t_{ig} (s)	Flux (kW/m^2)	t_{ig} (s)	Flux (kW/m^2)	t_{ig} (s)	Flux (kW/m^2)	t_{ig} (s)
8	NI	**10**	NI	**10**	NI	**15**	NI
9	438	11	452	**15**	NI	**17**	NI
10	395	15	238	**17**	NI	**18**	NI
12	242	20	129	**19**	NI	19	560
20	121	20	108	**20**	9	20	301
20	111	20	108	20	8	20	312
20	88	35	40	**20**	NI*	35	108
35	37	35	38	20	8	35	89
35	37	50	17	20	12	50	43
50	18	50	16	**35**	NI*	50	44
50	19			35	2		
				35	2		
				50	NI*		
				50	2		
				50	1		
				* Foil Side			

Engine Cooling Fan		Power Steering Fluid Reservoir		Windshield with Laminate		Blower Motor Housing	
Flux (kW/m^2)	t_{ig} (s)	Flux (kW/m^2)	t_{ig} (s)	Flux (kW/m^2)	t_{ig} (s)	Flux (kW/m^2)	t_{ig} (s)
15	NI	**20**	NI	**15**	NI	**8**	NI
17	NI	**20**	NI	**16**	NI	9	582
18	NI	**21**	NI	17	425	11	451
19	580	**22**	517	20	386	13	285
20	347	**23**	279	20	329	15	207
20	392	**25**	185	35	113	20	140
35	129	35	152	35	100	20	136
35	152	35	186	50	39	35	50
50	32	50	34	**50**	86	35	42
50	36	50	31			50	26
		50	37			50	23

Note: Heat fluxes that are in **BOLD** were not used in the calculation of FPI or TRP

Gas samples are analyzed using a ThermoNicolet Magna 560 FTIR spectrometer. A horizontal multi-holed, stainless steel sampling probe, with holes oriented downstream, is used to collect a representative sample from the Cone Calorimeter duct. This design minimizes particulate interference and ensures that sample is drawn across the full diameter of the duct. The probe has an inner diameter of 5 mm and outer diameter of 6 mm, and contains 9 holes: Five 2.36-mm diameter holes at the far end of the probe and four 1.70-mm holes nearest the outlet port. The upper end of the probe is closed.

The complete sampling system consists of (in order) the probe, a heated glass fiber filter, a heated PTFE-lined transfer line, a 0.2-L gas cell with a 2-m path length, a pressure transducer, a rotameter, desiccant (CaSO$_4$), and a pump. The flow rate through the system is monitored continuously via the rotameter, and is maintained at 2.7 L/min. The pathway is maintained at a constant temperature of 150°C from the outlet port to the gas cell to prevent condensation of the gas stream. The gas pressure in the line is typically maintained at a slight positive pressure relative to the

laboratory. A decrease in pressure is most often due to a buildup of particulate matter in the filter. If this is observed (via the pressure transducer), the glass fiber filter is replaced.

Sample is collected semi-continuously throughout each test. Eight infrared scans of the smoke sample are collected and added into a single infrared spectrum to improve the signal-to-noise ratio. The data represent an average concentration over the collection period, approximately 30 seconds. Collection times faster than those used significantly reduce the signal-to-noise ratio, obscuring low concentration data. Multiple spectra are obtained during the fire test, resulting in a concentration profile as a function of time.

Calibration of the spectrometer is conducted at the same temperature and pressure as the test program, using the same sampling parameters, to ensure accuracy at the point of sample as required by ASTM E 800. A calibration method based on the Beer-Lambert-Bouget Law is written using ThermoNicolet's Quant Setup 5.0 software. Beer's Law assumes concentration is linearly related to peak height or peak area of an infrared spectrum at a given wavenumber. Some compounds, such as CO, are nonlinear, and require extensive calibration and correction to provide consistent data across a range of concentrations.

Spectra representing a minimum of ten different concentrations are collected and used to correct the Quant method for nonlinearities. Certified master class gas mixtures are obtained for each compound blended in nitrogen. A gas divider is used on each to reduce the maximum certified concentration to 10, 20, 30, 40, 50, 60, 70, 80, 90, and 100% of the gas mixture, blended with 99.999% diatomic nitrogen. Correction coefficients are added to each curve in the Quant method. Table 22 shows the spectral concentrations and correction order.

Table 22. Maximum Calibration Concentration and Correction Order.

Compound	Maximum Concentration (ppm)	Correction Order
CO	7000	5th
CO_2	35,000	5th
HBr	600	3rd
HCl	3000	6th
HCN	140	5th
HF	600	4th
NO_x	350	5th
SO_2	120	5th
Water vapor	23,880	3rd

The samples used in this study are listed in Tables 23 and 24, and are the same samples used for the Cone Calorimeter testing described in Section 4.3.3.2. Table 23 lists the part numbers, sample descriptions, and material composition [4, 5] of each sample.   Spectra from each sample were analyzed to determine the concentrations of CO, CO_2, HBr, HCl, HCN, HF, NO_x, and SO_2 present in the smoke generated during the Cone Calorimeter tests.

Table 23. 1997 Chevrolet Camaro Test Samples Composition.

Part No.	Material ID	Composition	Contains
10296526	Front Wheel Well Liner	PP/PE copolymer	$[C_3H_6]_n$ / $[C_2H_4]_n$
10297291	Air Inlet	PP/PE	$[C_3H_6]_n$ / $[C_2H_4]_n$
10278015	Hood Insulator - Foil Side	Nylon 6 and phenolic binder (Novalac)	$[C_6H_{11}ON]_n$ and $C_{63}H_{48}O_{10}$
	Hood Insulator - Fiber side	Phenolic binder (Novalac)	$C_{63}H_{48}O_{10}$
52465337	Radiator Inlet/Outlet Tank	Nylon 6,6	$[C_{12}H_{22}O_2N_2]_n$
22098787	Engine Cooling Fan	Nylon 6	$[C_6H_{11}ON]_n$
26019594	Power Steering Fluid Reservoir	Nylon 6,6	$[C_{12}H_{22}O_2N_2]_n$
10310333	Laminated Windshield		
52458965	Heater Module Blower Motor Housing	Polypropylene	$[C_3H_6]_n$

Table 24. 1996 Dodge Caravan Test Samples Composition.

5235267AB	Battery Cover	Polypropylene	$[C_3H_6]_n$
4861057	Resonator Structure	Polypropylene	$[C_3H_6]_n$
53030508	Resonator Intake Tube	Ethylene propylene diene monomer	C_2H_4 and C_3H_6
4678345	Air Ducts	Polyethylene (A) or polypropylene (B)	$[C_2H_4]_n$ or $[C_3H_6]_n$
4683264	Brake Fluid Reservoir	Polypropylene	$[C_3H_6]_n$
4860446	Kick Panel Insulation Backing - Rubber side	Polyvinylchloride	$[C_2H_3Cl]_n$
4857041A	Headlight - Clear Lens	Polycarbonate	$[C_{16}H_{14}O_3]_n$
	Headlight - Black Casing	Polyoxy-methylene	$3[CH_2O]_n$
4716345B	Fender Sound Reduction Foam	Polystyrene	$[C_8H_8]_n$
4716832B	Hoodliner Face	polyethylene terephthalate	$[C_{10}H_8O_4]_n$
4716051	Windshield Wiper Structure	Glass reinforced thermoset polyester resin cross-linked with styrene	$[C_2H_4]_n$ and C_8H_8

4.3.3.5.3   Specimen Preparation

See Section 4.3.3.3 for information regarding the preparation of the samples used for these tests.

4.3.3.5.4   Supplemental Toxic Gas Measurement Results

Typical concentration versus time curves are shown in Figures 3 and 4. Tables 25 and 26 show CO and CO_2 concentration data for the Camaro and Caravan materials, respectively. The corresponding yields at 50 kW/m^2 are presented in Table 27. Yields at lower heat fluxes are generally lower. They are also less accurate because the concentrations are lower, in particular at 20 kW/m^2. Yields at lower heat fluxes are therefore not reported.

Tables 28 and 29 show HCN and NO_x concentration data for the nitrogen-containing materials. The corresponding yields at 50 kW/m^2 are presented in Table 30. HCl was detected for the only PVC that was tested. HCl concentrations and yields are given in Tables 31 and 32, respectively.

4.3.4   Smoke and Toxicity Tests

Based on the Cone Calorimeter results, three materials were selected for testing in both the IMO smoke chamber (Part 2 of Annex 1 to the FTP Code) and the NBS smoke chamber developed by the National Bureau of Standards. These materials represented the best, worst, and mid-level performers as evidenced from the CO concentration data collected during the Cone Calorimeter tests. The low-level material was also chosen in order to evaluate hydrogen chloride production relative to data collected from the Cone. The additional toxicity tests were conducted as part of the MVFRI project.

4.3.4.1   Test Procedures

Smoke toxicity measurements were performed in general accordance with Part 2 of Annex 1 to the IMO FTP Code, and in general accordance with Airbus Industrie ABD 0031. Each method uses a smoke chamber consisting of a 36 × 24 × 36-in. (914 × 610 × 914-mm) enclosure capable of developing and maintaining positive pressure during test periods. Both methods subject the sample to a radiant heat flux from an electrical heating element. For the IMO method, the heating element and sample are oriented horizontally; for the Airbus method, they are oriented vertically. Each method may be run with or without a pilot burner, referred to as *flaming* and *non-flaming*, respectively. The IMO method uses a single pilot flame mounted above the specimen, while the Airbus method uses an impinging six-tube pilot burner mounted between the specimen and the heating coil.
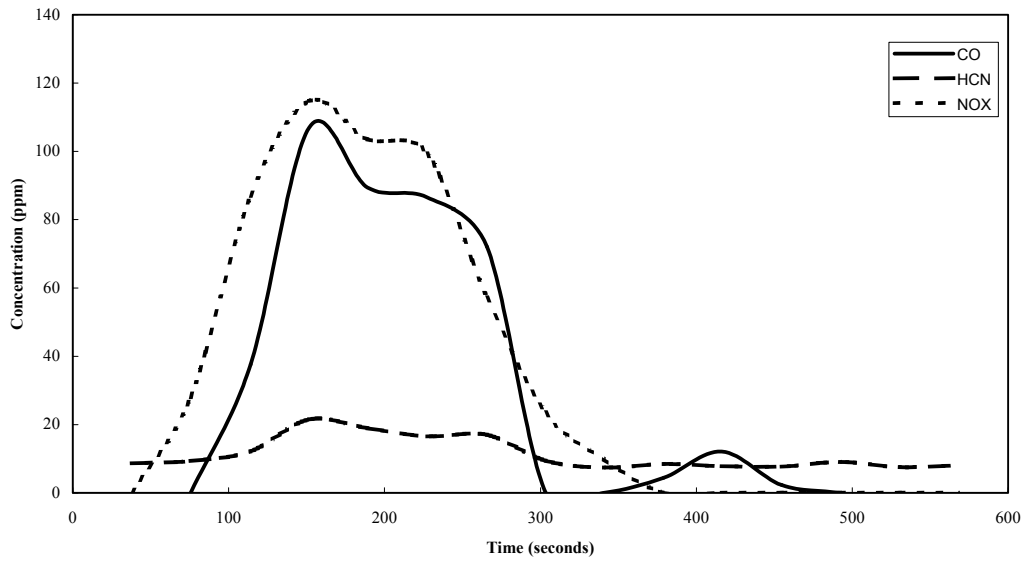
Figure 3. Concentration versus Time Curves for Brake Fluid Reservoir at 50 kW/m^2.
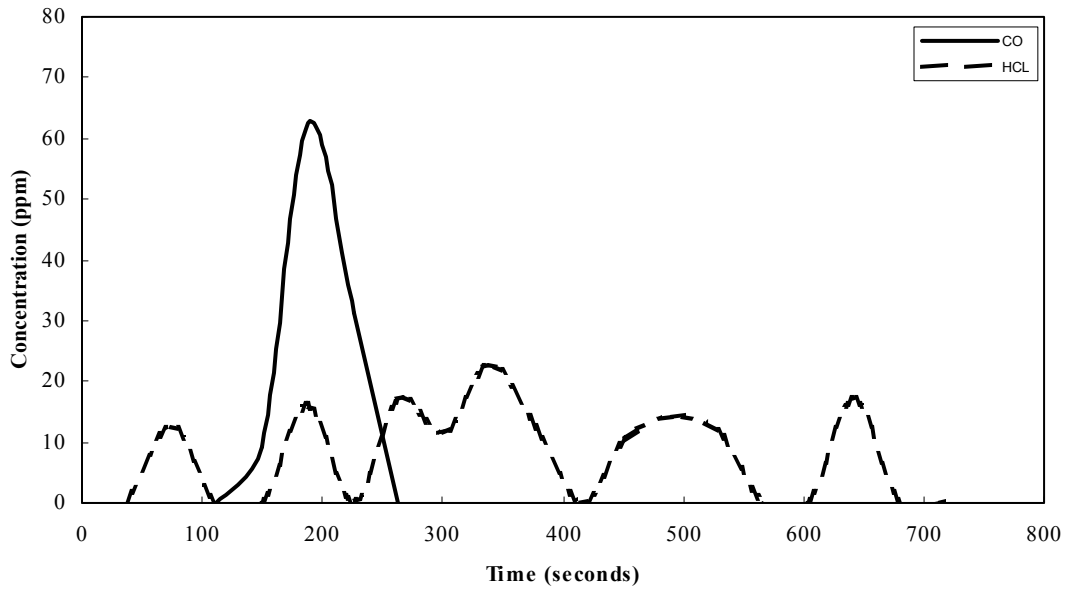
Figure 4. Concentration versus Time for Kick Panel Insulation at 35 kW/m^2.

Table 25. Maximum CO and CO$_2$ Concentrations for 1996 Dodge Caravan Parts.

Material Description	Composition	Flux (kW/m^2)	CO Max (ppm)			CO$_2$ at CO Max (ppm)			CO/CO$_2$ at Max CO		
			Test 1	Test 2	Average	Test 1	Test 2	Average	Test 1	Test 2	Average
Air Ducts (4678345)	PE or PP	20	97	109	103	6798	6667	6732	0.014	0.016	0.015
		35	166	158	162	9727	11054	10390	0.017	0.014	0.016
		50	189	225	207	9787	11801	10794	0.019	0.019	0.019
Battery Cover (5235267AB)	PP	20	39	12	26	4327	90	2209	0.009	NF	0.009
		35	50	35	43	4044	4272	4158	0.012	0.008	0.010
		50	83	55	69	5956	4749	5352	0.014	0.012	0.013
Brake Fluid Reservoir (4683264)	PP	20	95	101	98	6617	6762	6690	0.014	0.015	0.015
		35	259	85	172	13802	5831	9817	0.019	0.015	0.017
		50	205	202	204	10951	10580	10765	0.019	0.019	0.019
Fender Sound Reduction Foam (4716345B)	PS	20	152	39	95	3870	4327	4099	0.039	0.009	0.024
		35	163	176	170	3942	4572	4257	0.041	0.039	0.040
		50	173	153	163	4314	4093	4204	0.040	0.037	0.039
Headlight Lens - Black Casing (4857041A)	Polyoxy-methylene	20	5	5	5	70	77	73	NF	NF	NF
		35	NT	167	167	NT	399	399	NT	NF	NF
		50	253	269	261	5917	5612	5765	0.043	0.048	0.045
Headlight Lens - Clear Lens (4857041A)	PC	20	5	NT	5	63	NT	63	NF	NT	NF
		35	309	NT	309	7533	NT	7533	0.041	NT	0.041
		50	396	NT	396	7988	NT	7988	0.050	NT	0.050
Hoodliner Face (4716832B)	PET	20	322	326	324	265	287	276	NF	NF	NF
		35	361	432	397	352	250	301	NF	NF	NF
		50	227	187	207	385	411	398	NF	NF	NF
Kick Panel Insulation Backing - Rubber side (4860446)	PVC	20	26	38	32	2672	3107	2889	0.010	0.012	0.011
		35	63	72	67	4115	4200	4157	0.015	0.017	0.016
		50	60	46	53	3719	3420	3569	0.016	0.013	0.015
Resonator Intake Tube (53030508)	EPDM Rubber	20	78	57	67	4997	4512	4754	0.016	0.013	0.014
		35	106	116	111	6315	6653	6484	0.017	0.017	0.017
		50	130	112	121	7490	6921	7205	0.017	0.016	0.017
Resonator Structure (4861057)	PP	20	89	95	92	5489	5735	5612	0.016	0.017	0.016
		35	127	120	123	7570	6977	7273	0.017	0.017	0.017
		50	191	160	176	9221	7953	8587	0.021	0.020	0.020
Windshield Wiper Structure (4716051)	PE, PS	20	103	147	125	3307	4306	3806	0.031	0.034	0.033
		35	117	122	119	3664	3829	3747	0.032	0.032	0.032
		50	236	212	224	5995	5718	5856	0.039	0.037	0.038

NF = Not Flaming. NT = Not Tested.

Table 26. Maximum CO and CO$_2$ Concentrations for 1997 Chevrolet Camaro Parts.

Material Description	Composition	Flux (kW/m^2)	CO Max (ppm)			CO$_2$ at CO Max (ppm)			CO/CO$_2$ at Max CO		
			Test 1	Test 2	Average	Test 1	Test 2	Average	Test 1	Test 2	Average
Air Inlet (10297291)	PP, PE	20	24	76	50	3811	6092	4951	0.006	0.012	0.009
		35	145	186	166	10472	11622	11047	0.014	0.016	0.015
		50	234	241	237	13423	13360	13391	0.017	0.018	0.018
Engine Cooling Fan (22098787)	Nylon 6	20	5	5	5	392	53	222	NF	NF	NF
		35	NT	51	51	NT	300	300	NT	NF	NF
		50	112	137	124	378	423	401	NF	NF	NF
Front Wheel Well Liner (10296526)	PP, PE	20	66	69	68	4803	4862	4832	0.014	0.014	0.014
		35	77	52	64	5720	4428	5074	0.013	0.012	0.013
		50	89	366	227	6151	15908	11029	0.014	0.023	0.019
Heater Module Blower Motor Housing (52458965)	PP	20	43	38	40	3954	3422	3688	0.011	0.011	0.011
		35	69	69	69	4760	4444	4602	0.015	0.016	0.015
		50	107	95	101	5447	5153	5300	0.020	0.018	0.019
Hood Insulator - Fiber side (10278015)	Phenolic Binder	20	6	NT	6	17	NT	17	NF	NT	NF
		35	14	NT	14	432	NT	432	NF	NT	NF
		50	40	NT	40	664	NT	664	NF	NT	NF
Hood Insulator - Foil Side (10278015)	Nylon 6 and Phenolic Binder	20	6	NT	6	92	NT	92	NF	NT	NF
		35	5	NT	5	60	NT	60	NF	NT	NF
		50	10	NT	10	148	NT	148	NF	NT	NF
Laminated Windshield (10310333)		20	12	12	12	1724	396	1060	NF	NF	NF
		35	14	11	13	3332	3063	3197	0.004	0.003	0.004
		50	26	14	20	4079	4792	4435	0.006	0.003	0.005
Power Steering Fluid Reservoir (26019594)	Nylon 6,6	20	6	6	6	23	89	56	NF	NF	NF
		35	NT	84	84	NT	4200	4200	NT	0.020	0.020
		50	158	342	250	8554	16547	12550	0.018	0.021	0.020
Radiator Inlet/Outlet Tank (52465337)	Nylon 6,6	20	53	55	54	2696	3759	3227	0.020	0.015	0.017
		35	70	100	85	5764	7031	6397	0.012	0.014	0.013
		50	107	108	108	8236	7545	7891	0.013	0.014	0.014

NF = Not Flaming. NT = Not Tested.

Table 27. Average CO Yields at 50 kW/m².

Material Description	Composition	Flux (kW/m²)	CO Yield (mg/g)		
			Test 1	Test 2	Average
Air Ducts (4678345)	PE or PP	50	22	25	24
Battery Cover (5235267AB)	PP	50	15	11	13
Brake Fluid Reservoir (4683264)	PP	50	25	25	25
Fender Sound Reduction Foam (4716345B)	PS	50	53	50	52
Headlight Lens - Black Casing (4857041A)	Polyoxy-methylene	50	54	53	54
Headlight Lens - Clear Lens (4857041A)	PC	50	50	NT	50
Hoodliner Face (4716832B)	PET	50	148	136	142
Kick Panel Insulation Backing - Rubber side (4860446)	PVC	50	9.5	8.6	9.0
Resonator Intake Tube (53030508)	EPDM Rubber	50	25	16	21
Resonator Structure (4861057)	PP	50	28	28	28
Windshield Wiper Structure (4716051)	PE, PS	50	34	38	36
Air Inlet (10297291)	PP, PE	50	24	18	21
Engine Cooling Fan (22098787)	Nylon 6	50	13	16	15
Front Wheel Well Liner (10296526)	PP, PE	50	14	47	31
Heater Module Blower Motor Housing (52458965)	PP	50	26	24	25
Hood Insulator - Fiber side (10278015)	Phenolic Binder	50	50	NT	50
Hood Insulator - Foil Side (10278015)	Nylon 6 and Phenolic Binder	50	DNI	NT	DNI
Laminated Windshield (10310333)		50	3.5	1.9	2.7
Power Steering Fluid Reservoir (26019594)	Nylon 6,6	50	21	30	26
Radiator Inlet/Outlet Tank (52465337)	Nylon 6,6	50	12	14	13

NT = Not Tested. DNI = Did Not Ignite.

Table 28. Maximum HCN Concentrations for Nitrogen-Containing Materials.

Material Description	Composition	Flux (kW/m^2)	HCN Max (ppm)			CO$_2$ at HCN Max (ppm)			HCN/CO$_2$ at HCN Max		
			Test 1	Test 2	Average	Test 1	Test 2	Average	Test 1	Test 2	Average
Engine Cooling Fan (22098787)	Nylon 6	20	10	10	10	14	16	15	NF	NF	NF
		35	NT	15	15	NT	2151	2151	NT	0.0071	0.0071
		50	14	15	15	5254	4312	4783	0.0027	0.0034	0.0031
Hood Insulator - Foil Side (10278015)	Nylon 6 and Phenolic Binder	20	11	NT	11	18	NT	18	NF	NT	NF
		35	11	NT	11	13	NT	13	NF	NT	NF
		50	11	NT	11	26	NT	26	NF	NT	NF
Power Steering Fluid Reservoir (26019594)	Nylon 6,6	20	10	11	11	18	16	17	NF	NF	NF
		35	NT	16	16	NT	3558	3558	NT	0.0045	0.0045
		50	11	13	12	365	16547	8456	0.0304	0.0008	0.0156
Radiator Inlet/Outlet Tank (52465337)	Nylon 6,6	20	14	16	15	2548	3759	3153	0.0055	0.0043	0.0049
		35	19	18	18	6364	7031	6697	0.0030	0.0025	0.0028
		50	22	17	19	8236	7545	7891	0.0026	0.0022	0.0024

NF = Not Flaming. NT = Not Tested.

Table 29. Maximum NO$_x$ Concentrations for Nitrogen-Containing Materials.

Material Description	Composition	Flux (kW/m^2)	NO$_x$ Max (ppm)			CO$_2$ at NO$_x$ Max (ppm)			NO$_x$/CO$_2$ at NO$_x$ Max		
			Test 1	Test 2	Average	Test 1	Test 2	Average	Test 1	Test 2	Average
Engine Cooling Fan (22098787)	Nylon 6	20	19	17	18	308	657	482	NF	NF	NF
		35	NT	26	26	NT	2339	2339	NT	0.0110	0.0110
		50	58	63	60	5254	5422	5338	0.0110	0.0117	0.0113
Hood Insulator - Foil Side (10278015)	Nylon 6 and Phenolic Binder	20	30	NT	30	18	NT	18	NF	NT	NF
		35	11	NT	11	14	NT	14	NF	NT	NF
		50	23	NT	23	29	NT	29	NF	NT	NF
Power Steering Fluid Reservoir (26019594)	Nylon 6,6	20	17	19	18	17	20	19	NF	NF	NF
		35	NT	39	39	NT	4200	4200	NT	0.0094	0.0094
		50	18	32	25	8554	16547	12550	0.0021	0.0019	0.0020
Radiator Inlet/Outlet Tank (52465337)	Nylon 6,6	20	21	37	29	2696	3759	3227	0.0078	0.0099	0.0088
		35	81	95	88	6364	6995	6680	0.0127	0.0136	0.0131
		50	115	114	114	8236	8510	8373	0.0139	0.0133	0.0136

NF = Not Flaming. NT = Not Tested.

Table 30. Average HCN and NO$_x$ Yields for Nitrogen-Containing Materials at 50 kW/m^2.

Material Description	Composition	Flux (kW/m^2)	HCN Yield (mg/g)			NO$_x$ Yield (mg/g)		
			Test 1	Test 2	Average	Test 1	Test 2	Average
Engine Cooling Fan (22098787)	Nylon 6	50	5.0	4.0	4.5	11	12	12
Hood Insulator - Foil Side (10278015)	Nylon 6 and Phenolic Binder	50	DNI	NT	DNI	DNI	NT	DNI
Power Steering Fluid Reservoir (26019594)	Nylon 6,6	50	8.0	4.5	6.3	0.7	2.0	1.4
Radiator Inlet/Outlet Tank (52465337)	Nylon 6,6	50	5.1	4.8	5.0	15	14	15

DNI = Did Not Ignite. NT = Not Tested.

Table 31. Maximum HCl Concentrations for Chlorine-Containing Materials.

Material Description	Composition	Flux (kW/m^2)	HCl Max (ppm)			CO$_2$ at HCl Max (ppm)			HCl/CO$_2$ at Max HCl		
			Test 1	Test 2	Average	Test 1	Test 2	Average	Test 1	Test 2	Average
Kick Panel Insulation Backing - Rubber side (4860446)	PVC	20	15	12	13	1702	NF	1702	0.009	NF	0.009
		35	23	20	21	2206	1280	1743	0.010	0.016	0.013
		50	12	12	12	281	1528	905	NF	0.008	0.008

NF = Not Flaming.

Table 32. Average HCl Yields for Chlorine-Containing Materials at 50 kW/m^2.

Material Description	Composition	Flux (kW/m^2)	HCl Yield (mg/g)		
			Test 1	Test 2	Average
Kick Panel Insulation Backing - Rubber side (4860446)	PVC	50	4.2	1.1	2.7

For each method, the gas sampling and analysis were performed in a manner similar to that described in Section 4.3.3.5.1. The only significant difference in the gas sampling method is the sampling probe; for the IMO and Airbus methods, the sampling probe consists of a PTFE-lined stainless steel probe mounted to an intake port in the center of the top of the chamber and terminating in the geometrical center of the smoke chamber.

Each method specifies procedures and calculations to be used to determine the optical density of smoke generated by the sample during the course of a test.

4.3.4.2   Test Matrix

Test materials were chosen that showed high, low, and intermediate peak CO concentrations in the Cone Calorimeter. Information about the materials is shown in Table 33. Note that none of the materials contains any nitrogen, and only one of the materials (the PVC kick panel insulation [rubber side]) contained chlorine.

Table 33. Material Selection for Smoke and Toxicity Testing.

Part No.	Auto (see note)	Material ID	Composition	Contains	CO_{MAX} (ppm, from Cone Calorimeter)
4860446	Caravan	Kick Panel Insulation Backing - Rubber side	PVC	$[C_2H_3Cl]_n$	53
4857041A	Caravan	Headlight - Clear Lens	polycarbonate	$[C_{16}H_{14}O_3]_n$	396
4716832B	Caravan	Hoodliner Face	PET	$[C_{10}H_8O_4]_n$	207

Note: Caravan = 1996 Dodge Caravan

4.3.4.3   Specimen Preparation

All specimens were prepared in accordance with the method being implemented, either Part 2 of Annex 1 to the IMO FTP Code, or Airbus Industrie ABD 0031. Ten 3 × 3-in. specimens for each sample were prepared. The thickness of each sample as received was below the limits specified in the methods. The ABD 0031 specimens were predried at 60°C for 24 hours. Specimens for both test methods were then conditioned at 23°C and 50% relative humidity until they achieved constant mass. Prior to testing, all specimens were covered across the back, along the edges, and over the front periphery with a single sheet of aluminum foil. Specimens were backed with a sheet of ½-in. thick piece of non-combustible insulating material, and secured with a spring and retaining rod.

4.3.4.4   Smoke Toxicity Test Results

The results of smoke toxicity testing performed on the three materials listed in Table 33 are given in Tables 34 through 43. Each material was tested in duplicate for each test protocol. The results for each specimen and averages for each material are listed in the tables. Peak concentrations are expressed in parts per million (ppm) and average yields are expressed in mg/g for CO and HCl.

Table 34. Peak CO and HCl Concentrations (Airbus, Non-Flaming, 25 kW/m^2).

| Sample | Peak Concentration (ppm) | | | | | |
| | CO | | | HCl | | |
	Test 1	Test 2	Average	Test 1	Test 2	Average
Headlight Lens - Clear Lens (4857041A) Polycarbonate	4	2	3			
Hoodliner Face (4716832B) PET	2563	2095	2329			
Kick Panel Insulation Backing - Rubber side (4860446) PVC	528	731	629	510	631	571

Table 35. Average CO and HCl Yields (Airbus, Non-Flaming, 25 kW/m^2).

| Sample | Average Yield (mg/g) | | | | | |
| | CO | | | HCl | | |
	Test 1	Test 2	Average	Test 1	Test 2	Average
Headlight Lens - Clear Lens (4857041A) Polycarbonate	2	1	2			
Hoodliner Face (4716832B) PET	82	61	71			
Kick Panel Insulation Backing - Rubber side (4860446) PVC	10	12	11	22	32	27

Table 36. Peak CO and HCl Concentrations (Airbus, Flaming, 25 kW/m^2).

| Sample | Peak Concentration (ppm) | | | | | |
| | CO | | | HCl | | |
	Test 1	Test 2	Average	Test 1	Test 2	Average
Headlight Lens - Clear Lens (4857041A) Polycarbonate	470	532	501			
Hoodliner Face (4716832B) PET	2096	1765	1931			
Kick Panel Insulation Backing - Rubber side (4860446) PVC	1053	934	994	625	596	611

Table 37. Average CO and HCl Yields (Airbus, Flaming, 25 kW/m^2).

| Sample | Average Yield (mg/g) | | | | | |
| | CO | | | HCl | | |
	Test 1	Test 2	Average	Test 1	Test 2	Average
Headlight Lens - Clear Lens (4857041A) Polycarbonate	22	29	26			
Hoodliner Face (4716832B) PET	93	71	82			
Kick Panel Insulation Backing - Rubber side (4860446) PVC	28	31	30	26	28	27

Table 38. Peak CO and HCl Concentrations (IMO, Non-Flaming, 25 kW/m^2).

Sample	Peak Concentration (ppm)					
	CO			HCl		
	Test 1	Test 2	Average	Test 1	Test 2	Average
Headlight Lens - Clear Lens (4857041A) Polycarbonate	1	4	2			
Hoodliner Face (4716832B) PET	5860	4400	5130			
Kick Panel Insulation Backing - Rubber side (4860446) PVC	174	3	89	41	30	36

Table 39. Average CO and HCl Yields (IMO, Non-Flaming, 25 kW/m^2).

Sample	Average Yield (mg/g)					
	CO			HCl		
	Test 1	Test 2	Average	Test 1	Test 2	Average
Headlight Lens - Clear Lens (4857041A) Polycarbonate	1	1	1			
Hoodliner Face (4716832B) PET	228	131	179			
Kick Panel Insulation Backing - Rubber side (4860446) PVC	48	3	25	14	10	12

Table 40. Peak CO and HCl Concentrations (IMO, Flaming, 25 kW/m^2).

Sample	Peak Concentration (ppm)					
	CO			HCl		
	Test 1	Test 2	Average	Test 1	Test 2	Average
Headlight Lens - Clear Lens (4857041A) Polycarbonate	14	19	17			
Hoodliner Face (4716832B) PET	3470	4020	3745			
Kick Panel Insulation Backing - Rubber side (4860446) PVC	362	9	185	27	11	19

Table 41. Average CO and HCl Yields (IMO, Flaming, 25 kW/m^2).

Sample	Average Yield (mg/g)					
	CO			HCl		
	Test 1	Test 2	Average	Test 1	Test 2	Average
Headlight Lens - Clear Lens (4857041A) Polycarbonate	2	4	3			
Hoodliner Face (4716832B) PET	133	91	112			
Kick Panel Insulation Backing - Rubber side (4860446) PVC	7	2	4	1	4	3

Table 42. Peak CO and HCl Concentrations (IMO, Non-Flaming, 50 kW/m^2).

Sample	Peak Concentration (ppm)					
	CO			HCl		
	Test 1	Test 2	Average	Test 1	Test 2	Average
Headlight Lens - Clear Lens (4857041A) Polycarbonate	1845	838	1342			
Hoodliner Face (4716832B) PET	4189	2874	3532			
Kick Panel Insulation Backing - Rubber side (4860446) PVC	964	1012	988	1073	1251	1162

Table 43. Average CO and HCl Yields (IMO, Non-Flaming, 50 kW/m^2).

Sample	Average Yield (mg/g)					
	CO			HCl		
	Test 1	Test 2	Average	Test 1	Test 2	Average
Headlight Lens - Clear Lens (4857041A) Polycarbonate	63	85	74			
Hoodliner Face (4716832B) PET	139	160	150			
Kick Panel Insulation Backing - Rubber side (4860446) PVC	15	34	25	18	80	49

4.4   Intermediate-Scale Fire Tests

4.4.1   Introduction

A series of intermediate-scale fire tests was conducted on six automotive components: four Dodge Caravan parts and two Chevrolet Camaro parts. The test matrix for this testing is given in detail in Section 4.4.3. The testing was conducted in general accordance with ASTM E 1623-02b, *Standard Test Method for Determination of Fire and Thermal Parameters of Materials, Products, and Systems Using an Intermediate-Scale Calorimeter (ICAL)*.   Details and results for the intermediate-scale tests are provided below.

4.4.2   Test Procedure

All tests were conducted in general accordance with ASTM E 1623, in the vertical orientation, with customized specimen holders and a pilot flame. The tests were terminated after flameout and data were recorded as specified in ASTM E 1623. Figure 5 shows the apparatus and Figure 6 shows a close-up of the sample holder and drip pan. There were three major deviations from the test standard, and they are as follows:

1. *Pilot Flame*: the pilot used to ignite the pyrolysis gases was a small open flame (propane flowing through tubing) rather than a hot wire at the surface of the test specimen.

2. *Pilot Flame Insertion Time*: the flame was inserted in the stream of pyrolysis gases at a time that was calculated from the Cone Calorimeter ignition data. This was done to minimize heat release rate variations due to random ignition time fluctuations.

3. *Irregular Shaped Test Specimens*: test specimens were tested as whole components whenever possible, and this made it necessary to design specialized test fixtures to support the specimens.

Single ICAL tests were conducted at three heat flux levels: 20, 35, and 50 kW/m^2. The rationale for the choice of heat flux levels is discussed in Sections 3.1 and 3.4. Also, it was necessary

to perform the ICAL tests at the same irradiance as the Cone Calorimeter tests in order to facilitate the data analysis.

Figure 5. ICAL Apparatus.

4.4.3   Test Matrix

The parts and components of the Caravan and Camaro tested in the ICAL are listed in Table 44. The number of replicate tests at each heat flux level, and the page numbers in Appendix E where graphs of the primary results can be found are also given in this table. A total of 18 full ICAL tests was performed on six different component parts.

4.4.4   Specimen Preparation

Nearly all the test specimens were irregular in shape and size. The ICAL was developed for testing of planar specimens, so special sample holders were used to accommodate these odd-shaped automotive components. When possible, samples were prepared according to the procedure in ASTM E 1623. In most cases, however, parts were tested as whole components supported by a frame or fixture (substrate). Drip pans were used to catch burning pieces that fell during testing to maintain the mass loss rate measurement. Table 45 shows a photograph of each specimen attached to its substrate and in its sample holder prior, during, or after testing and each test specimen's initially exposed area.

Figure 6. Close-up of Test Frame and Drip Pan for ICAL Apparatus.

Table 44. ICAL Test Matrix.

Vehicle Type	Automotive Component	Full ICAL Tests			Appendix E Pages
		20 kW/m^2	35 kW/m^2	50 kW/m^2	
Dodge Caravan	Battery Cover	1	1	1	1-9
	Air Ducts	1	1	1	10-18
	Sound Reduction Foam	1	1	1	19-27
	Hood Liner Face	1	1	1	28-36
Chevrolet Camaro	Front Wheel Well Liner	1	1	1	37-45
	Windshield Laminate	1	1	1	46-54

Table 45. ICAL Sample Preparation Details.

Automotive Component	Photograph of Prepared Specimens on Substrate	Photograph of Prepared Specimens in Sample Holders	Initially Exposed Area (m^2)
Battery Cover			0.779
Air Ducts			0.520

Table 45. (Cont'd.). ICAL Sample Preparation Details.

Automotive Component	Photograph of Prepared Specimens on Substrate	Photograph of Prepared Specimens in Sample Holders	Initially Exposed Area (m²)
Sound Reduction Foam			0.533
Hood Liner Face			0.559
Front Wheel Well Liner			0.393

Table 45. (Cont'd.). ICAL Sample Preparation Details.

Automotive Component	Photograph of Prepared Specimens on Substrate	Photograph of Prepared Specimens in Sample Holders	Initially Exposed Area (m²)
Windshield with Laminate			0.788

4.4.5 ICAL Test Results

Complete results and graphs for ASTM E 1623 tests are compiled in Appendix E. Table 46 gives logistic information about the ICAL testing such as test number, material identification, incident heat flux, and data file name.

Table 47 summarizes the ICAL data, including peak heat release rate, total heat released, peak smoke production rate, total smoke produced, total mass loss, peak CO generation rate and total amount of CO produced.

Figures 7–12 show test photographs for the battery cover, the air ducts, the sound reduction foam, the hood liner face, the front wheel well liner, and the windshield, respectively.

Table 46. ICAL Test Information.

Test No.	Material Identification	Data File No.	Date Tested	Incident Heat Flux (kW/m^2)	Ignition Time (s)
1	Front Wheel Well Liner	030s3fw1	01/30/03	20	115
2	Battery Cover	031bc1a	01/31/03	20	55
3	Hood Liner Face	0313hl1	01/31/03	20	22
4	Sound Reduction Foam	0313sr1	01/31/03	20	4
5	Air Ducts	0313ad1	01/31/03	20	123
6	Windshield	0313wd1	01/31/03	20	300
7	Hood Liner Face	0343hl2	02/03/03	35	10
8	Sound Reduction Foam	0343sr2	02/03/03	35	7
9	Battery Cover	0343bc2	02/03/03	35	19
10	Air Ducts	0343ad2	02/03/03	35	42
11	Front Wheel Well Liner	0353fw2a	02/04/03	35	40
12	Windshield	0353wd2	02/04/03	35	120
13	Front Wheel Well Liner	0353fw3	02/04/03	50	20
14	Hood Liner Face	0353hl3	02/04/03	50	5
15	Sound Reduction Foam	0353sr3	02/04/03	50	3
16	Battery Cover	0363bc3	02/05/03	50	6
17	Windshield	0363wd3	02/05/03	50	66
18	Air Ducts	0363ad3	02/05/03	50	21

Table 47. ICAL Test Results Summary.

Test No.	Peak Heat Release Rate (HRR) (kW)	Total Heat Released (MJ)	Peak Smoke Production Rate (m²/s)	Total Smoke Produced (m²)	Peak CO Generation Rate (g/s)	Total CO Produced (g)	Total Mass Loss (g)
1	161	50	2.3	555	0.65	429	1041
2	200	16	0.9	51	0.49	133	365
3	48	12	1.4	148	1.53	635	867
4	159	19	3.3	199	0.64	131	417
5	447	132	8.4	1949	0.96	923	3027
6	43	32	0.2	108	0.40	539	675
7	84	16	5.0	133	1.66	590	887
8	159	14	7.7	290	1.05	157	397
9	288	16	2.1	92	0.76	383	401
10	664	125	9.2	1880	0.92	989	2940
11	495	51	6.3	691	1.24	468	1158
12	100	32	0.7	110	0.82	1144	692
13	802	55	9.7	530	1.20	345	1074
14	132	22	7.8	91	1.69	612	877
15	226	16	13.8	399	1.15	170	422
16	603	21	3.4	86	0.86	155	394
17	148	45	1.0	171	0.80	1150	814
18	709	123	11.1	1748	1.25	2025	2846

Figure 7. Battery Cover – ICAL Test in Progress.

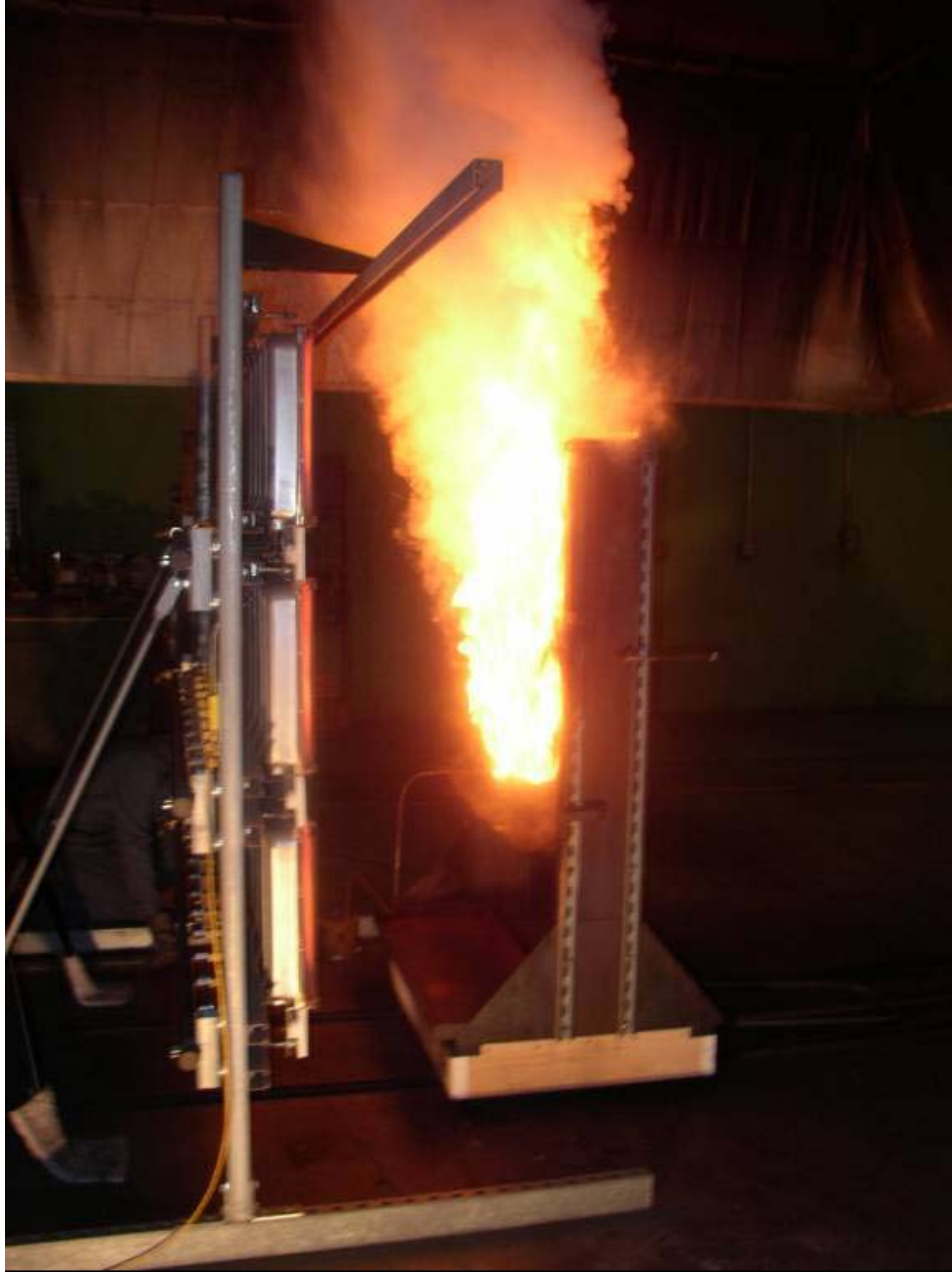**Figure 8. Air Ducts – ICAL Test in Progress.**

Figure 9. Sound Reduction Foam – ICAL Test in Progress.

Figure 10. Hood Liner Face – ICAL Test in Progress.

Figure 11. Front Wheel Well Liner – ICAL Test in Progress.

Figure 12. Windshield – ICAL Test in Progress.

4.5   Alternative Materials

The purpose of this task was to explore viable modifications to presently used automotive plastics that endow superior fire performance, and which can serve as suitable, economically viable modifications of standard automotive polymeric components. Surface coating technologies that were amenable to under the hood polymeric components were specifically sought-out in this task by employing surface engineering capabilities already established at SwRI. In particular, the potential benefits that surface metalization of standard polymeric materials might bring to the fire performance of such materials or components was determined experimentally under this task.

The hypothesis central to the surface metalization approach of the present study was that if the overall emissivity, the ability of a surface to emit radiant energy compared to that of a black body at the same temperature, could be significantly lowered in the engine compartment of an automobile, then for any given fire scenario the time to ignition of polymeric component materials would be lengthened and the rate of fire propagation would be reduced. In addition to the delay in ignition, proper selection of the low-emissivity coating may induce, upon ignition, a chemical mechanism,

through the interaction of the surface metal with the base polymer, by which the reaction local to the flame front yields an non-flammable product. From the perspective of the economic viability, such an approach, if successful, would not require the implementation of higher-cost base-polymer substitutes with improved fire performance or higher-cost fire-retardant additive packages for blending, but rather the surface properties of existing polymeric materials at the component level could be modified using a low-cost, scalable process.

To test this hypothesis, coupons of a sampling of the same polymeric components as were tested in the Cone Calorimeter were prepared in accordance with the surface properties and methods as follows. Thin films of pure aluminum (Al) and antimony (Sb) with near optical reflectance qualities were deposited, up to 3.6 μm in thickness, onto one face of the test coupon such that the edges of the test coupon were also coated. The emissivity values for these metals range from 0.06 to 0.07 (50-500°C). In addition to the pure metal, the corresponding thin-film oxide, aluminum oxide (Al_2O_3) and antimony oxide (Sb_2O_3), were formed on select test coupons. In all cases, vacuum-based physical vapor deposition (PVD) methods, employing an electron-beam hearth, were used to form the thin-films. For the corresponding oxides, however, the PVD (electron-beam) process was assisted with an energetic beam of oxygen ions to convert the pure-metal surface thin-film to its oxide form.

The heat release properties of the coated component materials were determined at a single heat flux value of 50 kW/m^2. The results of these measurements are compared with that of the corresponding uncoated specimens in Tables 48 and 49. For the purpose of comparing the heat release characteristics after ignition among all specimens, the mass-weighted peak rate of heat release (MWHRR) and mass-weighted total heat release (MWTHR) were calculated.

The results indicate that significant increases in the time to ignition (t_{ig}) can be realized from the low-emissivity coatings. However, in most cases, little change to the mass-weighted heat release properties were observed with some notable exceptions. In the case of unblended polypropylene component materials, *e.g.,* resonator structure, a slight decrease in the mass-weighted peak rate of heat release was observed for aluminum-coated specimens, whereas the integrated heat release (mass-weighted total heat release) remained unchanged. In order to visualize the trends for each parameter, the correlation between the parameters determined by the Cone Calorimeter for uncoated and coated specimens are plotted in Figure 13. Overall, pure aluminum coatings had the greatest impact on the time to ignition, regardless of the type of base polymer. It is interesting to note that the thin-film oxide form of both aluminum and antimony had in many instances a detrimental effect on the heat release properties of the specimen.

Table 48. Comparison Between Uncoated and Coated Component Materials from the Dodge Caravan.

| Dodge Caravan | | | | Uncoated | | | | | | Coated | | | | | |
| | | | | Heat Flux: 50 (kW/m²) | | | | | | Heat Flux: 50 (kW/m²) | | | | | |
Part No.	Description	Base Polymer Composition	Coating	Mass (g)	T$_{ig}$ (s)	Peak HRR (Kw/M²)	THR (MJ/m²)	Peak MWHRR (W/g)	MWTHR (kJ/g)	Mass (g)	T$_{ig}$ (s)	Peak HRR (Kw/M²)	THR (MJ/m²)	Peak MWHRR (W/g)	MWTHR (kJ/g)
4861057	Resonator Structure	Polypropylene	Aluminum (1.75 μm)	31.3	19	516.5	102.1	143.23	28.31	30.4	34.0	396	102.1	113.07	29.15
4861057	Resonator Structure	Polypropylene	Aluminum (3.6 μm)	31.3	19	516.5	102.1	143.23	28.31	35.2	184.0	479	135.9	118.12	33.51
4861057	Resonator Structure	Polypropylene	Antimony Oxide (3.2 μm)	31.3	19	516.5	102.1	143.23	28.31	29.8	74.0	553	122.4	161.08	35.65
4857041A	Headlight Structure	Polycarbonate	Aluminum (1.75 μm)	38.1	49	356	66.4	81.10	15.13	26.8	100.0	319	51.4	103.32	16.65
4857041A	Headlight Structure	Polycarbonate	Aluminum Oxide (3.2 μm)	38.1	49	356	66.4	81.10	15.13	26.3	73.0	389	61.9	128.38	20.43

Table 49. Comparison Between Uncoated and Coated Component Materials from the Chevrolet Camaro.

| Chevrolet Camaro | | | | Uncoated | | | | | | Coated | | | | | |
| | | | | Heat Flux: 50 (kW/m²) | | | | | | Heat Flux: 50 (kW/m²) | | | | | |
Part No.	Description	Base Polymer Composition	Coating	Mass (g)	T$_{ig}$ (s)	Peak HRR (Kw/M²)	THR (MJ/m²)	Peak MWHRR (W/g)	MWTHR (kJ/g)	Mass (g)	T$_{ig}$ (s)	Peak HRR (Kw/M²)	THR (MJ/m²)	Peak MWHRR (W/g)	MWTHR (kJ/g)
10297291	Air Inlet	Polyethylene/Polypropylene	Aluminum (1.75 μm)	21.55	16.5	758.5	81.5	305.51	32.83	22.6	189	718	86.7	275.76	33.30
10297291	Air Inlet	Polyethylene/Polypropylene	Aluminum (3.6 μm)	21.55	16.5	758.5	81.5	305.51	32.83	22.8	226	939	110.9	357.48	42.22
10297291	Air Inlet	Polyethylene/Polypropylene	Aluminum Oxide (3.2 μm)	21.55	16.5	758.5	81.5	305.51	32.83	21.2	84	1249	110.6	511.38	45.28
10296526	Front Wheel Well Liner	Polypropylene	Aluminum (1.75 μm)	23.3	18	526	62.6	195.95	23.32	19.5	100	648	55.3	288.44	24.62
10296526	Front Wheel Well Liner	Polypropylene	Antimony (3.6 μm)	23.3	18	526	62.6	195.95	23.32	24.7	50	826	83.9	290.27	29.48
10296526	Front Wheel Well Liner	Polypropylene	Antimony Oxide (2.9 μm)	23.3	18	526	62.6	195.95	23.32	24.3	32s	663	85.9	236.82	30.68
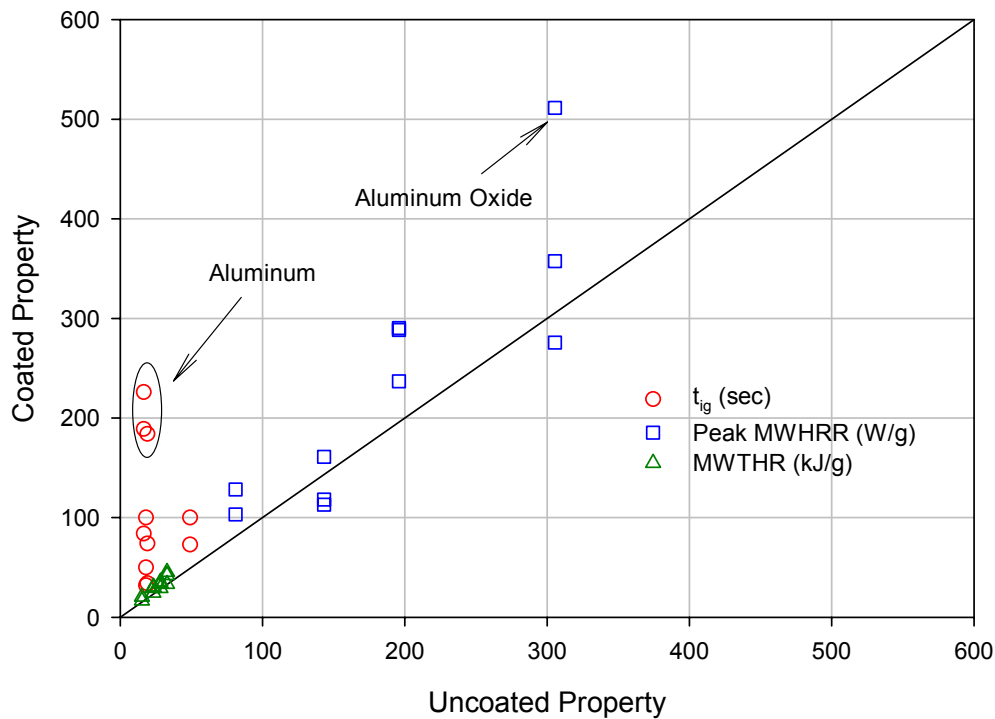
Figure 13. Correlation Between Uncoated and Coated Specimens .

While the heat release properties were not consistently altered in a beneficial way for the coated specimens, the significant delays observed in the time to ignition values have positive implications as will be discussed in Section 5.5. In particular, alternative alloy, oxide, and pure metal combinations may be engineered to endow a chemical mechanism by which the local flame reaction yields a non-combustible surface product. Insofar as aluminum, antimony, and their oxides are concerned, this post-ignition mechanism was not sufficiently active in these systems. Other choices, however, may be more suitable in this regard, while simultaneously providing significant delays in the time to ignition due to their low surface emissivities.

5.0   DATA ANALYSIS

5.1   Introduction

The primary objectives of the NHTSA project are:

1. To identify or develop a test methodology to determine an automotive material fire rating which best correlates to actual fire performance of the material in vehicle burns; and

2. To establish levels of performance using the test methodology that would significantly alter the fire outcome in terms of injury or survivability.

A secondary objective is to relate the performance of a material when tested according to the proposed methodology to fundamental thermal properties. This information will be useful for material suppliers and automotive components manufacturers in developing formulations that meet the new fire performance levels.

To accomplish these objectives, a detailed analysis was performed of the test data obtained as part of this study. This analysis is discussed below. An analysis of supplemental toxicity data is presented as well.

5.2   Test Methodology

The "test methodology" defines the test apparatus, the procedure that needs to be followed, and the results to be reported. Two distinct approaches have been used to develop a flammability test methodology for a particular application. These two approaches are based on very different philosophies and are referred to as the "traditional" and the "modern" approach, respectively.

A flammability test methodology developed according to the traditional approach measures one or several parameters that are believed to be an indication of real fire performance. FMVSS 302, for example, is a test that was developed in the 1970's according to the traditional approach. A small sample of a material is exposed to a Bunsen burner flame for 15 seconds and the primary measurement is the time for surface flame propagation over a distance of 10 in. Intuitively one would expect that a material with a lower propagation rate will perform better in a real fire than a material with a higher rate. Acceptance of a material for use in the occupant compartment of motor vehicles in the U.S. is therefore based on a maximum rate of propagation in the test. A second example of a popular test methodology that was developed according to a traditional approach is UL 94. Other examples are briefly discussed in Section 3.4.

Traditional flammability tests can serve a useful purpose. For example, it has been demonstrated that the lower number of fatalities in fires involving TV sets in the U.S. versus Europe can be attributed to the UL 94 V-0 requirement for the plastic TV housing in the U.S. [68]. However, these tests do not provide a complete and quantitative assessment of real fire performance. For example, it is logical to assume that the propagation rate of a flame over the surface of an automotive material in a real fire would be comparable to that in the FMVSS 302 test if the real ignition source is similar to that in the test. But what would happen if the real ignition source is twice as severe or

persists for more than 15 seconds, or if the surface of the material is in the vertical orientation? The results could be dramatically different, *i.e.*, the flame might propagate at a much faster rate and quickly result in a catastrophic fire. There are numerous examples of materials that pass the test with flying colors, but perform miserably under slightly more stringent real fire conditions.

Advances in fire dynamics and modeling have led to the development of a more sophisticated approach. This modern approach involves a hazard assessment. One or several key real fire scenarios are defined based on statistical surveys. For each scenario it is determined how materials and products contribute to the fire based on accident reports and full-scale fire test data. A model is developed to predict real fire performance on the basis of fire properties for the materials that are involved. The model can range in complexity from a relatively simple statistical correlation to a detailed computer simulation. A test methodology is developed to provide the properties that are needed for model input. The model can then be used to translate a specific fire performance level to a range of acceptable property values measured in the test.

Statistics reveal that there are two predominant scenarios that lead to fatalities in motor vehicle fires (see Section 3.1). The first scenario involves a rear-end collision that leads to a ruptured fuel tank and an underbody pool fire. The second scenario involves a front-end collision with a fire originating in the engine compartment that propagates to the passenger compartment. Thermal exposure conditions in the first scenario are much more severe than in the second scenario due to the overwhelming heat release rate by the burning fuel. It is unlikely in this scenario that any changes in the fire performance of exterior or interior materials will significantly affect survivability. In the second scenario, however, fire initiation and propagation is strongly affected by the flammability characteristics of the materials involved. This study, therefore, focuses on the second scenario.

Full-scale vehicle burn tests conducted at FM indicate that a fire originating in the engine compartment becomes a threat to trapped occupants in the passenger compartment when the heat release rate reaches approximately 400 kW (see Section 3.2). The model therefore must be capable of predicting fire growth in the engine compartment. A simple engine fire growth model will be developed in the next section. Without knowing the details of the engine fire growth model it can already be concluded that the input data will consist of ignition and heat release rate properties of the materials and components involved. This conclusion is based on similar fire growth models for upholstered furniture, electrical cable arrays, and interior finish [5, 6, 69-71]. A small-scale calorimeter such as the Cone Calorimeter or the FM Fire Propagation Apparatus can be used to obtain the ignition and heat release rate properties that are needed. The Cone Calorimeter was chosen for this study because it is more widely used and available at SwRI.

In conclusion, it is proposed to use the Cone Calorimeter as the new test methodology to evaluate the fire performance of automotive materials. The Cone Calorimeter test standard ASTM E 1354 provides a detailed description of the apparatus, procedure, and results that must be reported. The procedure does not specify the orientation of the sample, use of the retainer frame and spark igniter, and heat flux level. Cone Calorimeter tests are usually conducted in the horizontal orientation with the edge frame and spark igniter, and there is no reason to deviate from that practice for automotive materials. The issues of suitable heat flux levels and subset of results to be reported will be addressed in the next section.

5.3   Levels of Performance

5.3.1   Comparison Between Small and Intermediate-Scale Heat Release Rate Data

The analysis in this section is based on the premise that Cone Calorimeter data at the appropriate heat flux can be used to predict the heat release rate from objects in a real fire. Janssens and Urbas measured heat release rates of nine different wood panel and lumber products in the Cone Calorimeter and the ICAL apparatus [72]. All specimens were tested in the vertical orientation at 25, 35 and 50 kW/m^2. The intermediate-scale heat release rates were generally slightly higher, but within 10% of small-scale measurements. It can be concluded from that study that Cone Calorimeter data for wood products can indeed be used to predict the heat release rate from large surfaces, provided the small-scale data are obtained at heat fluxes that are representative of the thermal exposure conditions in the fire. The question is whether this conclusion can be extended to automotive materials, most of which sag, melt, and drip when heated. Figure 14 compares the peak heat release rates at three heat flux levels for the six automotive materials that were tested in the Cone Calorimeter and the ICAL apparatus (see Sections 4.3.3 and 4.4, respectively). The ICAL values were obtained by dividing the peak heat release rate in Table 47 by the initially exposed area in Table 45.
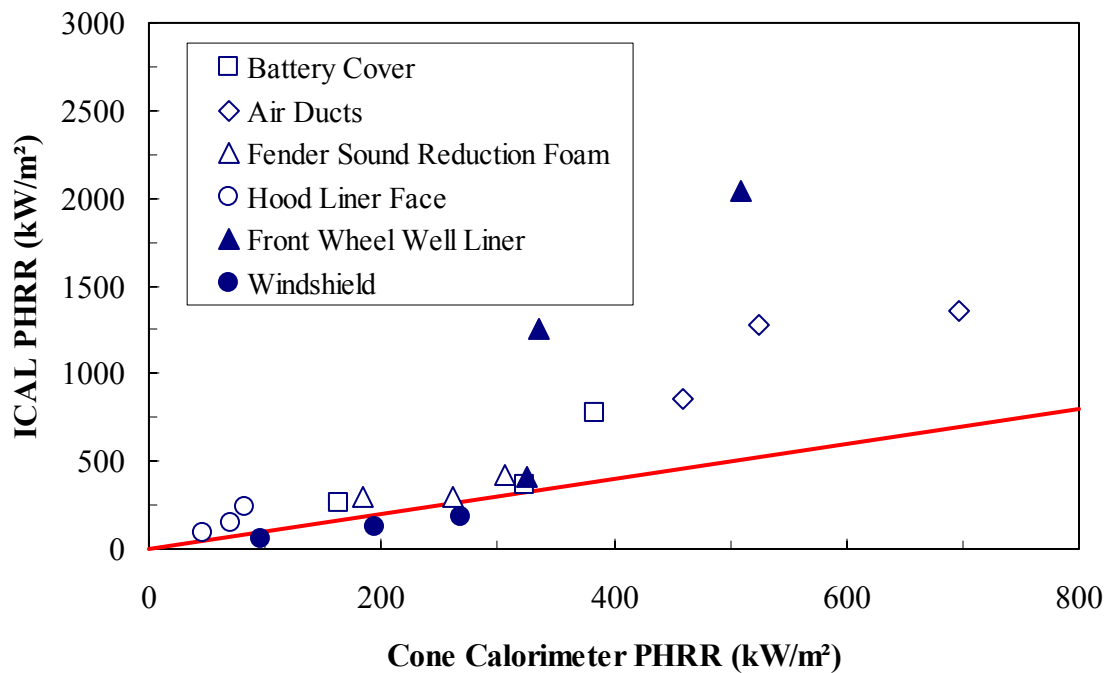
Figure 14. Comparison Between Peak Heat Release in the Cone Calorimeter and ICAL.

Figure 14 shows that there is a reasonable one-on-one relationship when the peak heat release rate in the Cone Calorimeter is 340 kW/m² or less. The peak heat release rate in the ICAL is much higher than that in the Cone Calorimeter when the latter exceeds 340 kW/m². This is the case for the battery cover at 50 kW/m^2, the fender sound reduction foam at 35 and 50 kW/m^2, and the air ducts at all three heat flux levels. This discrepancy can be attributed primarily to partial melting of the specimen into the catch pan, resulting in a pool fire below the specimen (see Figures 7, 8, and 11). The burning area under these conditions is (much) greater than the initially exposed area, which explains the higher heat release rate on a per-unit-area basis in the ICAL tests. Fortunately, the full-scale vehicle burn tests conducted at FM indicate that, although melting and dripping were observed, fire growth prior to spread to the passenger compartment is not significantly affected by pool fires developing beneath the engine (see Section 3.2). The effect of melting and dripping can therefore be largely ignored, and it is reasonable to assume that the heat release rate per unit area measured in the Cone Calorimeter is representative of that in a real engine fire.

5.3.2 *FM Fire Hazard Indices*

FM developed a procedure to assess the fire hazard of materials based on measurements in the Fire Propagation Apparatus [73]. The procedure involves measuring the time to ignition at

different heat flux levels between 10 and 60 kW/m^2 and heat release rate at 50 kW/m^2. The following fire hazard indices are calculated from the data:

1. *Critical Heat Flux (kW/m^2)* - The Critical Heat Flux (CHF) is the highest heat flux below which ignition does not occur for a very long (theoretically infinite) exposure time. The CHF can be estimated by extrapolation or by bracketing. The latter involves ignition tests at subsequently lower heat fluxes until ignition does not occur within 10-20 min. The former is determined as the intercept with the abscissa of a linear fit through thermally thin ignition points in a graph of the reciprocal of ignition time versus heat flux. Whether a material behaves as a thermally thin or a thermally thick solid depends on the physical thickness, thermal properties, and ignition time. Polymeric materials with a thickness of a few mm typically behave as a thermally thin solid at heat fluxes below 30 kW/m^2 [50].

2. *Thermal Response Parameter (kW-s$^{1/2}$/m^2)* – To determine the Thermal Response Parameter (TRP), the reciprocal of the square root of ignition time is plotted versus heat flux. The TRP is the reciprocal of the slope of a linear fit through thermally thick data points. Polymeric materials with a thickness of a few mm typically behave as a thermally thick solid at heat fluxes of 30 kW/m^2 or higher [50].

3. *Fire Propagation Index (m$^{5/3}$/kW$^{2/3}$-s$^{1/2}$)* – The Fire Propagation Index (FPI) is calculated from the following expression

$$FPI = 1000 \frac{\left(0.042\dot{Q}''\right)^{1/3}}{TRP} \tag{1}$$

where $\dot{Q}''$ is peak heat release rate in kW/m^2 measured in the Fire Propagation Apparatus at 50 kW/m^2.

Table 50 shows the CHF, TRP, and FPI values calculated based on the Cone Calorimeter ignition and heat release data presented in Section 4.3.3 and Appendix C.

Table 50. CHF, TRP, and FPI for Automotive Materials Tested in the Cone Calorimeter.

	Material	CHF (kW/m²) Extrapolation	CHF (kW/m²) Bracket	TRP (kW-s$^{1/2}$/m²)	HRR$_{peak}$ (kW/m²) (@ 50 kW/m²)	FPI (m$^{5/3}$/kW$^{2/3}$-s$^{1/2}$)
1996 Dodge Caravan	Headlight Assembly (Clear)	CHF > 20	23	200	312	11.8
	Battery Cover	19	19	100	384	25.3
	Resonator Structure	9	11	192	517	14.5
	Resonator Intake Tube	9	11	204	599	14.4
	Air Ducts	8	12	189	697	16.3
	Brake Fluid Reservoir	6	9	427	626	7.0
	Kick Panel Insulation	15	15	492	224	4.3
	Headlight Assembly (Black)	CHF > 20	37	112	401	22.9
	Fender Sound Reduction Foam	10	9	89	307	26.3
	Hood Liner Face	15	14	114	83	13.3
	Windshield Wiper Structure	10	11	381	323	6.3
1997 Chevrolet Camaro	Front Wheel Well Liner	6	8	220	526	12.8
	Air Inlet	9	10	174	759	18.2
	Hood Insulator	16	19	39	19	23.8
	Radiator Inlet/Outlet Tank	18	18	297	458	9.0
	Engine Cooling Fan	17	18	172	294	13.4
	Power Steering Fluid Reservoir	CHF > 20	21	159	655	19.0
	Windshield Laminate	2	16	238	269	9.4
	Blower Motor Housing	6	8	275	328	8.7

Tewarson suggests a critical value for the FPI of automotive materials of 10 m$^{5/3}$/kW$^{2/3}$-s$^{1/2}$ above which flame spread accelerates [50]. However, this value is based on data for the FM 25-ft corner test. What does an FPI of 10 m$^{5/3}$/kW$^{2/3}$-s$^{1/2}$ mean in terms of fire growth in the engine compartment of a motor vehicle? What is the corresponding time to reach a heat release rate of 400 kW? To answer these questions, a simple model will be developed in the next section to relate engine fire growth to ignition and heat release rate properties measured in the Cone Calorimeter.

5.3.3   *Simplified Model to Estimate Fire Growth in an Engine Compartment*

The rate of wind-aided flame spread over the surface of a material increases as the material releases more heat and is easier to ignite [74]. A higher heat release rate results in a longer flame and a larger area ahead of the flame front that is heated by the flame. The fire growth rate in a wind-aided flame spread scenario is thus expected to increase with increasing ratios of heat release rate to ignition time for the corresponding thermal exposure conditions. Figure 15 shows a plot of peak heat release rate per unit area measured at 50 kW/m² in the ICAL apparatus divided by ignition time versus the FPI. Although there are two outliers, the plot indeed shows that the ratio increases as the FPI increases and *vice versa*. This, however, still does not answer the questions that were raised in the previous section. A more detailed analysis is needed to find the answers.
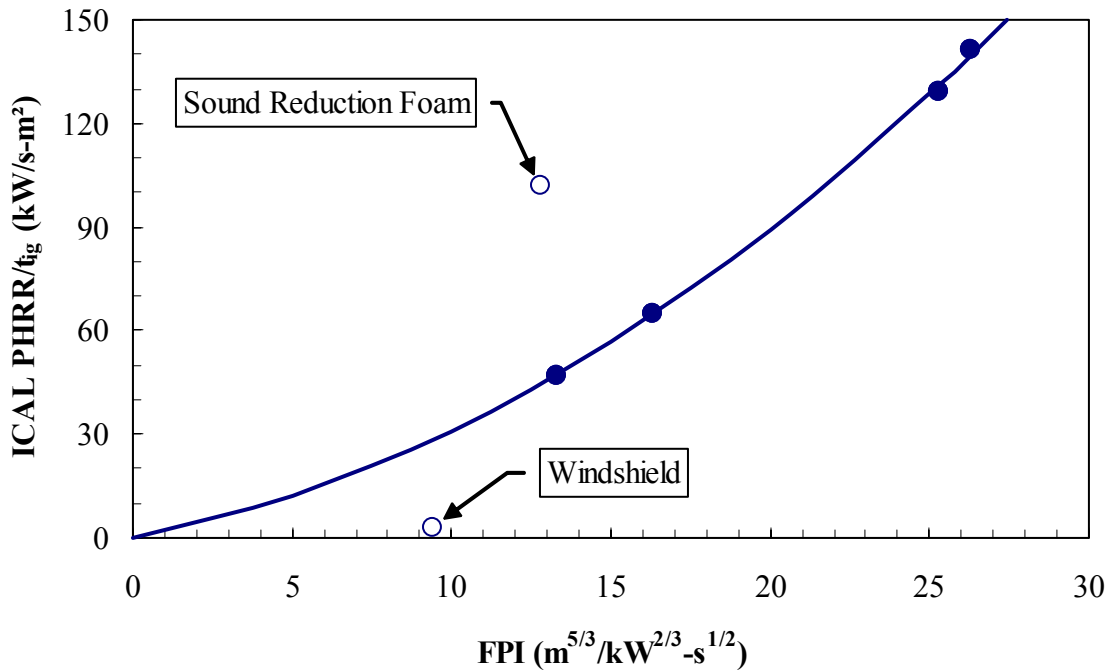
Figure 15. Comparison Between Peak Heat Release in the Cone Calorimeter and ICAL.

It is very difficult to predict fire growth for a complex geometry such as the collection of objects with varying composition that are found in the engine compartment of a motor vehicle. The following assumptions are made to simplify the problem so that an engineering model can be developed:

1. All materials are replaced with the material that has the worst fire performance.

2. All materials are redistributed in a continuous horizontal slab with an area equal to that of the hood.

The first assumption is definitely conservative because replacing a material with an inferior material will accelerate fire growth. Whether the second assumption is conservative is perhaps not so obvious. For example, a wood crib burns at a faster rate than a solid slab of wood with the same width and length because radiation is trapped inside the void spaces between the sticks.   This radiation effect is probably not nearly as significant for an engine compartment. Moreover, it seems reasonable to assume that flames will spread at a faster rate over a horizontal surface than between plastic components that are separated by air gaps and metal parts.

The fire growth estimates in this study are based on a simplified version of Atreya's model to predict flame spread over a horizontal slab of wood [75]. Atreya used Orloff's approach to calculate the radiant heat flux distribution from the flame to the fuel surface. The incident radiant heat flux is the highest at the center and drops off by 20-35% at the edge of the burning area. The radiant heat flux to the fuel surface ahead of the flame front decreases as a function of $(R/L)^3$, where R is the radius of the burning area and L is the distance to the center of the burning area. For the engine fire growth model it is assumed that the radiant heat flux from the flame to the burning surface is uniform. The uniform radiant heat flux is estimated at 35 kW/m^2 based on Atreya's equations applied to a 400 kW fire with a radius of 0.5 m. The incident heat flux to the fuel surface ahead of the flame front is also assumed to be 35 kW/m^2 between L/R = 1 and L/R = 1.5 and 0 kW/m^2 beyond L/R = 1.5. Figure 16 compares the simplified uniform radiant heat flux profile to Atreya's profile. The actual radiant heat flux from the flame to the burning fuel surface is slightly higher than 35 kW/m^2, but it is assumed equal to the heat flux to the fuel ahead of the flame front, so that the model only requires heat release rate data at a single heat flux level.
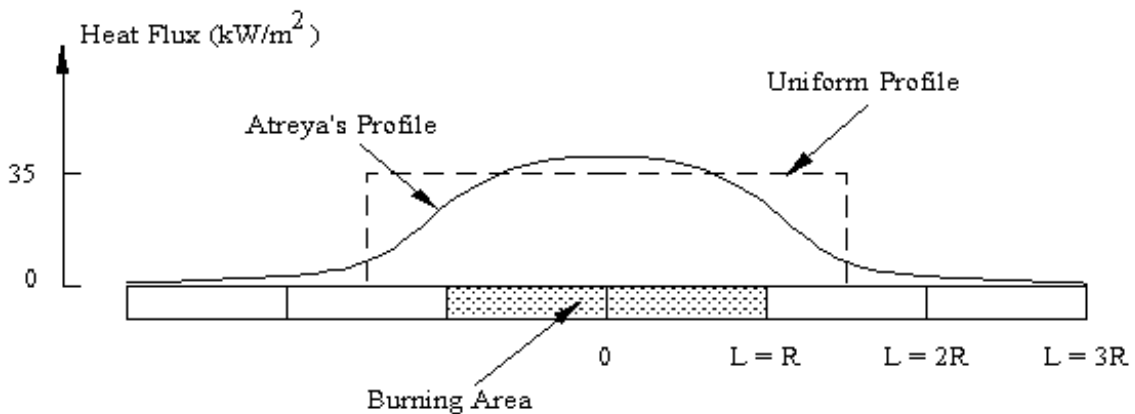

Figure 16. Approximation of Radiant Heat Flux Distribution.

The engine fire growth model assumes that initially a circular area with a radius of 0.05 m is exposed to 35 kW/m^2 and ignites after a period equal to the corresponding ignition time measured in the Cone Calorimeter. The subsequent heat release rate is estimated as the product of the peak heat release rate at 35 kW/m^2 measured in the Cone Calorimeter and the area of the burning surface (0.0079 m^2). An average heat release rate at a higher heat flux is probably more consistent, but the peak heat release rate at 35 kW/m^2 is used to minimize the Cone Calorimeter data needed. After a period equal to the average Cone Calorimeter ignition time at 35 kW/m^2 an annular region ahead of the flame front ignites. The width of this region is half the radius of the initial burning region, so that the radius of the burning area increases by 50%. After a period equal to three times the Cone Calorimeter ignition time, the radius of the burning area will increase by 50% again. This process

will continue until the heat release rate reaches 400 kW. Figure 17 shows an example of the fire growth model for a material with a peak heat release rate of 255 kW/m^2 at 35 kW/m^2.
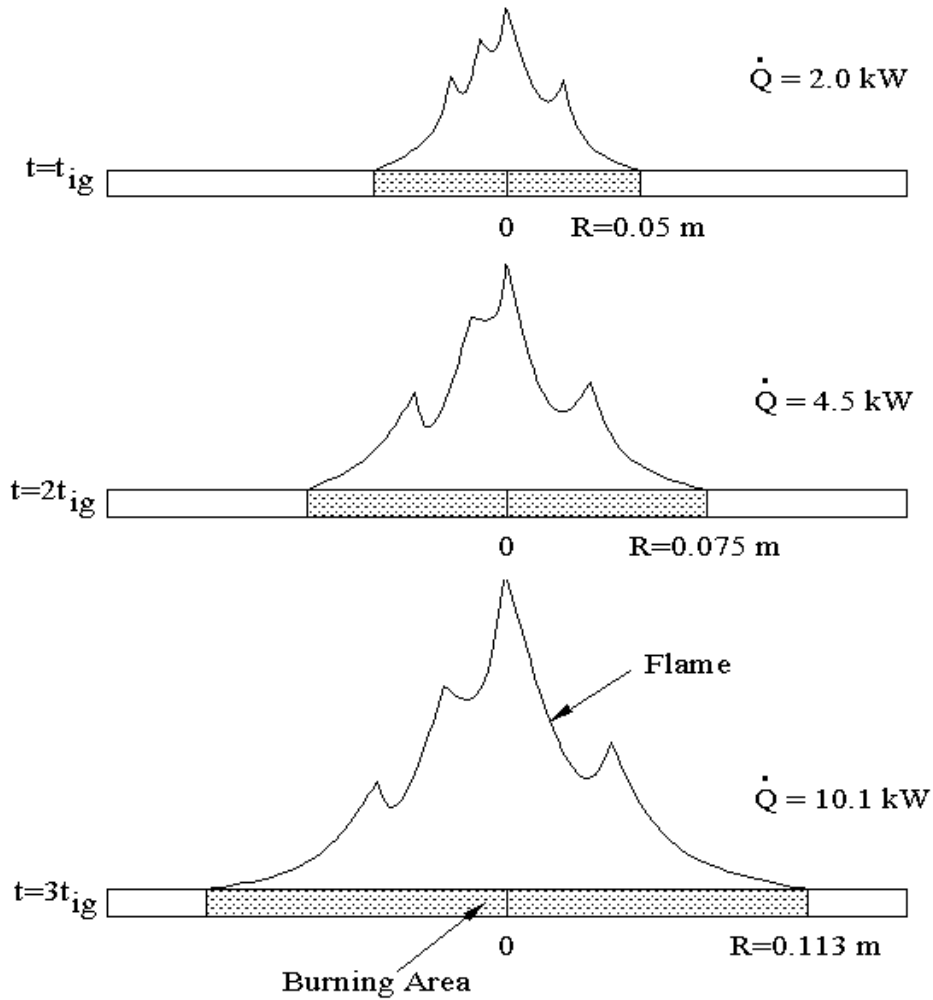
Figure 17. Simple Engine Fire Growth Model.

The resulting exponential fire growth model can be represented by the following expression:

$$\dot{Q} = A_0 \dot{Q}'' (1.5)^{\dfrac{2(t - t_{ig})}{t_{ig}}} \tag{2}$$

where $\dot{Q}$ is the heat release rate of the fire in kW, A_0 is the area initially ignited (assumed to be 0.0079 m^2), $\dot{Q}''$ is the peak heat release rate measured in the Cone Calorimeter at 35 kW/m^2, t is the time in sec, and t_{ig} is the time to ignition measured in the Cone Calorimeter at 35 kW/m^2. The time to

reach 400 kW when the fire becomes a threat to trapped occupants in the passenger compartment (see Section 3.2.4) can therefore be calculated from

$$t = t_{ig}\left[1 + 1.233 \ln\left(\frac{400}{0.0079\dot{Q}''}\right)\right] \tag{3}$$

Table 51 gives the time to reach 400 kW based on Equation (3) for the 18 materials that were tested in the Cone Calorimeter. Figure 18 presents the time to reach 400 kW as a function of the FPI. It can be observed from this figure that any material with an FPI of 10 $m^{5/3}/kW^{2/3}$-$s^{1/2}$ or less requires at least 10 minutes to reach the 400 kW threshold. Note that only Cone Calorimeter data at a single heat flux level are required by the model, while ignition data at multiple heat flux levels are needed to calculate the fire hazard indices used by FM. Figure 19 is based on peak 30-second average heat release rate measured at 50 kW/m^2 and leads to the same conclusions as Figure 18, which further justifies using Cone Calorimeter data at a single heat flux level.

Table 51. Time to 400 kW Based on Engine Fire Growth Model.

|	Material	t_{ig} (s)	$\dot{Q}''$ (kW/m^2)	$t_{400\,kW}$ (s)	$t_{400\,kW}$ min : sec
Dodge Caravan	Headlight Assembly (Clear)	278	385	1952	32 : 32
	Battery Cover	39	297	287	4 : 47
	Resonator Structure	64	417	443	7 : 23
	Resonator Intake Tube	72	434	497	8 : 17
	Air Ducts	68	560	443	7 : 23
	Brake Fluid Reservoir	270	499	1808	30 : 08
	Kick Panel Insulation	605	205	4720	78 : 40
	Headlight Assembly (Black)	74	158	603	10 : 03
	Fender Sound Reduction Foam	12	251	88	1 : 28
	Hood Liner Face	29	71	269	4 : 29
	Windshield Wiper Structure	252	233	1926	32 : 06
Chevy Camaro	Front Wheel Well Liner	66	390	465	7 : 45
	Air Inlet	48	686	306	5 : 06
	Hood Insulator	6	21	63	1 : 03
	Radiator Inlet/Outlet Tank	305	344	2187	36 : 27
	Engine Cooling Fan	102	158	831	13 : 51
	Power Steering Fluid Reservoir	129	217	997	16 : 37
	Windshield Laminate	157	187	1242	20 : 42
	Blower Motor Housing	104	268	775	12 : 55
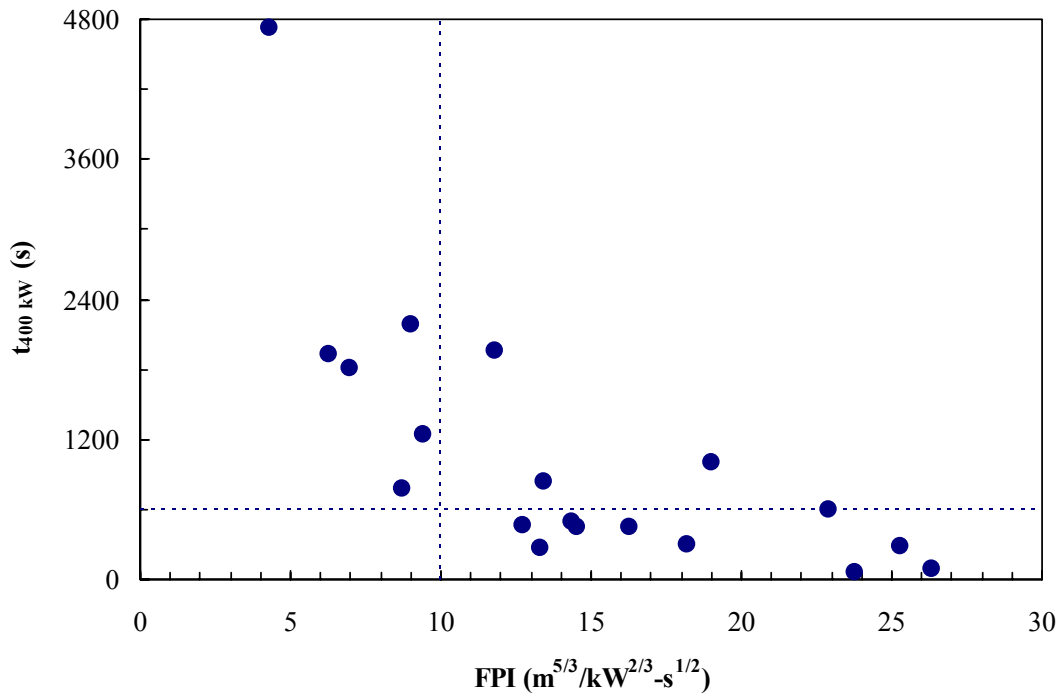
Figure 18. Time to Reach 400 kW Based on PHRR Measured at 35 kW/m^2 versus FPI.
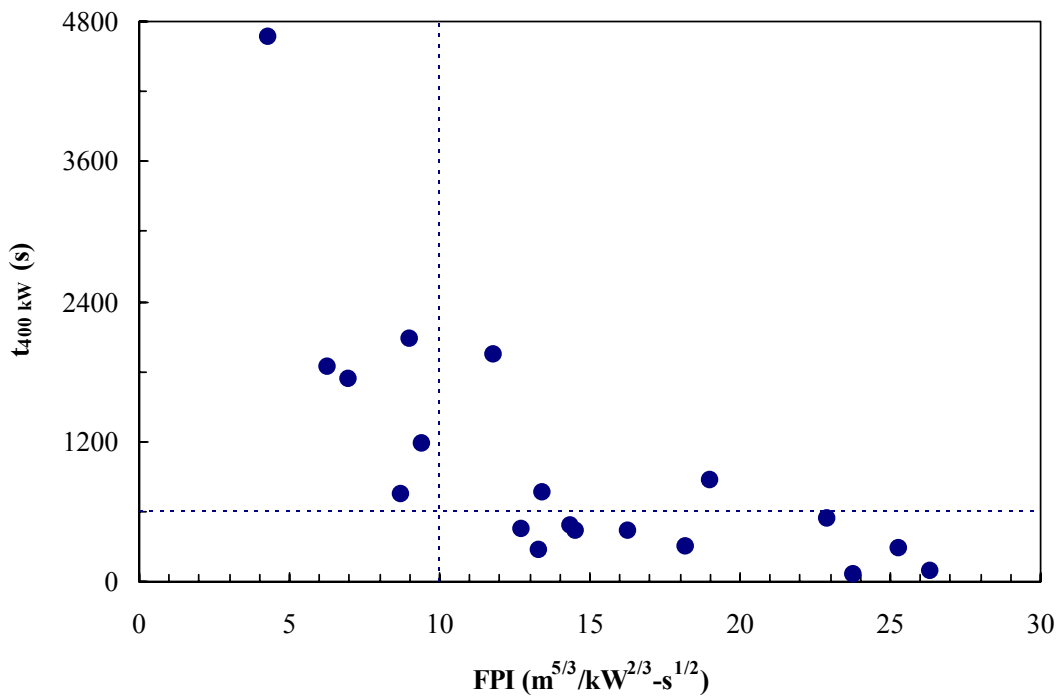

Figure 19. Time to Reach 400 kW Based on 30 s PHRR Measured at 50 kW/m^2 versus FPI .

5.3.4 Relationship Between Cone Calorimeter Data and FMVSS 302 Performance

In the previous section, an approximate relationship was developed between Cone Calorimeter data and the rate of fire growth in the engine compartment of an automobile. To put things in perspective, it is also useful to establish a relationship between Cone Calorimeter data and FMVSS 302 performance. That is the subject of this section.

Lyon demonstrated that the limiting heat release rate, HRR_0, correlates well with performance in the UL 94 and Limiting Oxygen Index (LOI) tests [76]. For example, plastics that meet the requirements for a UL 94 V-0 classification appear to have a limiting heat release rate below a critical value, HRR^*, of approximately 100 kW/m^2. HRR_0 is the intercept with the ordinate of a linear fit through data points in a plot of heat release rate measured in the Cone Calorimeter versus heat flux. The slope of the linear fit is the Heat Release Parameter (HRP). $HRR_0 < HRR^* \cong$ 100 kW/m^2 indicates that the heat release rate of the material under zero external heat flux is not sufficient to support combustion and upward flame propagation after removal of the Bunsen burner flame in the vertical UL 94 test. Figure 20 shows an example of how HRR_0 and HRP are determined. Unfortunately Lyon does not specify whether to use peak or average heat release rates. Table 52 gives HRR_0 and HRP values for the 18 automotive materials that were tested in this study based on four different heat release rate parameters. Figures 21-24 show plots of the propagation rate in the FMVSS 302 test versus the four different sets of HRR_0 values.
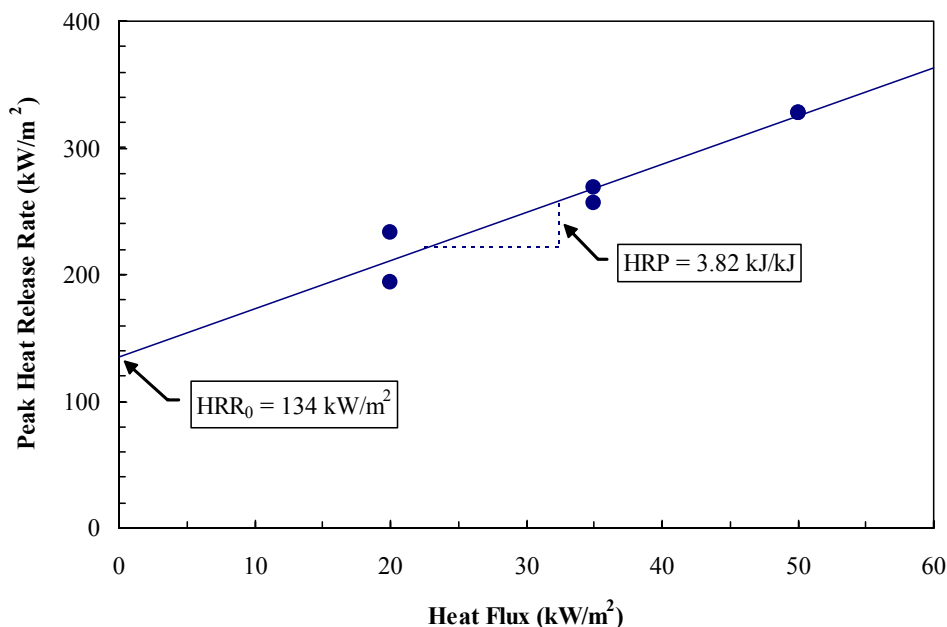

Figure 20. Lyon's Heat Release Rate Parameters.

Table 52. HRR$_0$ and HRP for Automotive Materials Tested in the Cone Calorimeter.

| Material	Peak		Peak 30 s Average		180 s Average		Test Average	
	HRR$_0$ (kW/m^2)	HRP (kJ/kJ)	HRR$_0$ (kW/m^2)	HRP (kJ/kJ)	HRR$_0$ (kW/m^2)	HRP (kJ/kJ)	HRR$_0$ (kW/m^2)	HRP (kJ/kJ)
Headlight Assembly (Clear)	346	1.10	244	2.97	117	3.37	133	1.07
Battery Cover	65	6.63	119	4.63	61	1.70	-6	4.22
Resonator Structure	227	5.43	227	5.27	166	4.38	37	5.42
Resonator Intake Tube	125	8.82	134	7.55	101	3.42	-58	5.92
Air Ducts	284	7.90	285	7.32	204	2.87	108	1.72
Brake Fluid Reservoir	158	9.75	158	9.48	85	6.62	12	6.78
Kick Panel Insulation	154	1.48	150	1.42	53	2.25	38	1.42
Headlight Assembly (Black)	-201	10.27	-222	10.53	-377	12.60	-286	9.40
Fender Sound Reduction Foam	107	4.12	79	5.03	71	2.73	23	3.42
Hood Liner Face	41	0.85	45	0.64	2	1.17	29	0.20
Windshield Wiper Structure	103	3.72	139	3.50	121	0.73	49	1.18
Front Wheel Well Liner	136	7.26	175	5.40	107	2.48	37	1.48
Air Inlet	510	5.04	502	4.42	192	4.21	36	4.21
Hood Insulator	11	0.28	3	0.62	1	0.02	6	0.29
Radiator Inlet/Outlet Tank	40	8.68	187	5.30	159	4.13	-18	4.75
Engine Cooling Fan	-128	8.17	-127	8.08	-142	7.72	-67	4.54
Power Steering Fluid Reservoir	-444	18.87	-426	18.27	-289	12.23	-249	9.40
Windshield Laminate	-15	5.75	-5	5.17	28	1.58	7	1.52
Blower Motor Housing	134	3.82	132	3.82	73	4.13	16	4.40
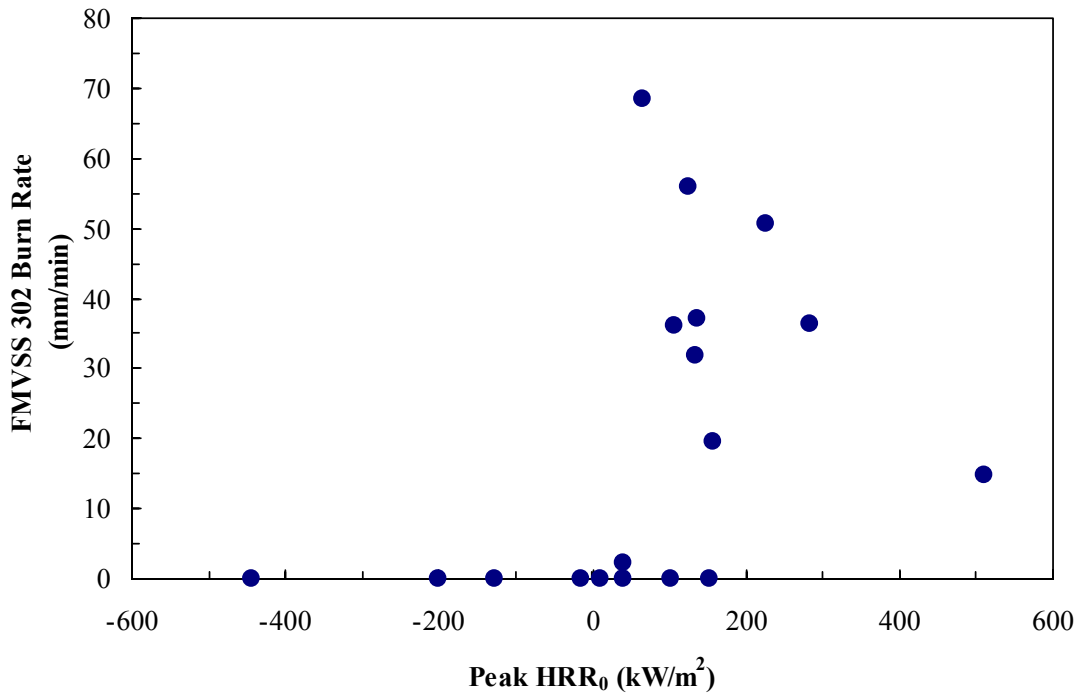
Figure 21. FMVSS 302 Burn Rate Versus HRR$_0$ Based on Peak HRR.
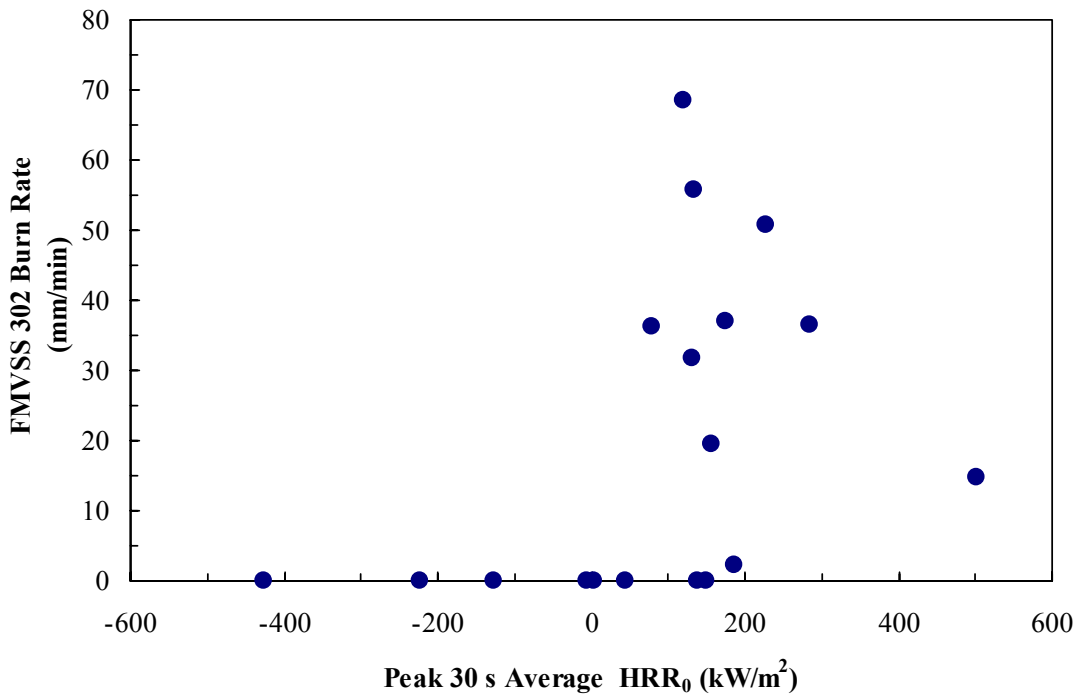
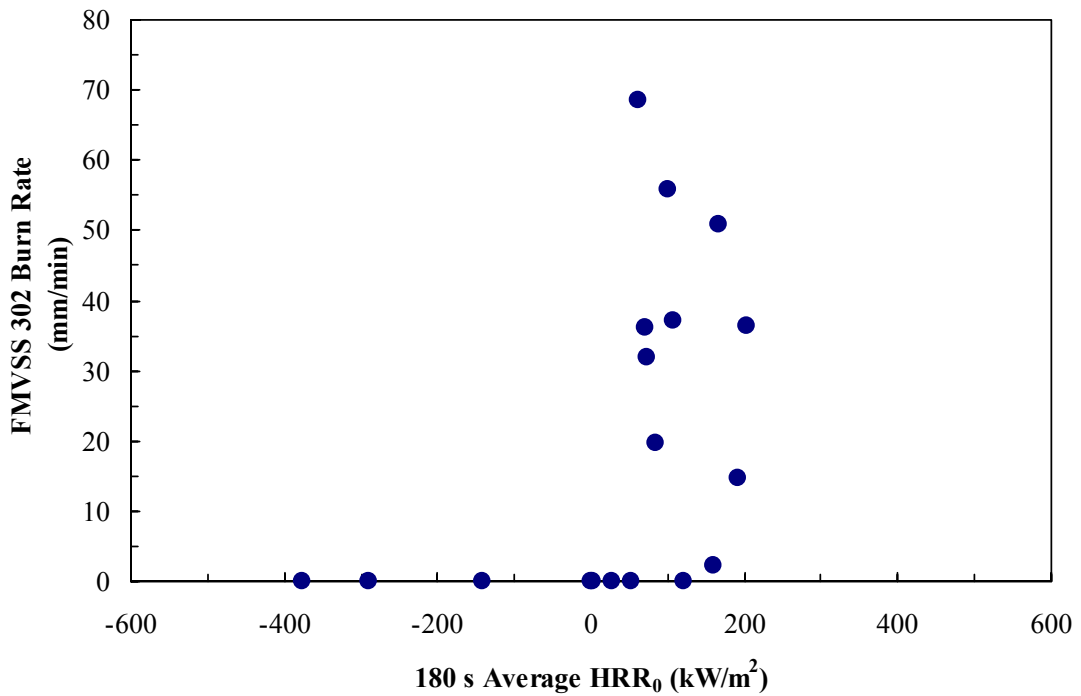**Figure 22. FMVSS 302 Burn Rate Versus HRR$_0$ Based on Peak 30 s Average HRR.**

Figure 23. FMVSS 302 Burn Rate Versus HRR$_0$ Based on 180 s Average HRR.
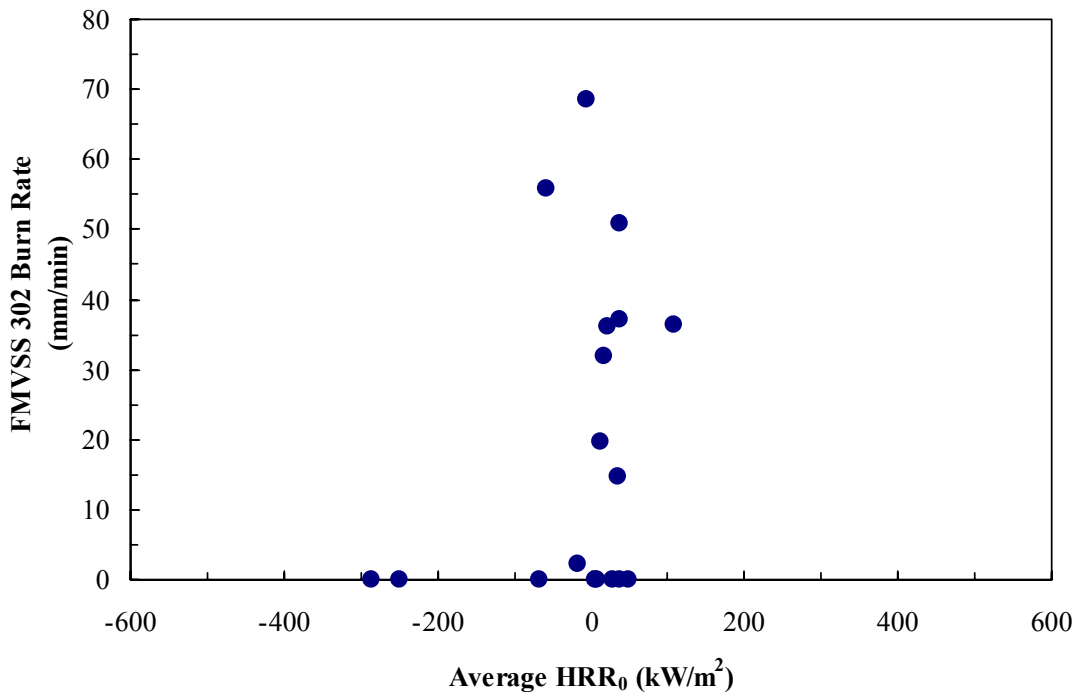
Figure 24. FMVSS 302 Burn Rate Versus HRR$_0$ Based on Average HRR.

Figures 21-24 indicate that HRR$_0$ is not a good indicator of flame propagation in the FMVSS 302 test. In a more recent paper, Lyon proposed using the Fire Hazard Parameter (FHP) to rank materials more consistently with UL 94 V performance [77]. The FHP is defined as follows:

$$FHP \equiv \frac{HRR_0}{HRR^*} + HRP \qquad (4)$$

The FHP is actually proportional to the heat release rate at a heat flux level equal to HRR*.

Lyon's improved correlations therefore indicate that heat release rate at a heat flux higher than zero is a better predictor of performance in a small flame propagation test such as UL 94 V and FMVSS 302. To explore this, the burn rate in the FMVSS 302 was plotted as a function of the heat release rate at 20, 35, and 50 kW/m^2 calculated from HRR$_0$ + 20 × HRP, HRR$_0$ + 35 × HRP, and HRR$_0$ + 50 × HRP, respectively. These plots were generated for the four different sets of HRR$_0$ and HRP values presented in Table 52. The best plot of the 12 that were generated is based on the peak heat release rate at 35 kW/m^2 (see Figure 25). This figure indicates that a flame will not propagate to the second mark in the FMVSS 302 test if the peak heat release rate in the Cone Calorimeter at 35 kW/m^2 does not exceed 250 kW/m^2. The figure also shows that there is a poor correlation between peak heat release rates that exceed 250 kW/m^2 and FMVSS 302 burn rates.
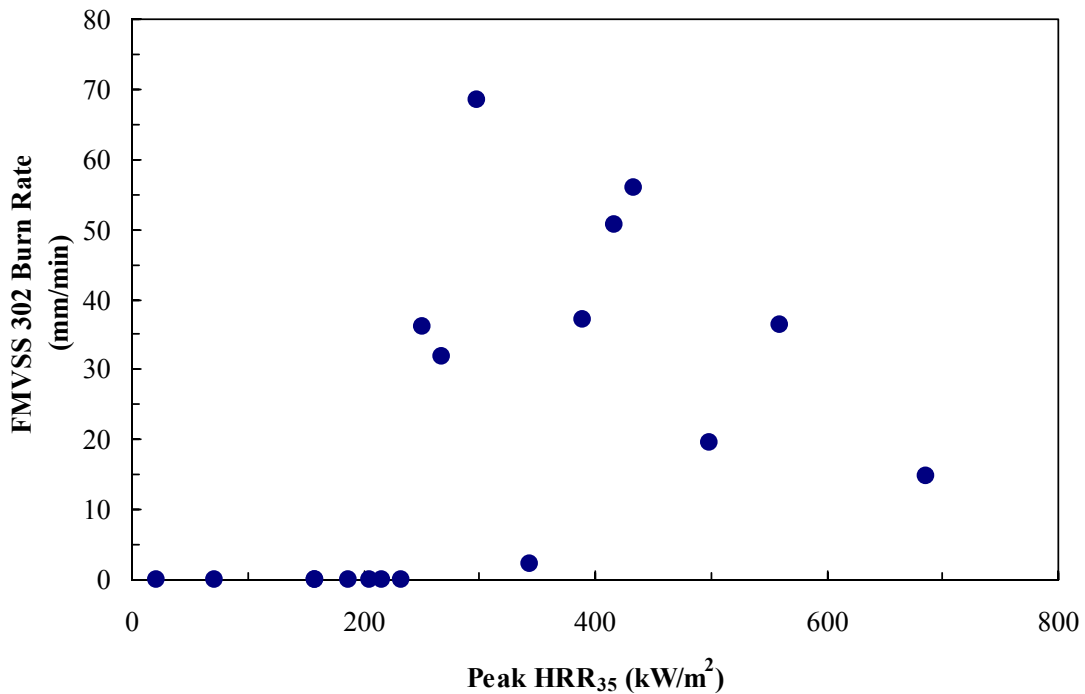
Figure 25. FMVSS 302 Burn Rate Versus Peak HRR at 35 kW/m^2.

Figure 26 is a plot of FMVSS 302 burn rate versus peak heat release rate divided by ignition time at 35 kW/m^2. The use of this ratio is motivated by the fact that the flame length of a laminar diffusion flame is proportional to the heat release rate. The assumption is that the distance ahead of the flame front heated by the flame divided by the time to ignite the heated material is expected to correlate well with the burn rate. Except for a few outliers, the agreement is reasonable. A ratio of 12 or less appears to be a sufficient condition to pass the FMVSS 302 test requirement.

5.3.5   Fire Performance Graph

The results obtained in the previous two sections are summarized in graphical form in Figure 27. A data point that falls below a specific curve indicates that the performance criteria associated with the curve are expected to be met. For example, consider a material that ignites in 45 seconds and releases heat at a peak rate of 100 kW/m^2 when tested in the Cone Calorimeter at 35 kW/m^2. The resulting data point is below the curve that corresponds to an engine fire growth rate of 0 to 400 kW in 6 minutes. Since the data point is below the curve, more than 6 minutes will be required to reach 400 kW. However, the data point is above the curve for 8 minutes. The time to reach 400 kW is therefore expected to be between 6 and 8 minutes. The data point is also below the FMVSS 302 line, which indicates that the material is expected to meet the FMVSS 302 requirements.
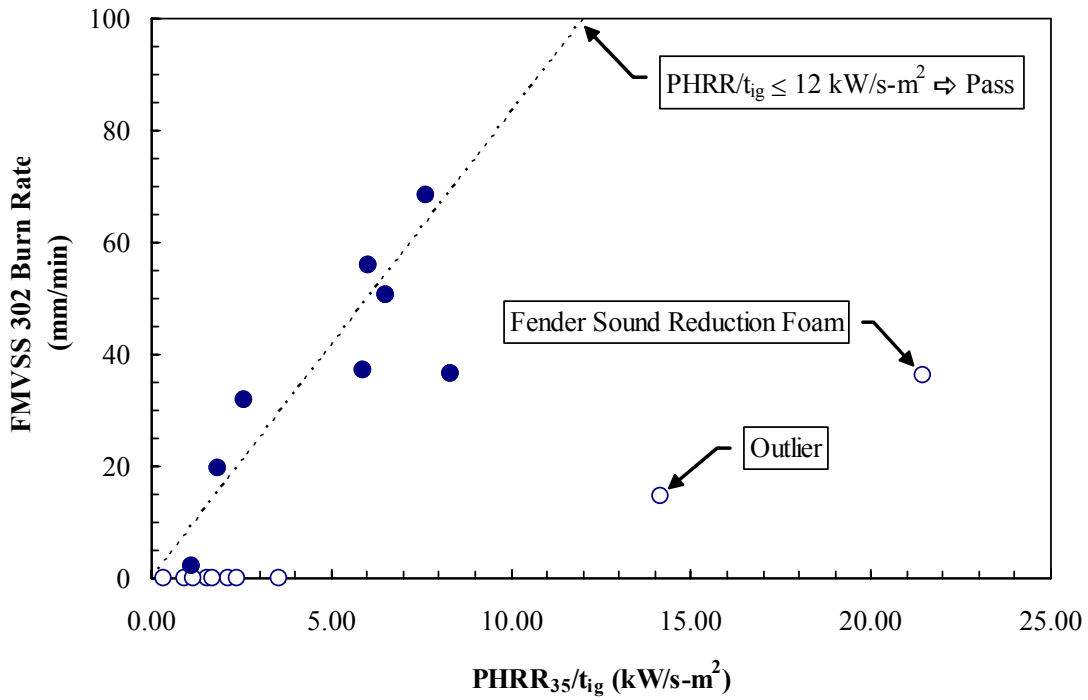
Figure 26. FMVSS 302 Burn Rate Versus Peak HRR/t_{ig} at 35 kW/m^2.
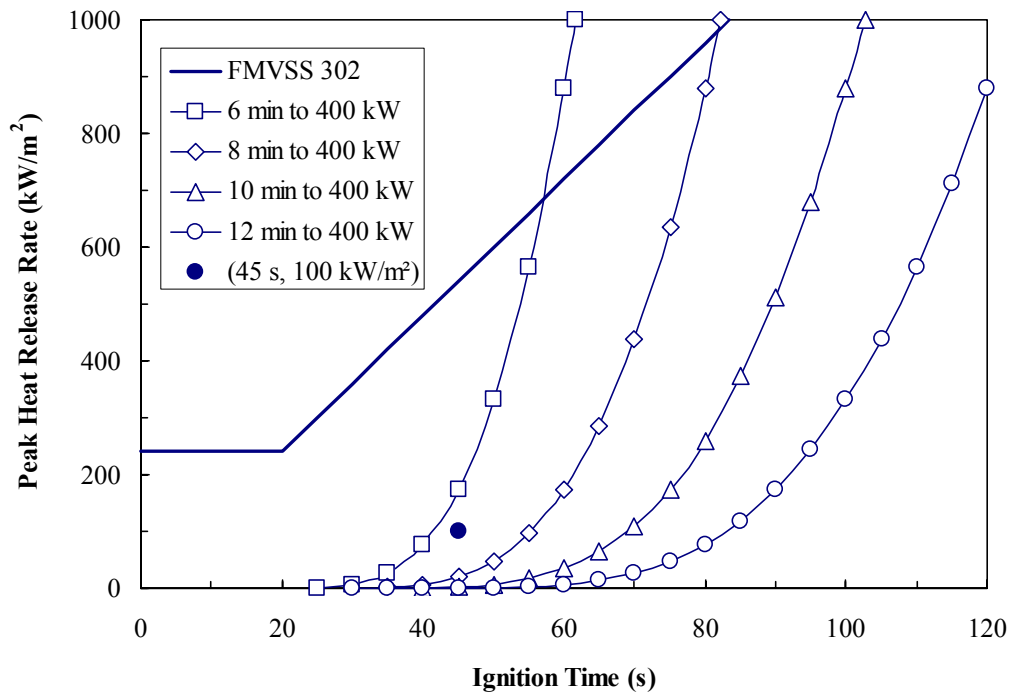

Figure 27. Fire Performance Graph.

Figure 28 shows the FMVSS 302 performance graph with the data points for the 18 materials that were tested. Two data points fall slightly above the FMVSS 302 line. These are the points for the fender sound reduction foam and the second outlier in Figure 26. This indicates that the performance graph provides a sufficient, but not a necessary condition to meet the FMVSS 302 requirements.
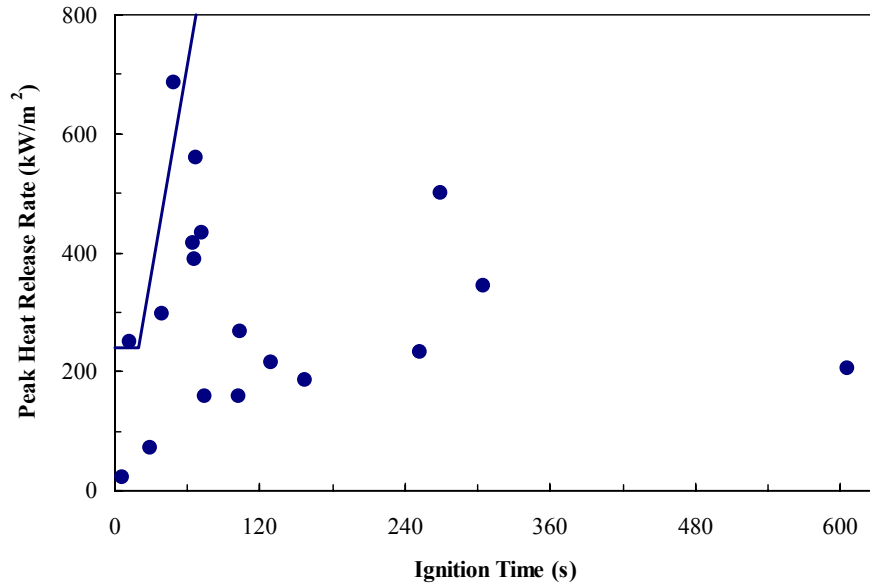
Figure 28. FMVSS 302 Performance Graph.

5.4   Analysis of Supplemental Smoke Toxicity Measurements and Tests

5.4.1   Comparison to Literature Values

Tewarson has published CO yield data for a variety of polymeric materials generated using the ASTM E 2058 Fire Propagation Apparatus designed by FM [78]. Table 53 shows a comparison between the CO yields measured for the materials used in this study from the MVFRI project and Tewarson's data. The reported values for the PE, PP materials and the nylons are averages of the results obtained from the samples listed in the table.

There is reasonable agreement between the results from the MVFRI project and Tewarson's data for the PE/PP, PC, and PS materials. The poor agreement between the values for the nylon and PVC materials may be an indication of significant differences between the actual materials used in this study and Tewarson's work. The lower values generally seen in this study may be reflective of the difference in ventilation between the Cone Calorimeter and the Fire Propagation Apparatus.

Table 53. Comparison of CO Yields Between This Study and Tewarson's Data.

| Material | CO Yields (mg/g) | | Number of Samples | Included Samples | |
	Tewarson	Measured Values		Vehicle	Sample
PE, PP	24	24±6	7	1996 Dodge Caravan	Air Ducts (4678345), Battery Cover (5235267AB), Brake Fluid Reservoir (4683264), Resonator Structure (4861057)
				1997 Chevrolet Camaro	Air Inlet (10297291), Front Wheel Well Liner (10296526), Heater Module Blower Motor Housing (52458965)
PC	54	50	1	1996 Dodge Caravan	Headlight Lens - Clear Lens (4857041A)
Nylons	38	18±7	3	1997 Chevrolet Camaro	Engine Cooling Fan (22098787), Power Steering Fluid Reservoir (26019594), Radiator Inlet/Outlet Tank (52465337)
PS	60	52	1	1996 Dodge Caravan	Fender Sound Reduction Foam (4716345B)
PVC	63	9	1	1996 Dodge Caravan	Kick Panel Insulation Backing - Rubber side (4860446)

5.4.2   Comparison of Cone Calorimeter Results with Smoke Box Measurements

The three materials tested as described in Section 4.3.4 were chosen based upon their performance in the Cone Calorimeter, as described in Section 4.3.3.5. Specifically, the Kick Panel Insulation Backing - Rubber Side (Part # 4860446) was chosen for its low CO_{MAX} value, the Hoodliner Face (Part # 4716832B) was chosen for its intermediate CO_{MAX} value, and the Headlight – Clear Lens (Part # 4857041A) was chosen for its high CO_{MAX} value.

Peak CO concentration data from the two smoke box tests show a different ranking of the three materials (see Table 54). At the 25 kW/m^2 exposures, the Headlight material produces the lowest CO concentrations and yields, rather than the highest. The other two samples are ordered as based on the Cone data. The Headlight material shows an increase in CO levels relative to the other two materials in the 50 kW/m^2 IMO test.

5.4.3   Application of Limits

Airbus, Bombardier, and the IMO all require that materials meet certain limits on the concentration of gases measured during a standard smoke box measurement. These limits are listed in Table 55.

Table 54. Sumary of CO Concentrations and Yields in Smoke Box Tests.

Method	Exposure	Part	Average Concentration (ppm)	Average Yield (mg/g)	Peak Concentration (ppm)	Peak Yield (mg/g)
Airbus	25FL	4857041A Headlight - Clear Lens	278	25.8	500.9	
		4716832B Hoodliner Face	927	82.2	1930.6	
		4860446 Kick Panel Insulation Backing - Rubber Side	653	29.5	993.6	
	25NF	4857041A Headlight - Clear Lens	0	0	0	
		4716832B Hoodliner Face	909	71	2329	
		4860446 Kick Panel Insulation Backing - Rubber Side	212	11	630	
IMO	25FL	4857041A Headlight - Clear Lens		1	17	8
		4716832B Hoodliner Face		90	3745	171
		4860446 Kick Panel Insulation Backing - Rubber Side		6	185	13
	25NF	4857041A Headlight - Clear Lens		0	2	0
		4716832B Hoodliner Face		148	5130	245
		4860446 Kick Panel Insulation Backing - Rubber Side		23	87	44
	50NF	4857041A Headlight - Clear Lens		103	1342	137
		4716832B Hoodliner Face		215	3532	362
		4860446 Kick Panel Insulation Backing - Rubber Side		32	988	42

Table 55. Toxic Gas Concentration Limits for Different Test Procedures.

	Airbus	Bombardier	IMO
CO_2	None	90000	None
CO	1000	3500	1450
HF	100	100	600
HCl	150	500	600
HBr	None	100	600
NO_x	100	100	350
HCN	150	100	140
SO_2	100	100	120

Airbus ABD 0031 requires that the average concentration of each gas as measured according to AITM 3.0005 shall not exceed the listed limits. Bombardier's SMP 800-C also places limits on the average concentrations observed, but specifies wet chemistry. Part 2 of Annex 1 to the IMO FTP Code places limits on the peak concentration observed during the test.

These limits have been applied to the measured gas concentrations listed in Section 4.3.4.4. The results are listed in Tables 58 through 60. As shown in the tables, the Kick Panel Insulation Backing - Rubber Side (Part # 4860446) failed to meet the criteria set by Airbus, due to excessive HCl formation in both flaming and non-flaming modes. It also failed to meet the IMO criteria due to excessive HCl production during the 50 kW/m^2 exposure. The Hoodliner Face (Part # 4716832B) failed to meet the criteria set by the IMO due to excessive CO production at both exposures and flaming modes. All materials met the Bombardier specifications.

Table 56. Performance Compared to Airbus +Acecptance Criteria.

	Sample	Average Concentration (ppm)			
		CO	CO$_2$	HCl	NO$_x$
25FL	Headlight Lens - Clear Lens (4857041A) Polycarbonate	278	7635	0	0
	Hoodliner Face (4716832B) PET	927	4039	0	0
	Kick Panel Insulation Backing - Rubber side (4860446) PVC	653	7273	461	0
25NF	Headlight Lens - Clear Lens (4857041A) Polycarbonate	3	82	0	0
	Hoodliner Face (4716832B) PET	908	1579	0	0
	Kick Panel Insulation Backing - Rubber side (4860446) PVC	212	2061	399	0
Limits		1000	none	150	100
Result	Headlight Lens - Clear Lens (4857041A) Polycarbonate	Pass	NA	Pass	Pass
	Hoodliner Face (4716832B) PET	Pass	NA	Pass	Pass
	Kick Panel Insulation Backing - Rubber side (4860446) PVC	Pass	NA	FAIL	Pass

Table 57. Performance Compared to Bombardier Acceptance Criteria.

	Sample	Average Concentration (ppm)			
		CO	CO$_2$	HCl	NO$_x$
25FL	Headlight Lens - Clear Lens (4857041A) Polycarbonate	278	7635	0	0
	Hoodliner Face (4716832B) PET	927	4039	0	0
	Kick Panel Insulation Backing - Rubber side (4860446) PVC	653	7273	461	0
25NF	Headlight Lens - Clear Lens (4857041A) Polycarbonate	3	82	0	0
	Hoodliner Face (4716832B) PET	908	1579	0	0
	Kick Panel Insulation Backing - Rubber side (4860446) PVC	212	2061	399	0
Limits		3500	90000	500	100
Result	Headlight Lens - Clear Lens (4857041A) Polycarbonate	Pass	Pass	Pass	Pass
	Hoodliner Face (4716832B) PET	Pass	Pass	Pass	Pass
	Kick Panel Insulation Backing - Rubber side (4860446) PVC	Pass	Pass	Pass	Pass

Table 58. Performance Compared to IMO Acceptance Criteria.

	Sample	Average Concentration (ppm)			
		CO	CO_2	HCl	NO_x
25FL	Headlight Lens - Clear Lens (4857041A) Polycarbonate	17	5991	0	0
	Hoodliner Face (4716832B) PET	3745	15873	0	0
	Kick Panel Insulation Backing - Rubber side (4860446) PVC	185	2406	19	0
25NF	Headlight Lens - Clear Lens (4857041A) Polycarbonate	2	221	0	0
	Hoodliner Face (4716832B) PET	5130	5631	0	0
	Kick Panel Insulation Backing - Rubber side (4860446) PVC	89	793	36	0
50NF	Headlight Lens - Clear Lens (4857041A) Polycarbonate	1342	NT	0	0
	Hoodliner Face (4716832B) PET	3532	5170	0	0
	Kick Panel Insulation Backing - Rubber side (4860446) PVC	988	18329	1162	77
Limits		1450	none	600	350
Result	Headlight Lens - Clear Lens (4857041A) Polycarbonate	Pass	NA	Pass	Pass
	Hoodliner Face (4716832B) PET	FAIL	NA	Pass	Pass
	Kick Panel Insulation Backing - Rubber side (4860446) PVC	Pass	NA	FAIL	Pass

5.4.4   *Use of Yields Measured in the Cone Calorimeter to Determine Toxic Hazard*

The yields measured in the Cone Calorimeter (see Section 4.3.3.4) in theory can be used to determine the toxic hazard to occupants in the passenger compartment from the products of combustion generated in an engine fire. However, this calculation is very complex. First it would be necessary to determine the burning rate of each part in the engine compartment as a function of time. The product of burning rate and yield of a particular toxic gas is equal to the generation rate of that gas. Thus, based on the yields and mass loss rates, it is possible to determine the generation rate of different toxic gases as a function of time for each component. Next, it is necessary to determine how the generated toxic gases are diluted by entrained air and how the resulting gas mixture migrates into the passenger compartment. This leads to concentration versus time curves of the gas mixture to which occupants of the passenger compartment are exposed. A Fractional Effective Dose can be calculated to determine the time to incapacitation and lethality [79]. There are obviously many sources of uncertainty in these calculations, but modeling smoke transport from the fire to the passenger compartment appears to be by far the most difficult part of the problem. In addition, because the full-scale vehicle burn tests at FM demonstrated that toxicity appears to be a secondary issue (see Section 3.2), the effort to perform toxic hazard calculations can hardly be justified.

5.5 Alternative Materials

Section 4.5 explores the use of metallic coatings to improve the fire performance of automotive materials. Table 59 shows how the various coatings and thicknesses affect ignition time and peak heat release rate in the Cone Calorimeter at 50 kW/m^2. It takes more time to ignite the coated specimens, but in some cases the peak heat release rate is higher than for the uncoated specimens. The former improves fire performance while the latter adversely affects it. Unfortunately, Cone Calorimeter data for the coated specimens are not available at 35 kW/m^2 and the net effect on the fire growth rate according to Equation 2 cannot be calculated. Table 59 gives the times to reach 400 kW based on the ignition time and peak heat release rate at 50 kW/m^2. These times are obviously much shorter than those given in Table 48, but the calculations show that all coatings result in a significantly lower fire growth rate. It can be concluded, therefore, that application of a metallic coating presents a viable approach to improve the fire performance of automotive materials and bring their hazard below a specified level.

Table 59. Effect of Coatings on the Fire Hazard of Automotive Materials.

Vehicle	Component	Coating	Uncoated			Coated		
			t_{ig} (s)	PHRR (kW/m^2)	$t_{400\ kW}$ (s)	t_{ig} (s)	PHRR (kW/m^2)	$t_{400\ kW}$ (s)
Caravan	Resonator Structure	1.75 μm Aluminum	19	517	126	34	396	237
Caravan	Resonator Structure	3.6 μm Aluminum	19	517	126	184	479	1242
Caravan	Resonator Structure	3.2 μm Antinmony Oxide	19	517	126	74	553	486
Caravan	Headlight	1.75 mm Aluminum	49	356	349	100	319	725
Caravan	Headlight	3.2 μm Antimnony Oxide	49	356	349	73	389	511
Camaro	Front Wheel Well Liner	1.75 μm Aluminum	18	526	119	100	648	637
Camaro	Front Wheel Well Liner	3.6 μm Antimony	18	526	119	50	826	304
Camaro	Front Wheel Well Liner	2.9 μm Antimony Oxide	18	526	119	32	663	203
Camaro	Air Inlet	1.75 μm Aluminum	17	759	102	189	718	1181
Camaro	Air Inlet	3.6 μm Aluminum	17	759	102	226	939	1337
Camaro	Air Inlet	3.2 μm Aluminum Oxide	17	759	102	84	1249	467

6.0 CONCLUSIONS AND RECOMMENDATIONS

The objectives of the NHTSA project are to develop a small-scale test methodology to rate automotive materials consistent with actual fire performance in vehicle burns and to establish levels of performance for this test methodology that would significantly alter the fire outcome in terms of injury or survivability.

It is demonstrated in Section 5.3 that the FMVSS 302 test, which is currently required for interior materials, is relatively mild and corresponds to a low level of performance in actual vehicle

fires. Moreover, it is a pass/fail type test and it may not be possible to change the acceptance criteria so that actual fire performance is sufficiently improved to result in the desired reduction of motor vehicle fire injuries and fatalities.

It is also shown in Section 5.3 that the Cone Calorimeter provides quantitative data that can be used to determine the heat release rate of a growing engine fire as a function of time. Full-scale vehicle burn tests have shown that post-crash engine fires become a threat to occupants trapped in the passenger compartment when the heat release rate reaches approximately 400 kW. Consequently, the time to this critical condition for a specific material can be determined on the basis of the following equation

$$t_{cr} = t_{ig}\left[1 + 1.233 \ln\left(\frac{400}{0.0079\dot{Q}''}\right)\right]$$

where t_{cr} is the time to a critical condition (heat release rate of 400 kW) in sec, t_{ig} is the time to ignition measured in the Cone Calorimeter at 35 kW/m^2, and $\dot{Q}''$ is the peak heat release rate measured in the Cone Calorimeter at 35 kW/m^2.

Based on NHTSA's goal for a reduction of the number of fatalities and injuries in motor vehicle fires, it is recommended that statistics of post-crash fires originating in the engine compartment be analyzed to determine the corresponding shortest time for fire spread into the passenger compartment, t_{min}. If materials are used so that the actual time is equal to or greater than t_{min}, the expected number of fatalities will be equal to or less than the desired number.

In summary, it is suggested that candidate materials for components in the engine compartment be tested in the Cone Calorimeter at 35 kW/m^2, and that acceptance be based on the requirement that $t_{cr} \geq t_{min}$.

To validate this concept, it is proposed that a number of comparative full-scale fires tests be conducted. It was demonstrated in this study that the use of metallic coatings is a viable option to improve fire performance and delay fire growth in the engine compartment of a motor vehicle. Therefore, it is suggested that at least two experiments be conducted. Both experiments involve the same make and vehicle model. The vehicle is first tested without any modifications. Surfaces of plastic components in the engine compartment are treated with a metallic coating prior to the second test. The fire initiates in the engine compartment and temperatures, heat fluxes and toxic gas species are measured to determine the time to untenable conditions for occupants in the passenger

compartment. To provide more validity, additional tests could be performed with a different type of vehicle. Full-scale tests also provide an opportunity to evaluate the effect of flammable or combustible liquid spills.

The NHTSA project only addresses materials of plastic components in the engine compartment. Motor vehicle fires that originated in the passenger compartment would have to be analyzed to determine whether the same Cone Calorimeter criteria are adequate, or whether they can or should be changed to meet specific survivability objectives for this fire scenario. A similar analysis would also have to be performed to address fires that involve a rear-end collision and subsequent underbody pool fire. For this scenario it may not be possible to meet survivability objectives through material performance specifications, and other fire protection strategies may have to be explored (fire-resistant boundaries, fire suppression systems, etc.)

The MVFRI project involved additional measurements of toxic gases in the duct for most of the Cone Calorimeter tests. Concentrations of CO, CO_2, HCl, HCN, and NO_x were measured continuously during each test with an FTIR spectrometer. The concentration measurements were used to calculate yields, *i.e.*, the total mass of each toxic gas generated during flaming combustion divided by the mass loss of the fuel over the same period. CO yields obtained in this study are comparable in magnitude, but consistently lower than values reported in the literature for the same generic classes of materials. This can be explained by the fact that the literature values were obtained in the Fire Propagation Apparatus (ASTM E 2058) under reduced ventilation conditions compared to the Cone Calorimeter.

The measured yields can be used to calculate a fractional effective dose in a real engine fires is also discussed.

Three materials were selected from the set of 18 for an evaluation in two commonly used toxicity test procedures. The Airbus ABD 0031 procedure is based on the NBS smoke chamber (ASTM E 662) and involves supplemental gas analysis. The IMO smoke and toxicity test procedure is detailed in Part 2 of Annex 1 to the FTP code and is based on a modified version of the NBS smoke chamber as described in ISO standard 5659 Part 2. Both procedures specify acceptance criteria that include limiting concentrations of CO, HCl, HCN, NO_x, and a few additional gases. The three materials that were selected had the lowest, median, and highest peak CO concentrations in the Cone Calorimeter tests of all the materials that were tested. The material with low peak CO concentration was a PVC and exceeded the limits for HCl in the IMO and Airbus tests. The material with median CO in the Cone Calorimeter failed the IMO test, and the material with high CO in the Cone

Calorimeter marginally met the IMO and Airbus requirements. It can be concluded from these tests that the CO concentrations in the Cone Calorimeter are not consistent with those in box-type toxicity tests. This can be explained by the fact that plenty of excess air is continuously supplied in the Cone Calorimeter, while the atmosphere in the IMO and Airbus smoke chambers typically becomes vitiated during a test.

7.0   REFERENCES

[1]   M. Miller, M. Janssens, and J. Huczek, "Development of a New Procedure to Assess the Fire Hazard of Materials Used in Motor Vehicles," SwRI, San Antonio, TX, Draft Final Report SwRI Project No. 18.03614, 2003 (Under Review).

[2]   J. Santrock, "Demonstration of Enhanced Fire Safety Technology - Fire Retardant Materials - Part 1: Full Scale Vehicle Fire Tests of a Control Vehicle and a Test Vehicle Containing an HVAC Module," General Motors Corporation, Warren, MI October 22, 2002.

[3]   T. Ohlemiller and J. Shields, "Burning Behavior of Selected Automotive Parts from a Minivan," National Institute of Standards and Technology, Gaithersburg, MD NISTIR 6143, August 1998.

[4]   T. Ohlemiller and J. Shields, "Burning Behavior of Selected Automotive Parts from a Sports Coupe," National Institute of Standards and Technology, Gaithersburg, MD NISTIR 6316, April 2001.

[5]   B. Sundström, "Fire Safety of Upholstered Furniture - The Final Report on the CBUF Research Programme," Interscience Communications, London, England EUR 16477 EN, 1995.

[6]   S. Grayson, P. Van Hees, U. Vercelotti, H. Bruelet, and A. Green, "The FIPEC Report: Fire Performance of Electric Cables," Interscience Communications, London, England SMT4-CT96-2059, 2000.

[7]   I. Wichman, "A Review of Literature of Material Flammability, Combustion and Toxicity Related to Transportation," Michigan State University, East Lansing, MI January 30, 2002.

[8]   K. Strom and A. Hamer, "Post-Crash Fire Modeling - Software for Characterization of the Hazards Posed by Heat and Exposure to Toxic Agents Associated with Fire," GM R&D and Planning, Warren, MI October 22, 2002.

[9]   J. Santrock, "Study of Flammability of Materials - Identification of the Base Polymers in Selected Components and Parts from a 1997 Chevrolet Camaro by Pyrolysis/Gas Chromatography/Mass Spectroscopy," General Motors Corporation, Warren, MI August 12, 2002.

[10]   J. Santrock, "Evaluation of Motor Vehicle Fires Initiation and Propagation, Part 4: Propagation of an Underbody Gasoline Pool Fire in a 1996 Passenger Van," General Motors Corporation, Warren, MI 2002.

[11]   J. Santrock, "Study of Flammability of Materials - Identification of the Base Polymers in Selected Components and Parts from a 1997 Ford Explorer by Pyrolysis/Gas Chromatography/Mass Spectroscopy and Attenuated Total Reflectance/Fourier Transform Infrared Analysis," General Motors Corporation, Warren, MI August 12, 2002.

[12]   J. Santrock, A. Tewarson, and P. Wu, "Study of Flammability of Materials - Flammability Testing of Automotive Heating Ventilation and Air Conditioning Modules Made from

Polymers Containing Flame Retardant Chemicals," General Motors Corporation, Warren, MI August 12, 2002.

[13]   J. Santrock, "Study of Flammability of Materials - Determination of Mol-% Ethylene in Propylene/Ethylene Copolymer Samples by Pyrolysis/Gas Chromatography/Mass Spectroscopy Analysis," General Motors Corporation, Warren, MI August 12, 2002.

[14]   J. Santrock, "Evaluation of Motor Vehicle Fires Initiation and Propagation, Part 9: Propagation of a Rear-Underbody Gasoline Pool Fire in a 1998 Sport Utility Vehicle," General Motors Corporation, Warren, MI October 22, 2002.

[15]   J. Santrock, "Evaluation of Motor Vehicle Fires Initiation and Propagation, Part 10: Propagation of a Mid-Underbody Gasoline Pool Fire in a 1998 Sport Utility Vehicle," General Motors Corporation, Warren, MI October 22, 2002.

[16]   J. Santrock, "Evaluation of Motor Vehicle Fires Initiation and Propagation, Part 6: Propagation of an Underbody Gasoline Pool Fire in a 1997 Rear Wheel Drive Passenger Car," General Motors Corporation, Warren, MI June 14, 2002.

[17]   J. Santrock and D. Kohonen, "Study of Flammability of Materials - Flammability Properties of Engine Compartment Fluids Other than Gasoline - Autoignition Characteristics of Non-Gasoline Motor Vehicle Fluids on Heated Surface," General Motors Corporation, Warren, MI March 29, 2002.

[18]   J. Santrock, "Study of Flammability of Materials - Flammability Properties of Engine Compartment Fluids Other than Gasoline - Gas Chromatography/Mass Spectroscopy Analysis," General Motors Corporation, Warren, MI March 29, 2002.

[19]   J. Santrock, "Evaluation of Motor Vehicle Fires Initiation and Propagation, Part 7: Propagation of an Engine Compartment Fire in a 1997 Rear Wheel Drive Passenger Car," General Motors Corporation, Warren, MI August 12, 2002.

[20]   T. Ohlemiller, "Influence of Flame-Retarded Resins on the Burning Behavior of a Heating, Ventilating and Air Conditioning Unit from a Sports Coupe," National Institute of Standards and Technology, Gaithersburg, MD NISTIR 6748, June 2002.

[21]   T. Ohlemiller, "The Effect of Polymer Resin Substitution on the Flammability of a Standardized Automotive Component in Laboratory Tests," National Institute of Standards and Technology, Gaithersburg, MD NISTIR 6745, June 2002.

[22]   J. Jensen and J. Santrock, "Evaluation of Motor Vehicle Fires Initiation and Propagation, Part 8: Crash Tests on a Sports-Utility-Vehicle," General Motors Corporation, Warren, MI January, 2002.

[23]   J. Jensen and J. Santrock, "Evaluation of Motor Vehicle Fires Initiation and Propagation, Part 11: Crash Tests on a Front-Wheel Drive Passenger Vehicle," General Motors Corporation, Warren, MI August 12, 2002.

[24]   L. Griffin, B. Davies, and R. Flowers, "Studying Passenger Vehicle Fires with Exisiting Databases," Texas A&M, College Station, TX January 2002.

[25]   B. Davies and L. Griffin, "A Clinical Evaluation of the Death Investigations for 206 Decendents Who Died in Passenger Vehicles that Experienced Post-Crash Fires," Texas A&M, College Station, TX January 2002.

[26]   L. Shields, R. Scheibe, T. Angelos, and R. Mann, "Case Studies of Motor Vehicle Fires," University of Washington, Seattle, WA January, 2001.

[27] J. Santrock, "Evaluation of Motor Vehicle Fires Initiation and Propagation, Part 3: Propagation in an Engine Compartment Fire in a 1996 Passenger Van," General Motors Corporation, Warren, MI August 30, 2001.

[28] J. Jensen and J. Santrock, "Evaluation of Motor Vehicle Fires Initiation and Propagation, Part 5: Crash Tests on a Rear Wheel Drive Passenger Car," General Motors Corporation, Warren, MI September 7, 2001.

[29] L. Griffin and R. Flowers, "An Evaluation of Fatal and Incapacitating Injuries to Drivers of Passenger Vehicles that Experienced Post-Crash Fires in North Carolina (1991-1996)," Texas A&M, College Station, TX April 2001.

[30] L. Griffin, "Comparison of Crash-Involved Passenger Vehicles [Containing One or More Fatally-Injured Occupants] that Did or Did Not Experience Fires (FARS 1994-1996)," Texas A&M, College Station, TX April 2001.

[31] I. Abu-Isa and S. Jodeh, "Thermal Properties of Automotive Polymers: III. Thermal Characteristics and Flammability of Fire Retardant Polymers," *Materials Research Innovations*, vol. 4, pp. 135-143, 2001.

[32] I. Abu-Isa and S. Jodeh, "Thermal Properties of Automotive Polymers: V. Flammability Test for Fire Retardant Polymers," Delphi Central Research & Development Center, Warren, MI September 7, 2001.

[33] K. Strom, A. Hamer, and R. Karlsson, "Burn Hazard Assessment Model," GM R&D and Planning, Warren, MI May 31, 2000.

[34] A. Hamins, "Evaluation of Active Suppression in Simulated Post-Collision Vehicle Fires," National Institute of Standards and Technology, Gaithersburg, MD NISTIR 6379, November 2000.

[35] I. Abu-Isa and S. Jodeh, "Thermal Properties of Automotive Polymers: IV. Thermal Gravimetric Analysis and Differential Scanning Calorimetry of Selected Parts from a Chevrolet Camaro," Delphi Central Research & Development Center, Warren, MI 2000.

[36] I. Abu-Isa and S. Jodeh, "Thermal Properties of Automotive Polymers: III. Thermal Characteristics and Flammability of Fire Retardant Polymers," Delphi Central Research & Development Center, Warren, MI 2000.

[37] I. Wichman, J. Beck, B. Oladipo, R. McMasters, and E. Little, "Theoretical and Experimental Study of Thermal Barriers Separating Automobile Engine and Passenger Compartments," Michigan State University, East Lansing, MI 10-31-99, October 31, 1999.

[38] A. Tewarson, I. Abu-Isa, D. Cummings, and D. LaDue, "Characterization of the Ignition Behavior of Polymers Commonly Used in the Automotive Industry," presented at Sixth International Symposium of Fire Safety Science, Poitiers, France, 1999.

[39] R. Scheibe, L. Shields, and T. Angelos, "Field Investigation of Motor Vehicle Collision Fires," 1999.

[40] J. Ierardi, "A Computer Model for Fire Spread from Engine to Passenger Compartmentsin Post-Collision Vehicles," in *Center for Firesafety Studies*. Worcester, MA: Worcester Polytechnic Institute, 1999, pp. 205.

[41] P. Eichbrecht, "Crash Test Protocol Development for Fuel System Integrity Assesment," General Motors Corporation, Warren, MI december 13, 1999.

[42] L. Shields, R. Scheibe, and T. Angelos, "Motor-Vehicle Collision-Fire Analysis Method and Results," University of Washington, Seattle, WA 1998.

[43]   T. Ohlemiller and T. Cleary, "Aspects of the Motor Vehicle Fire Threat from Flammable Liquid Spills on a Road Surface," National Institute of Standards and Technology, Gaithersburg, MD NISTIR 6147, August 1998.

[44]   J. Lavelle, D. Kononen, and J. Nelander, "Field Data Improvements for Fire Safety Research," presented at 16th International Technical Conference on the Enhanced Safety of Vehicles, Windsor, ON, 1998.

[45]   D. LaDue III and D. Kononen, "A Searchable Fire Safety Bibliography," presented at 16th International Technical Conference on the Enhanced Safety of Vehicles, Windsor, ON, 1998.

[46]   J. Jensen and J. Santrock, "Evaluation of Motor Vehicle Fire Initiation and Propagation, Vehicle Crash and Fire Propagation Test Program," presented at 16th International Technical Conference on the Enhanced Safety of Vehicles, Windsor, ON, 1998.

[47]   A. Hamins, "Evaluation of Intumescent Body Panel Coatings in Simulated Post-Accident Vehicle Fires," National Institute of Standards and Technology, Gaithersburg, MD NISTIR 6157, April 1998.

[48]   I. Abu-Isa, D. Cummings, D. LaDue, and A. Tewarson, "Thermal Properties and Flammability Behavior of Automotive Polymers," presented at 16th International Technical Conference on Enhanced Safety of Vehicles, Windsor, Canada, 1998.

[49]   I. Abu-Isa, "Thermal Properties of Automotive Polymers: II. Thermal Conductivity of Selected Parts from a Dodge Caravan," General Motors Research & Development Center, Warren, MI 1998.

[50]   A. Tewarson, "A Study of the Flammability of Plastics in Vehicle Components and Parts," Factory Mutual Research, Norwood, MA FMRC J.I.OB1R7.RC, October 1997.

[51]   L. Griffin, "An Assessment of the Reliability and Validity af the Information on Vehicle Fires Contained in the Fatal Accident Reporting System (FARS)," Texas A&M, College Station, TX 1997.

[52]   L. Watson, S. Deaton, J. Gamble, D. Sugg, S. Tzortzis, and M. Mcleary, "Fire Statistics United Kingdom, 2000," Home Office, London, England Product Code FS/PPU/2765, February 20, 2002.

[53]   USFA, "Highway Vehicle Fires," in *Topical Fire Research Series*, vol. 2: United States Fire Administration, 2001.

[54]   M. Hirschler, D. Hoffman, J. Hoffman, and E. Kroll, "Fire Hazard Associated with Passenger Cars and Vans," presented at Fire and Materials 2003, San Francisco, CA, 2003.

[55]   D. Joyeux, J. Kruppa, L. Cajot, J. Schleich, P. Van de Leur, and L. Twilt, "Demonstration of Real Fire Tests in Car Parks and High Buildings," CTICM June 2002.

[56]   D. Stroup, L. DeLauter, J. Lee, and G. Roadermel, "Passenger Minivan Fire Tests," National Institute of Standards and Technology, Gaithersburg, MD FR 4011, 2001.

[57]   C. Steinert, "Experimental Investigation of Burning and Fire Jumping Behavior of Automobiles (in German)," *VFDB*, vol. 49, pp. 163-172, 2000.

[58]   C. Jayakody, D. Myers, and C. Ogburn, "Fire-Resistant Cushioning for the Transportation Industry," presented at Fire Risk & Hazard Assessment Research Application Symposium, Baltimore, MD, 2002.

[59]   S. Grayson and M. Hirschler, "Fire Performance of Plastics in Car Interiors," presented at Flame Retardants 2002, London, England, 2002.

[60] R. Bailey and G. Blair, "Small Scale Laboratory Flammability Testing and Real Automotive Interior Fires: A Comparison," presented at Fire Retardants Trends and Advances, Philadelphia, PA, 2001.

[61] M. Shipp, "Vehicle Fires and Fire Safety in Tunnels," presented at Tunnel Fires and Escape from Tunnels, Washington, DC, 2001.

[62] D. Barber and D. Proe, "Practical Design Applications for Real Car Fire Test Data," presented at Engineered Fire Protection design ... Applying Fire Science to Fire Protection Problems, San Francisco, CA, 2001.

[63] J. Zicherman, "Polymer Products in Rail and Bus Applications: Fire Risk, Fire Hazard Assessment and Field Experience," presented at Fire and Materials 2003, San Francisco, CA, 2003.

[64] M. Stevens, "Fiber Reinforced Plastics in Mass Transportation Industry," presented at Fire and Materials, San Francisco, CA, 2001.

[65] R. Johnson and L. Wuethrich, "Flammability of Automotive Child Restraint Seats for Use in Aircraft," Federal Aviation Administration, Atlantic City, NJ DOT/FAA/AR-TN01/42, November 2001.

[66] U. Sorathia, T. Gracik, J. Ness, M. Blum, A. Le, B. Scholl, G. Long, and B. Lattimer, "Fire Safety of Marine Composites," presented at Bridging the Centuries with SAMPE's Materials and Processes Technology, Long Beach, CA, 2000.

[67] Y. Le Tallec, A. Sainrat, V. Le Sant, S. Méral, P. Gil, P. Briggs, S. Messa, and H. Breulet, "The Firestarr Project - Fire Protection of Railway Vehicles," presented at Fire and Materials 2001, San Francisco, CA, 2001.

[68] J. Roed, "Low Voltage Directive," presented at FIRESEL 2003, Borås, Sweden, 2003.

[69] U. Wickström and U. Göransson, "Full-Scale/Bench-Scale Correlations of Wall and Ceiling Linings," *Journal of Fire and Materials*, vol. 16, pp. 15-22, 1992.

[70] B. Östman and L. Tsantaridis, "Smoke Production in the Cone Calorimeter and the Room Fire Test," *Fire Safety Journal*, vol. 17, pp. 27-43, 1991.

[71] B. Östman and R. Nussbaum, "Correlation between Small-Scale Rate of Heat Release and Full-Scale Room Flashover for Wall Linings," presented at Second International Symposium of Fire Safety Science, Tokyo, Japan, 1988.

[72] M. Janssens and J. Urbas, "Comparison of Small and Intermediate Scale Heat Release Data," presented at Interflam '96, Cambridge, England, 1996.

[73] F. Chu and A. Tewarson, "Standard Method of Test for Material Properties using the FMRC Flammability Apparatus," Factory Mutual Research, Norwood, MA FMRC J.I.OBOJ4.BU, February 1997.

[74] J. Quintiere, "Surface Flame Spread," in *SFPE Handbook of Fire Protection Engineering*, P. DiNenno, Ed. Quincy, MA: NFPA, 2002, pp. Section 2, 246-257.

[75] A. Atreya, "Pyrolysis, Ignition, and Fire Spread on Horizontal Surfaces of Wood." Cambridge, MA: Harvard University, 1983.

[76] R. Lyon, "Fire and Flammability," presented at Fire and Materials 2003, San Francisco, CA, 2003.

[77] R. Lyon, "Fire & Flammability," presented at FIRESEL 2003, Borås, Sweden, 2003.

[78]   A. Tewarson, "Generation of Heat and Chemical Compounds in Fire," in *SFPE Handbook of Fire Protection Engineering*, P. DiNenno, Ed. Quincy, MA: NFPA, 2002, pp. Section 3, 82-161.

[79]   D. Purser, "Toxicity Assessment of Combustion Products," in *SFPE Handbook of Fire Protection Engineering*, P. DiNenno, Ed. Quincy, MA: NFPA, 2002, pp. Section 2, 83-171.